

**THE STUDY OF HYDROXYAPATITE REINFORCED POLYLACTIC ACID
COMPOSITES FOR ORTHOPEDIC APPLICATIONS**

A Dissertation

presented to

the Faculty of the Graduate School

at the University of Missouri

In Partial Fulfillment

of the Requirements for the Degree

Doctor of Philosophy

by

RICHARD JOSEPH LEBENS III

Dr. Hao Li, Dissertation Supervisor

MAY 2014

© Copyright by Richard J. Lebens III 2014

All Rights Reserved

The undersigned, appointed by the Dean of the Graduate School, have examined the
dissertation entitled

**THE STUDY OF HYDROXYAPATITE REINFORCED POLYLACTIC ACID
COMPOSITES FOR ORTHOPEDIC APPLICATIONS**

Presented by Richard Joseph Lebens III
A candidate for the degree of
Doctor of Philosophy in Mechanical Engineering
And hereby certify that in their opinion it is worthy of acceptance

Professor Hao Li

Professor Craig A. Kuhns, MD

Professor Yuyi Lin

Professor Stephen Lombardo

Professor Douglas Smith

Professor Qingsong Yu

DEDICATION

This dissertation is dedicated to my loving family without their support this would not have been possible, especially to my wife Mary and children Richard and Eleanor.

ACKNOWLEDGMENTS

The path to obtain my PhD in mechanical engineering has been a long and fascinating journey. Fortunately, I have been very lucky to have the encouragement, guidance, and support of many people. I would like to express my genuine appreciation and gratitude to all the people who assisted me on this journey, although it would be impossible to name them all.

First, I would like to sincerely thank my advisor, Dr. Hao Li, without whose help my path would have been extremely different. I am very grateful for the tremendous amount of time and patience Dr. Li has shown to me. I am so lucky to have worked with such an admirable and respectful supervisor and friend. Thank you very much for your understanding, guidance and passion.

I would like to express my gratitude to all my committee members in my comprehensive examination and my dissertation, Dr. Craig Kuhns, Dr. Stephen Lombardo, Dr. Yuyi Li, Dr. Douglas Smith and Dr. Qingsong Yu for their valuable suggestions and time.

I also would like to take this time to acknowledge my current and past colleagues Dr. Liang Chen, Dr. Meng Chen, Dr. Andrew Ritts, Dr. Young Jo Kim, Mr. Joseph Mcrate, Dr. Wen Ritts, Ms. Bonnie Walker, Dr. Adam Blumhagen, Mr. David Golub, Mr. Xin Sun, Mr. John Jones, Dr. Xiaoqing Dong, Mr. Qing Hong, Mrs. Liling Liu, Ms. Kathryn Giddens, Mr. Johnathan Schottler, Ms. Hana Dye, Mr. Craig Wilkins, Mr. Tyler Arthur, and Mr. Adam Joyce for their collaboration, discussion, meaningful assistance, friendship, and making the work enjoyable and exciting. Finally, I would like to thank my parents for their unconditional love and support throughout my life. Additionally, I am grateful for the love and support of my amazing wife, son Richard IV, daughter Eleanor.

TABLE OF CONTENTS

Acknowledgments	ii
LIST OF ILLUSTRATIONS	viii
LIST OF TABLES	xii
LIST OF ABBREVIATIONS	xiii
Abstract	xiv
Chapter 1. General Introduction	1
References	7
Chapter 2: The Application of Taguchi Method® Optimization Design of Experiment to Determine Single Screw Injection Molding Parameters for Polylactic Acid Composites for Orthopedic Application	11
2.1 Chapter 2 Abstract	11
2.2 Introduction	12
2.3 Materials and Methods	13
2.3.1 <i>Injection Molding Procedure</i>	14
2.3.2 <i>Flexural testing</i>	15
2.3.3 <i>Tensile testing</i>	16
2.3.4 <i>Taguchi Method® Design of Experiment</i>	16
2.4 Results	19
2.5 Discussion	21
2.6 Conclusion	24
References	25
Chapter 3: Fabrication and Mechanical Evaluation of Polylactic Acid Composites Containing Hydroxyapatite Nanofibers for Orthopedic Applications	27
3.1 Chapter 3 Abstract	27
3.2 Introduction	28
3.3 Materials and Methods	30
3.3.1 <i>Hydroxyapatite Nanofiber Synthesis</i>	30
3.3.2 <i>HA/PLA Composite Fabrication</i>	31
3.3.3 <i>Characterization</i>	31

3.3.3.1 <i>Viscosity Measurement</i>	31
3.3.3.2 <i>Mechanical Testing</i>	32
3.3.3.3 <i>Morphology</i>	32
3.3.3.4 <i>Differential Scanning Calorimetry (DSC)</i>	32
3.4 Results	33
3.5 Discussion	41
3.5.1 <i>Polymer Nanocomposites Filler</i>	41
3.5.2 <i>Polymer Matrix</i>	44
3.5.3 <i>Polymer Interfacial Region</i>	46
3.5.4 Conclusions	47
3.6 Conclusion	47
References	49
Chapter 4: Mechanical Evaluation of Polylactic Acid and Hydroxyapatite Composites Following 24-hour Immersion in Simulated Physiological Environment	55
4.1 Chapter 4 Abstract.....	55
4.2 Introduction	56
4.3 Materials and Methods.....	59
4.3.1 <i>HA whiskers and polylactic acid composite</i>	59
4.3.2 <i>Mechanical testing</i>	60
4.3.3 <i>Characterization</i>	61
4.4 Results	61
4.5 Discussion	65
4.6 Conclusion	70
References	72
Chapter 5: Mechanical Evaluation of Hybrid Polylactic Acid Hydroxyapatite Micro- and Nano-composite for Orthopedic Fixation Applications	77
5.1 Chapter 5 Abstract.....	77
5.2 Introduction	78
5.3 Methodology	81
5.3.1 <i>Materials</i>	81
5.3.2 <i>Fabrication</i>	81

5.3.3 Testing	82
5.4 Results & Discussion	82
5.4.1 Mechanical Evaluation	82
5.4.2 Scanning Electron Microscopy	84
5.5 Conclusions	86
References	87
Chapter 6: Polylactic Acid Composites Containing Hydroxyapatite in Simulated Body Environment for Orthopedic Fixation Application: A 24 Week Study	92
6.1 Chapter 6 Abstract.....	92
6.2 Introduction	93
6.3 Materials and Methods	94
6.3.1 Polylactic acid/hydroxyapatite composite fabrication.....	94
6.3.2 Degradation in vitro.....	95
6.3.3 Mechanical evaluation	95
6.3.4 Weight loss and water absorption.....	96
6.3.5 Scanning electron microscopy (SEM).....	96
6.4 Results & discussion	96
6.4.1 Mechanical properties.....	96
6.4.2 Physiological evaluations	102
6.4.3 Scanning electron microscopy of fracture surface.....	107
6.5 Conclusions	110
References	112
Chapter 7: Accelerated <i>In Vitro</i> Study of Surface Modified Hydroxyapatite (HA) Reinforced Polylactic Acid Composite: A 56 Day Study.....	114
7.1 Chapter 7 Abstract.....	114
7.2 Introduction	115
7.3 Materials & Methods.....	116
7.3.1 Materials	116
7.3.2 Methods	116
7.4 Results	117
7.4.1 Mechanical evaluation	117
7.4.2 Mass retention	119
7.4.3 Visual examination.....	119

7.4.4 <i>Geometric examination and water absorption</i>	120
7.4.5 <i>pH evaluation</i>	120
7.5 Discussion	121
7.5.1 <i>Accelerated degradation procedure</i>	121
7.5.2 <i>Mechanical evaluation</i>	122
7.6 Conclusions	123
References	125
Chapter 8: Parametric Analysis and Optimization of Orthopedic Interference Screws in Relation to Pullout Resistance	127
8.1 Chapter 8 abstract.....	127
8.2 Introduction	128
8.3 Materials and Methods	129
8.3.1 <i>Finite Element Model</i>	129
8.3.2 <i>Taguchi Method[®] for parametric study</i>	130
8.3.3 <i>Artificial Neural Network</i>	132
8.4 Results	133
8.5 Discussion	137
8.5.1 <i>FEA</i>	137
8.5.2 <i>Taguchi Method</i>	138
8.5.3 <i>Artificial Neural Network (ANN)</i>	139
8.6 Conclusions	140
References	141
Appendix I: Fabrication and Mechanical Evaluation of Hydroxyapatite and Polylactic acid (HA/PLA) Nanocomposites using Hot Pressing	143
A.1 Abstract	143
2.2 Introduction	144
A1.3 Materials and Methods	146
A1.3.1 <i>Hydroxyapatite nanofiber</i>	146
A1.3.2 <i>Polylactic acid</i>	147
A1.3.3 <i>HA nanofiber surface modification</i>	147
A1.3.4 <i>Hot pressing fabrication of PLA & HA/PLA</i>	148
A1.3.5 <i>Taguchi method</i>	150
A1.3.6 <i>Mechanical testing: three point bending</i>	151

<i>A1.3.7 Scanning electron microscope fracture surface</i>	152
A1.4 Results	153
<i>A1.4.1 Mechanical testing</i>	153
<i>A1.8.2 Scanning electron microscope</i>	156
A1.9 Discussion	157
A1.10 Conclusion.....	159
References:	161
Vita.....	165

LIST OF ILLUSTRATIONS

2.1 PLA in the form of pellets (size 1-3 mm diameter) for injection molding study prior to processing.....	14
2.2 Schematic diagram of a mixing tip used to enhance distribution and dispersion. This screw is considered in applications requiring significant mixing.....	15
2.3 Experimental setup for three point bending and flexural samples as molded in injection molding procedure.....	15
2.4 Experimental setup for tensile test and tensile samples designed to show the injection molding procedure for evaluation of tensile strength.....	16
2.5 Mechanical strength from injection molding design of experiment average flexural strength (▨) and average tensile strength (▩) NatureWorks Ingeo 3251	20
2.6 Response graph signal to noise ratio from injection molding design of experiment study.....	20
3.1 SEM images of hydroxyapatite as synthesized by wet chemical method	33
3.2 (a) Digital camera image of PLA pellets prior to milling; and (b) digital camera and (c) optical microscope images of PLA powder after milling and sieving procedure	34
3.3 The bending strength (a), bending modulus (a), tensile strength (b), and tensile modulus (b) of the pure PLA and PLA/HA composites filled with different HA nanofiber mass fractions.....	36
3.4 Stress versus strain relationship from tensile testing Pure PLA, 1 wt. % HA NF, 2 wt. % HA NF, 5 wt. % HA NF, 10 wt. % HA NF (a 1 percent strain is inserted for visualization purpose only) (a), and toughness energy and strain at failure of tensile tested HA nanofiber composites(b).....	37
3.5 SEM fracture surface morphology HA/PLA composite 0 wt% (a), 2 wt% (b), 5 wt% (c), and 10 wt% (d) demonstrating single nanofiber pullout (short white arrows), nanofiber bundle pullout (long white arrow), and fracture artifact pores (black arrows)..	38
3.6 Differential scanning calorimetry (DSC) of PLA and HA/PLA composite following processing and fabrication (+ denotes the T _g , and * denotes the T _m).....	39

4.1 Young's modulus (tensile) values of polylactic acid/hydroxyapatite composite containing 0 to 30 wt. % HA-w. Dashed line represents Young's modulus of pure PLA.....	62
4.2 The dependence of flexural strength and tensile strength on hydroxyapatite whisker (HA-w) mass fraction, flexural strength dry (◆), 24-hour immersion flexural strength (▲), dry tensile strength (■), and 24-hour immersion strength (●). Dashed line represents flexural and tensile strength of pure PLA in the dry state (*, *P= 0.05).....	63
4.3 SEM micrographs of polylactic acid/hydroxyapatite whisker composites and fracture surface from three –point bending test. (a) 5 wt% HA-w, (b) 10 wt% HA-w, (c) 20 wt% HA-w, and (d) 30 wt% HA-w.....	64
5.1 Flexural strength and modulus from 3-point bending HA/PLA composites containing various weight fractions of HA whiskers and nanofibers.....	83
5.2 Scanning electron microscopy of flexural fracture surface containing Hydroxyapatite whiskers and nanofibers a.) 30 wt% HA, b.) 40 wt% HA, c.) 50 wt% HA, d.) 60 wt% HA.....	85
6.1 Mechanical evaluation (Flexural and Tensile) with varying loading rates of HA through 24-week immersion in simulated body fluid 0 wt% HA, 5 wt% HA, 30 wt% HA, 50 wt% HA.....	98
6.2 Stress versus strain relationship following immersion 0 wt% HA, 5 wt%, 30 wt%, 50 wt% HA (1% separation added for visualization purpose): A. represents results at 0 weeks, B. at 8 weeks, C. at 16 weeks, and D. at 24 weeks.....	101
6.3 Cross-sectional area variations following immersion in simulated body fluid with various loading rates of HA 0 wt% HA, 5 wt% HA, 30 wt% HA, 50 wt% HA.....	103
6.4 Percentage water absorption of flexural bending specimens with varying loading rates of HA immersed in simulated body fluid after 24 weeks at 0 wt. % HA, 5 wt% HA, 30 wt% HA, and 50 w% HA.....	104
6.5 The dependence of mass retention on immersion time in PBS with various loading rates of HA filler: 0 wt%, 5 wt%, 30 wt%, and 50 wt%.....	105
6.6 The dependence of pH in the vicinity of degrading HA/PLA composites as they relate to immersion times at 0 wt% HA, 5 wt% HA, 30 wt% HA, and 50 wt% HA.....	106
6.7 Pure PLA tensile specimens degraded in PBS at 37 °C.....	107

6.8 Scanning electron microscopy of the fractured surface of bending specimens following mechanical evaluation A) 5 wt% HA–NF B) 30 wt% HA (5 wt% HA-NF/25 wt% HA-w), and C) 50 wt% HA (5 wt% HA-NF/45 wt% HA-w). Arrows depict single fiber pull-out, and circle shows HA nanofiber bundles.....	109
6.9 SEM fracture surface of 30 wt% HA whisker and nanofiber/polylactic acid composite. (Arrows refer to fiber, dashed arrows represent broken HA whisker, encircled areas represent holes from whisker pull-out, and hexagons highlight HA whisker facet unbroken).....	110
7.1 Variation of flexural strength with immersion time in PBS at 50 °C.....	118
7.2 Variation of mass with immersion in PBS at 50 °C	119
7.3 The pH variation over immersion intervals with various weight fraction HA	121
8.1 Setup for FEA pullout.....	130
8.2 Screw geometric parameters and detail of mesh.....	131
8.3 Maximum von Mises stress resulting from pullout of Screw 6.....	133
8.4 Signal to noise plots of the total von Mises stress at each level of each design parameter.....	134
8.5 Stress distributions between screw and bone thread geometry in screw (a) and bone (b).....	136
A1.1 Hydroxyapatite fibers created by wet chemical precipitation method.....	147
A1.2 The complete hot pressing procedure:: (A) Pure PLA pellets and methylene chloride solution are first added; (B) pellets are completely dissolved in methylene chloride solution (C) HA is mixed with PLA using ultra-sonic horn and mechanical assistance (D) Methylene chloride solvent forms an HA/PLA solution (E) Methylene chloride is evaporated using a vacuum oven (F) From vacuum oven HA/PLA emerges as a composite disk (G) Hot pressing procedure yields (H) mold removal and (I) samples are cut and tested in three point bending on universal texture analyzer.	149
A1.3 Schematic diagram of the three point flexural test designed according to ASTM standard D790.....	151

A1.4 Scanning electron microscope (SEM Quanta) used to image the fracture surface of HA/PLA composite.....	153
A1.5 Flexural strength from Taguchi method ® for processing study	154
A1.6 Flexural strength average from hot pressed samples of PLA with silane modified HA fibers.....	155
A1.7 Flexural modulus of PLA and HA/PLA for hot pressed samples.....	155
A1.8 Stress versus strain graph of high molecular weight PLA and HA/PLA for hot pressed samples where an offset of 0.025 was used for visualization purpose	156
A1.9 Scanning electron micrograph of fracture surface of hot press specimen under three point bending: (A) pure PLA (b) 5% HA (C) 10% HA (D) 15% HA (E) 20% HA (F) 25% HA	157

LIST OF TABLES

Table	Page
2.1 Experimental procedure using Taguchi design of experiment L16.....	18
2.2 Percentage contribution from Taguchi design of experiment on injection molding ...	21
3.1 Absolute viscosity measurements of PLA following milling and injection molding...	35
3.2 Thermal characteristics melting temperature (T_m), glass transition temperature (T_g), and crystallinity (X_c) of PLA and HA/PLA composites.....	40
6.1 Dependence of strain to failure of HA/PLA composite filled with various mass fraction hydroxyapatite.....	100
7.1 The cross section and water absorption variation of HA/PLA composite immersed in PBS at 50 °C.....	120
8.1 Geometric parameters of screws	132
8.2 Percentage contribution of thread geometric parameter to screw and bone maximum stress.....	135
8.3 Maximum von Mises stress in screw and bone from finite element analysis.....	135
A1.1 Parameters evaluated for fabrication of HA/PLA composite using Taguchi method.....	151

LIST OF ABBREVIATIONS

HA- hydroxyapatite
HA NF- hydroxyapatite nanofiber
HA-w -hydroxyapatite whisker
CS- calcium sulfate
CaP- calcium phosphate
 β -TCP- beta tri calcium phosphate
PLA- poly lactic acid
PLLA- poly-L-lactic acid
PDLA- poly-D-lactic acid
SR-PLA- self-reinforced polylactic acid
 γ -MPS -methacryloxymethyltrimethylsilane
PEEK- polyetheretherketone
PGA- Polyglycolic acid
PLGA- poly (lactic-co-glycolic) acid
HDPE- high density polyethylene
PMMA- poly methyl methacrylate
FEA- finite element analysis
SEM- scanning electron microscope
DSC- differential scanning calorimetry
T_g- glass transition temperature
T_m- melting temperature
X_c- crystallization percent
PBS- phosphate buffered saline

**THE STUDY OF HYDROXYAPATITE REINFORCED POLYLACTIC ACID
COMPOSITES FOR ORTHOPEDIC APPLICATIONS**

Richard Joseph Lebens III

Dr. Hao Li, Dissertation Supervisor

ABSTRACT

Poly(lactic acid) and calcium phosphate ceramic composite are widely accepted in orthopedic fixation and are mainly replacing metal soft tissue fixation devices, such as interference screws and suture anchors. However, the critical disadvantages of poor biological properties and poor mechanical strength compared to metal devices have left much to be desired in bioabsorbable orthopedic implant materials. In order to develop a more ideal calcium phosphate based polymer composite material, we have conducted the following studies: i.) Synthesis of Hydroxyapatite nanofibers and microfibers (whisker), ii.) Fabrication and evaluation of HA/PLA composite's structure and processing methods, and iii.) An in-vitro immersion study of composite to simulate degradation behavior in vivo. After systematic evaluation and in depth analysis of the experimental results, it was concluded that: i.) the use of small loading rates of hydroxyapatite nanofiber, such as 5 wt%, significantly improve the mechanical strength and toughness, ii.) maintenance in mechanical strength was observed with 10 wt% hydroxyapatite nanofibers, 30 wt% hydroxyapatite whisker formed by molten salt method, and with 40 wt% hybrid composite of nanofiber and whisker (5 wt% HANF and 35 wt% HA whisker), iii.) in

vitro immersion demonstrated hydroxyapatite's viability in a simulated physiological condition maintaining strength after 24 weeks immersion with 5 wt% hydroxyapatite composite, with no substantial physical changes, and iv.) surface modification demonstrated strength retention of 25 wt% Hydroxyapatite hybrid composite in an accelerated immersion study. These substantial improvements in the present study may greatly impact the development of absorbable hydroxyapatite/Poly(lactic acid) (HA/PLA) composite for use in soft tissue fixation and likely experience the same improved biological properties with the high mass fraction of hydroxyapatite composites.

CHAPTER 1. GENERAL INTRODUCTION

1.1 Chapter 1 Abstract

Interference screws and suture anchors have widely been used for attaching soft tissue in arthroscopic surgery and sports medicine, such as for anterior cruciate ligament (ACL) reconstruction. It is estimated that there are as many as 400,000 cases of anterior cruciate ligament fixation [1-3] and 250,000 shoulder repairs [4] each year in the United States. Polymer-based screws and suture anchors for ACL reconstruction are quickly replacing metallic devices due to several advantages. Polymers offer less complicated revision surgeries, better postsurgical imaging, less removal operations, and significantly reduce the risk of graft damage [5-9]. The variety of bioabsorbable polymer interference screws and suture anchors made from polylactic acid (PLA), polyglycolic acid (PGA), and their copolymers (poly (lactic-co-glycolic) acid (PLGA)) are preferred materials by the majority of orthopedic surgeons. These bioabsorbable polymer implants, however, have suffered from implant fracture, fibrous defect after resorption, and well-documented inflammatory responses resulting from rapid degradation [10-16].

In order to address the aforementioned drawbacks, great efforts have recently been focused on the fabrication and development of PLA and PLGA-based composites incorporated with bioactive ceramics, such as hydroxyapatite (HA) [17-20], calcium sulfate (CS) [21, 22], or β -Tricalcium phosphate (β -TCP) [23]. Several brands of interference screws made of polymer composites, including Biocomposite Interference, Bio-Intrafix, Biolok Tapered, BioRCI-HA, BioSure HA, Biosteon Wedge, CompositTCP, Matryx, and Milagro BR, are commercially available in the market now. *In vitro* degradation tests revealed that the addition of HA into PLA can reduce the incidence of

foreign body response and inflammation reaction [24], while an *in vivo* study on small animal models have shown HA-PLA composites have excellent biodegradability and osteoconductivity [25]. Since 2008, *in vivo* studies on ovine animal models have revealed significantly increased bone formation and decreased inflammatory response with HA-PLA composite interference screws, in comparison with the standard polymer interference screws after 12 months [26] and 24 months [27] implantation. Clinical trial results with two year follow up also showed that no inflammatory response was noted in all the 40 patients implanted with BioRCI-HA (75% PLLA/25% HA) and Bilok (70% PLLA/30% β -TCP) composite interference screws [28].

The greatest challenge to such bioceramic polymer composites is that the mechanical strength of composites containing HA, CS or β -TCP particles or short crystal whiskers generally decreases after the addition of the ceramic phase, especially with mass fraction filler around 20-40%. With the addition of HA, CS or β -TCP particles or crystal whiskers, the PLA or other polymers become brittle [29-31], which have led to catastrophic failures during insertion [32, 33]. Experimental results indicated that a small mass fraction (5-10 wt%) of HA nanofibers (HANF), with great potential to improve the composites' biocompatibility and osteoconductivity, can improve mechanical strength, tensile strain at failure (toughness), and elastic modulus (rigidity) of PLA composite.

Compared to bioceramic particles and short whiskers used in existing bioresorbable composites, HA nanofibers, which are several times stronger than stainless steel, can provide a much better reinforcing effect. HA nanofibers also have the potential to provide a near ideal biocompatibility allowing the screws or anchors to support the patient's biological properties and thereby promote healing. The rationales for using

nanofibers instead of nanoparticles, microparticles, or microfibers are: 1) the mechanical strength of ceramic nanofibers can reach the maximum/theoretical value with nanoscale diameter; and 2) the load transfer is roughly proportional to the length (aspect ratio) up to a maximum value. Tooth [34-36], bone [37, 38], and shell [39, 40] are all nanocomposites in nature composed of nanoscale, hard, inorganic building blocks (minerals) in a soft organic matrix. The ultra-long nanofiber reinforced composites have mechanical properties superior to those containing spherical nanoparticles or short nanofibers. Compared to the pure PLA control, the bending strength, tensile strength and elastic modulus of 5 wt% HA/PLA composites were increased by 45.8%, 23.3% and 40.0%, respectively

A relatively high loading rate of HA and/or TCP has proven to be crucial in eliminating inflammatory responses, stimulate bone growth (improve osteoconductivity), and also improve the rigidity of bioabsorbable implants [26, 28, 41]. However, it has also been well accepted that there is a very small percolation threshold for nanomaterials in polymer composites, beyond which the addition of more nanomaterials inevitably degrades the mechanical strength of the polymer composites [42, 43]. In the present study, the increase in mechanical strength, with the addition of HA nanofibers, was limited to 5 wt%. This indicates that this composite is coming close to this percolation threshold. With 10 wt% HA NF, the mechanical reinforcement is diminished, although the modulus is greatly improved.

In the present study, HA nanofibers, alone, cannot achieve a high HA mass fraction for optimized biological properties and desired rigidity. As a result, microsized HA should be used to achieve a high mass fraction. HA microfibers were chosen in this

study for their better reinforcing properties compared to microparticles. The most popular method of fabrication of HA microfibers (whiskers) are hydrothermal (wet chemical) methods, which can generate whiskers of $2.3 \pm 0.8 \mu\text{m}$ in diameter and $18.0 \pm 8.9 \mu\text{m}$ long [29]. Nanofibers made with the hydrothermal method at low temperature are very strong because their strength is not sensitive to defects, but microfibers made at such conditions may have many defects and much lower strength [44]. Compared to hydrothermal hydroxyapatite whiskers (HA-w), HA-w made at $1190 \text{ }^\circ\text{C}$ can provide much better reinforcing effects. As an example, hydrothermal HA whiskers in PEEK led to a 57.8% loss in tensile strength and 92.3% loss in strain to failure [30]. With samples of 25 wt% HA whiskers made at $1190 \text{ }^\circ\text{C}$ in PLA, the flexural strength increased to 109.3 MPa from 95.5 MPa, representing a 14.8% increase from the pure specimen; the tensile strength decreased to 60.0 MPa from 65.0 MPa, an 8.3% decrease; and the elastic modulus increased to 5.3 GPa from 3.4 GPa, a 44.2% increase.

In order to increase the mass fraction of HA to improve biological properties, different sized HA microfibers and nanofibers were used. The maximum mass fraction without mechanical property degradation becomes higher as the void spaces from large fillers are filled with smaller fillers. It is hypothesized that the combination of HA fibers with diameters at $\sim 100 \text{ nm}$, $1\text{-}2 \mu\text{m}$, and $10 \mu\text{m}$ may lead to a composite with both superior biological properties and mechanical properties. The hypothesis is 1) the ultra-long and super strong HA nanofibers at small loading rate, such as 5%, will significantly improve PLA mechanical strength and toughness; 2) the HA nanofibers, made of biomimetic method inspired by bone mineralization with very large surface areas (for surface reactions) and some defects (less stable than HA made at elevated temperatures),

can significantly improve the composite biocompatibility and osteoconductivity; 3) the combination of HA nanofibers and microfibers may lead to a composite with high HA mass fraction for better biocompatibility and a modulus closer to cortical bone, and also superior toughness and strength for fewer catastrophic failures. With this hybrid composite construction, the increase in bending strength from 0 wt% (107.9 ± 4.1 MPa) HA to 30 wt% HA (119.4 ± 2.7 MPa) was 17.5%. Even with 60 wt% HA, the strength of the composite was 93.0 ± 2.4 MPa, a decrease of only 13.8%. The bending modulus at 60 wt% was greatly increased to 9.1 ± 0.4 GPa (165%) from 3.4 ± 0.1 GPa in pure PLA

This study will demonstrate how improvements in mechanical properties of hybrid composites can apply to a variety of bioabsorbable orthopedic implants. These improved implants can address different clinical needs with performance superior to existing devices. In order to validate the material for use as an orthopedic implant device, a better understanding of its materials' properties in physiological conditions is required. This is critically important as early success with increasing the strength of PLA using self-reinforcement were lost after immersion in physiological environment. Furthermore, it is necessary to maintain the improved biological properties, as described in literature, with increasing amounts of HA. This dissertation's research accomplished this goal with *in vitro* immersion and accelerated immersion testing using HA/PLA composites enhanced by the addition of 5 wt% HA nanofibers, thereby maintaining the flexural strength. Furthermore, 81.5% of the tensile strength was retained *in vitro* through 16 weeks, and 25 wt% HA samples retained 97.2% (115.2 ± 4.5 MPa) and 95.1% (105.4 ± 8.0 MPa) flexural strength at 28 simulated weeks. Another improvement was a stable pH

reading for the fluid in the vicinity of the PLA/HA composite throughout both the 24-week test and the 56-day accelerated test (52 weeks simulated).

With the promising results from the immersion of HA/PLA composites in physiological conditions, preliminary work focused on the development and optimization of orthopedic implantable devices through the development of improved interference screws. In order to maximize the benefits of this new hybrid composite, an interference screw thread geometry was designed to primarily resist pullout. Using the combination of finite element analysis (FEA), the Taguchi Method[®] and artificial neural network (ANN), the time spent in creating models and simulation was greatly decreased. In this study the parameters which have high impact on pullout strength were determined as minor diameter and screw half angle. Additionally, a decrease in the maximum stress in the bone and screw was achieved.

It is believed that hybrid HA/PLA composites will lead to a variety of bioabsorbable orthopedic implants that can address different clinical needs with performance superior to existing materials. With positive outcomes in the present study, developments in orthopedic fixation devices to improve patient outcome can now be considered in suture anchors and interference screws, as well as other bone screws and plates for craniofacial applications. In addition, the knowledge gained in this project will benefit research in other fields, such as hard tissue engineering, dental composites, and development of other fiber reinforced composites.

References

- [1] Murray, M.M., P. Vavken, and B. Fleming, *The ACL Handbook: Knee Biology, Mechanics, and Treatment*. 2013: Springer.
- [2] Arendt, E.A., *OKU orthopaedic knowledge update: Sports medicine 2*. Vol. 2. 1999: Amer Academy of Orthopaedic.
- [3] Vavken, P. and M.M. Murray, *Translational studies in anterior cruciate ligament repair*. Tissue Engineering Part B: Reviews, 2009. **16**(1): p. 5-11.
- [4] Kuhn, J.E., *Effectiveness of physical therapy in treating atraumatic full-thickness rotator cuff tears: a multicenter prospective cohort study*. Journal of Shoulder and Elbow Surgery, 2013.
- [5] Zantop, T., *Graft Laceration and Pullout Strength of Soft-Tissue Anterior Cruciate Ligament Reconstruction: In Vitro Study Comparing Titanium, Poly-D,L-Lactide, and Poly-D,L-Lactide–Tricalcium Phosphate Screws*. Arthroscopy: The Journal of Arthroscopic & Related Surgery, 2006. **22**(11): p. 1204-1210.
- [6] Middleton, J.C. and A.J. Tipton, *Synthetic biodegradable polymers as orthopedic devices*. Biomaterials, 2000. **21**(23): p. 2335-2346.
- [7] Warden, W.H., D. Chooljian, and D.W. Jackson, *Ten-year magnetic resonance imaging follow-up of bioabsorbable poly-L-lactic acid interference screws after anterior cruciate ligament reconstruction*. Arthroscopy: The Journal of Arthroscopic & Related Surgery, 2008. **24**(3): p. 370. e1-370. e3.
- [8] Pihlajamäki, H., J. Kinnunen, and O. Böstman, *In vivo monitoring of the degradation process of bioresorbable polymeric implants using magnetic resonance imaging*. Biomaterials, 1997. **18**(19): p. 1311-1315.
- [9] Disegi, J. and H. Wyss, *Implant materials for fracture fixation: a clinical perspective*. Orthopedics, 1989. **12**(1): p. 75.
- [10] AndreasWeiler, *Biodegradable Implants in Sports Medicine: The Biological Base*. The Journal of Arthroscopic and Related Surgery, 2000. **16**(03).
- [11] Ma, C.B., *Hamstring anterior cruciate ligament reconstruction: a comparison of bioabsorbable interference screw and endobutton-post fixation*. Arthroscopy: The Journal of Arthroscopic & Related Surgery, 2004. **20**(2): p. 122-128.
- [12] Bostman, O., *Foreign-body reactions to fracture fixation implants of biodegradable synthetic polymers*. Journal of Bone & Joint Surgery, British Volume, 1990. **72**(4): p. 592-596.

- [13] Weiler, A., *Foreign-Body Reaction and the Course of Osteolysis After Polyglycolide Implants For Fracture Fixation Experimental Study in Sheep*. Journal of Bone & Joint Surgery, British Volume, 1996. **78**(3): p. 369-376.
- [14] Busfield, B.T. and L.J. Anderson, *Sterile pretibial abscess after anterior cruciate reconstruction from bioabsorbable interference screws: a report of 2 cases*. Arthroscopy: The Journal of Arthroscopic & Related Surgery, 2007. **23**(8): p. 911. e1-911. e4.
- [15] Kwak, J.H., *Delayed intra-articular inflammatory reaction due to poly-L-lactide bioabsorbable interference screw used in anterior cruciate ligament reconstruction*. Arthroscopy: The Journal of Arthroscopic & Related Surgery, 2008. **24**(2): p. 243-246.
- [16] Konan, S. and F. Haddad, *A clinical review of bioabsorbable interference screws and their adverse effects in anterior cruciate ligament reconstruction surgery*. The Knee, 2009. **16**(1): p. 6-13.
- [17] Takayama, T., M. Todo, and A. Takano, *The effect of bimodal distribution on the mechanical properties of hydroxyapatite particle filled poly(L-lactide) composites*. Journal of the Mechanical Behavior of Biomedical Materials, 2009. **2**(1): p. 105-112.
- [18] Macarini, L., *Poly-L-lactic acid — hydroxyapatite (PLLA-HA) bioabsorbable interference screws for tibial graft fixation in anterior cruciate ligament (ACL) reconstruction surgery: MR evaluation of osteointegration and degradation features*. La Radiologia Medica, 2008. **113**(8): p. 1185-1197.
- [19] Kasuga, T., *Preparation and mechanical properties of polylactic acid composites containing hydroxyapatite fibers*. Biomaterials, 2001. **22**(1): p. 19-23.
- [20] Mathieu, L.M., P.E. Bourban, and J.A.E. Mason, *Processing of homogeneous ceramic/polymer blends for bioresorbable composites*. Composites Science and Technology, 2006. **66**(11-12): p. 1606-1614.
- [21] Murariu, M., *Polylactide compositions. Part 1: Effect of filler content and size on mechanical properties of PLA/calcium sulfate composites*. Polymer, 2007. **48**(9): p. 2613-2618.
- [22] Miroslaw Pluta, *Polylactide compositions. II. Correlation between morphology and main properties of PLA/calcium sulfate composites*. Journal of Polymer Science Part B: Polymer Physics, 2007. **45**(19): p. 2770-2780.
- [23] Stephane Aunoble, *Biological performance of a new beta-TCP/PLLA composite material for applications in spine surgery: In vitro and in vivo studies*. Journal of Biomedical Materials Research Part A, 2006. **78A**(2): p. 416-422.

- [24] David D. Hile, Stephen A. Doherty, and Debra J. Trantolo, *Prediction of resorption rates for composite polylactide/hydroxylapatite internal fixation devices based on initial degradation profiles*. Journal of Biomedical Materials Research Part B: Applied Biomaterials, 2004. **71B**(1): p. 201-205.
- [25] Hasegawa, S., *A 5-7 year in vivo study of high-strength hydroxyapatite/poly(L-lactide) composite rods for the internal fixation of bone fractures*. Biomaterials, 2006. **27**(8): p. 1327-1332.
- [26] Hunt, J. and J. Callaghan, *Polymer-hydroxyapatite composite versus polymer interference screws in anterior cruciate ligament reconstruction in a large animal model*. Knee Surgery, Sports Traumatology, Arthroscopy, 2008. **16**(7): p. 655-660.
- [27] *Arthex BioComposite Interference Screws for ACL and PCL Reconstruction*.
- [28] Tecklenburg, K., *Prospective evaluation of patellar tendon graft fixation in anterior cruciate ligament reconstruction comparing composite bioabsorbable and allograft interference screws*. Arthroscopy: The Journal of Arthroscopic & Related Surgery, 2006. **22**(9): p. 993-999.
- [29] Roeder, R.K., M.M. Sproul, and C.H. Turner, *Hydroxyapatite whiskers provide improved mechanical properties in reinforced polymer composites*. Journal of Biomedical Materials Research Part A, 2003. **67A**(3): p. 801-812.
- [30] Converse, G.L., W. Yue, and R.K. Roeder, *Processing and tensile properties of hydroxyapatite-whisker-reinforced polyetheretherketone*. Biomaterials, 2007. **28**(6): p. 927-935.
- [31] Wright-Charlesworth, D.D., et al., *In vitro flexural properties of hydroxyapatite and self-reinforced poly(L-lactic acid)*. Journal of Biomedical Materials Research Part A, 2006. **78A**(3): p. 541-549.
- [32] Weiler, A., *The influence of screw geometry on hamstring tendon interference fit fixation*. The American Journal of Sports Medicine, 2000. **28**(3): p. 356-359.
- [33] Weiler, A., *Biodegradable interference screw fixation exhibits pull-out force and stiffness similar to titanium screws*. The American Journal of Sports Medicine, 1998. **26**(1): p. 119-128.
- [34] Tesch, W., *Graded microstructure and mechanical properties of human crown dentin*. Calcif Tissue Int, 2001. **69**(3): p. 147-57.
- [35] Warshawsky, H., *Organization of crystals in enamel*. Anat Rec, 1989. **224**(2): p. 242-62.

- [36] Weiner, S., *Peritubular dentin formation: crystal organization and the macromolecular constituents in human teeth*. J Struct Biol, 1999. **126**(1): p. 27-41.
- [37] Landis, W.J., *The strength of a calcified tissue depends in part on the molecular structure and organization of its constituent mineral crystals in their organic matrix*. Bone, 1995. **16**(5): p. 533-44.
- [38] Landis, W.J., *Structural relations between collagen and mineral in bone as determined by high voltage electron microscopic tomography*. Microsc Res Tech, 1996. **33**(2): p. 192-202.
- [39] Kamat, S., *Structural basis for the fracture toughness of the shell of the conch Strombus gigas*. Nature, 2000. **405**(6790): p. 1036-40.
- [40] Currey, J.D., *Mechanical properties of mollusc shell*. Symp Soc Exp Biol, 1980. **34**: p. 75-97.
- [41] Macarini, L., *Poly-L-lactic acid — hydroxyapatite (PLLA-HA) bioabsorbable interference screws for tibial graft fixation in anterior cruciate ligament (ACL) reconstruction surgery: MR evaluation of osteointegration and degradation features*. La Radiologia Medica, 2008. **113**(8): p. 1185-1197.
- [42] Rong, M.Z., *Improvement of tensile properties of nano-SiO₂/PP composites in relation to percolation mechanism*. Polymer, 2001. **42**(7): p. 3301-3304.
- [43] Vaia, R.A. and H.D. Wagner, *Framework for nanocomposites*. Materials Today, 2004. **7**(11): p. 32-37.
- [44] Gao, H., *Materials become insensitive to flaws at nanoscale: lessons from nature*. Proc Natl Acad Sci U S A, 2003. **100**(10): p. 5597-600.

CHAPTER 2: THE APPLICATION OF TAGUCHI METHOD[®] OPTIMIZATION DESIGN OF EXPERIMENT TO DETERMINE SINGLE SCREW INJECTION MOLDING PARAMETERS FOR POLYLACTIC ACID COMPOSITES FOR ORTHOPEDIC APPLICATION

2.1 Chapter 2 Abstract

The use of bioabsorbable polymers in medical devices has grown in the past 30 years. While fabrication of these devices is mainly done by injection molding, the availability of good and substantial fabrication procedures using injection molding is not available. In the present study, injection molding was utilized to form bending and tensile specimens for mechanical evaluation. The Taguchi Method[®] was used to design experiments performed using an L16 orthogonal array to understand the effect of each molding parameter. From the Taguchi Method[®] experiment design, an optimal process was created, which resulted in a flexural and tensile strength 30.9% and 36.2% higher than that reported by the manufacturer. It also revealed the strong influence of injection speed and acceleration to mechanical strength. The use of injection molding in orthopedic medical devices should be strongly considered as it has proven to be a very reliable and convenient method for the fabrication of bioabsorbable polymer, especially for PLA-based devices, as shown in the present study.

Keywords: Injection molding, Taguchi Design of Experiment, Fabrication, Mechanical evaluation

2.2 Introduction

The use of polymers in orthopedic devices has had a positive impact on the quality of care in recent years. Poly(methyl methacrylate) (PMMA), first used in dental applications in 1936, was one of the first polymers used in a medical application [1]. Since its first use, the development of polymer biomaterials has expanded for use in other medical applications. In the past 30 years, polymer degradable biomaterials have been very attractive to orthopedic fixation applications starting with absorbable sutures made of polyglycolic acid (PGA) and polylactic acid (PLA) approved in the 1960s [2]. The main positive impacts of bioabsorbable polymer biomaterials are that they make non-imaging artifacts and do not require surgical removal. Such biodegradable materials have been used in fixation screws, plates and drug delivery systems in the orthopedic field [3]. Currently, approved biodegradable polymer biomaterials include poly(dioxane) (PDS), poly(trimethylene carbonate), poly(ϵ -caprolactone), polyglycolic, polylactic acid (PLA) and their copolymers [3]. In this category of biodegradable polymer biomaterials, PLA is one of the most significantly studied due to its high strength and biocompatibility.

Polylactic acid has demonstrated its value as a material for orthopedic fixation devices in applications such as interference screws, suture anchors and craniomaxillofacial screws and plates. These devices have had a positive impact on patient care and recovery. Unfortunately, limited information is available specifically for processing medical-grade polymers.

Medical devices made from the absorbable polymer, PLA, are commonly made using an injection molding technique. In the injection molding process, PLA is melted and a ram or screw type plunger is utilized to force molten plastic into a mold cavity.

Other methods for fabrication of PLA and PLA composites developed in research are hot pressing or extrusion to plates or bars followed by machining to final dimensions, and casting according to final device geometry. Unfortunately, limitations of researched fabrication methods sometimes lead to an imperfect model for final device manufacture.

Numerous studies have focused on the fabrication of PLA due to its sensitivity to temperature and the processing method. However, limited work with injection molding has been studied, despite the fact it is the most prevalent fabrication method for PLA medical devices. Limited data on parameter effects during injection molding, such as injection molding speed and acceleration, is published.

In the present study, mechanical testing specimens were created with the injection molding procedure in order to understand its impact on the fabrication of medical devices. Injection molding parameters were optimized using the Taguchi Method[®]. Parameter percent contributions are examined to form an optimal fabrication method. Based on the present study, a recommended fabrication method is assessed.

2.3 Materials and Methods

Commercially available polylactic acid (PLA), Ingeo[™] 3251—an injection molding grade, was used in this study (NatureWorks, Minnetonka, MN, USA) This grade of PLA is a non-medical grade used to optimize processing.

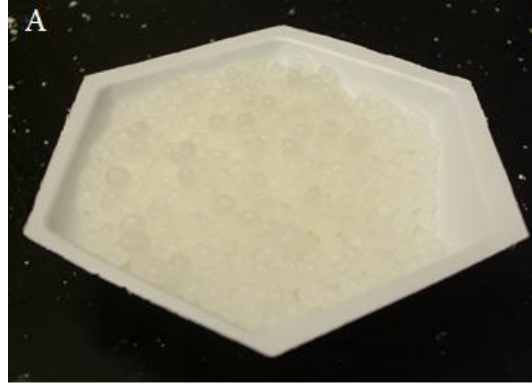


Figure 2.1. PLA in form of pellets (size 1-3 mm diameter) for injection molding study prior to processing

2.3.1 Injection Molding Procedure

In the present study, ASTM D638 dumbbell shaped specimens were made for tensile testing, and flexural test specimens were made for three point bend testing [4, 5]. Both test specimens were created with a two-part design mold, where half the geometry is milled on each side. This mold type allows for easy removal and good quality parts. A family mold was used so that multiple samples may be made with one shot. Single screw injection molding in the present study is similar to the conventional injection molding techniques used by Altpeter et al. [6]. In a typical fabrication procedure, polylactic acid (PLA) resin was introduced into the barrel where a combination of heat and screw RPM were utilized to allow the PLA polymer to flow and be fabricated into testing specimens. For this process, the screw RPM was set to 200 and barrel temperatures were set to 330 °F (rear), 350 °F (front), and 360° F (nozzle). In this injection molding process, velocity was used to control the injection at 1 in/sec. Furthermore, a mixing tip further enhanced the dispersion of filler materials for future study as seen in Figure 2. Once the PLA passed this mixing tip it was then forced through a nozzle with pressure into the mold to form the final part. A packing pressure was maintained for 12 seconds at 4,000 psi before part was removed from the mold [7-9].

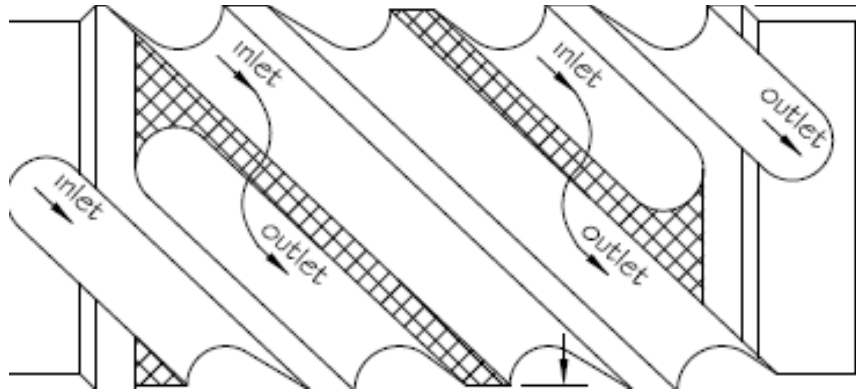


Figure 2.2. Schematic diagram of a mixing tip used to enhance distribution and dispersion. This screw is considered in applications requiring significant mixing.

2.3.2 Flexural testing

To evaluate the flexural modulus and strength of the fabricated PLA, three point bending tests were conducted using ASTM standard D790. The test involved loading of the specimen to failure at a constant rate of 5 mm/min using a span length of 20 mm in a three point bending fixture. Using an Instron 3367 (Instron, Grove City, PA, USA) universal testing machine, load was calculated using a 500 N load cell, and displacement data was obtained via cross-head motion to evaluate the ultimate flexural strength. Additionally, flexural modulus was obtained as the linear portion from the stress-strain curve.

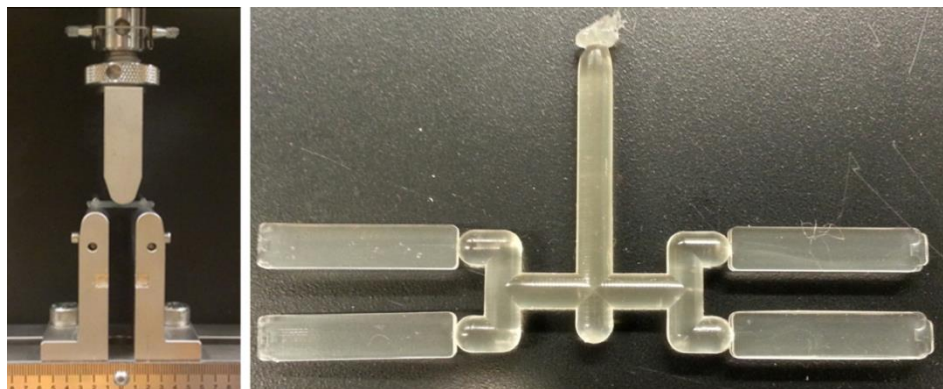


Figure 2.3. Experimental setup for three-point bending and flexural samples as molded in injection molding procedure for evaluation of flexural strength.

3.3.3 Tensile testing

Tensile strength was evaluated using ASTM standard D638 [4]. From this standard test specimen, type V was chosen. In this testing, load was measured using an Instron 3367 universal testing system (Instron, Grove City, PA, USA) with a 5000 N load cell, and strain was measured using a 7.62 mm strain gauge. The strain gauge used sharp knife edges to accurately measure the change in distance as the sample elongated. If samples were elongated past strain gauge maximal length, the cross head movement was used to measure displacement. From this test, an ultimate tensile strength was obtained, and tensile moduli were recorded.

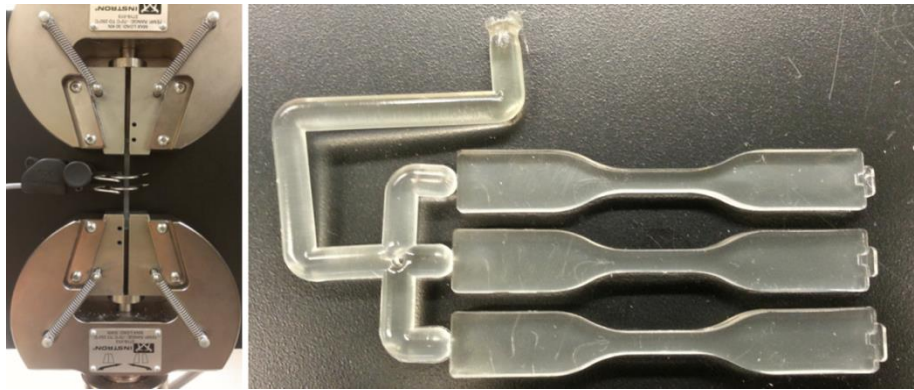


Figure. 2.4. Experimental setup for tensile test and tensile samples designed to show the injection molding procedure for evaluation of tensile strength

2.3.4 Taguchi Method® Design of Experiment

The Taguchi Method® for design of experiment (DOE) was used for control of the injection molding processing procedure. The objective value for the injection molding procedure was the bending strength and tensile strength of produced samples. In addition, a visual determination was also made for a good final product to ensure no voids or molding defects were formed. Parameters studied using the Taguchi method were barrel temperatures, injection speeds and accelerations, packing pressure, back pressure during

fill, and screw RPM. An L16 orthogonal array was chosen, which can handle up to 15 parameters, to study the flexural and tensile strengths produced by these processing techniques. From these experiments a percentage contribution was calculated which determined each parameter's overall impact on the material's final properties. To determine the effect of each of the variables, a signal to noise ratio was developed [10]. Furthermore, a percentage contribution was generated from the mean of each factor and from the change generated by the same signal from the 16 experiments. This change is representative of a response level for each factor. Following this, a sum of squares was calculated for each individual factor and used to find the percentage contribution.

$$SN = \sum_{i=1}^{n \text{ experiments}} \eta_i^2 \quad (1)$$

$$m = \frac{\sum_i^n \eta_i}{n} \quad (2)$$

$$Response = m_{A1} - m_{A2} \quad (3)$$

$$S_x = n_{A1}(m_{A1} - m)^2 + n_{A2}(m_{A2} - m)^2 + \dots \quad (4)$$

$$\rho = \frac{S_x}{S_{total}} * 100 \quad (5)$$

where n is the experiment number, A is the level, and i is the trial number [10-12].

After this processing, all parameters are maintained and unaltered to achieve uniformity in processing between samples. Parameters and factor levels for each experiment are shown in Table 2.1 and Figure 2.5.

Table 2.1. Experimental procedure using Taguchi design of experiment L16

Experiment	Rear Heater	Front Heater	Nozzle Heater	Inject step 1 Velocity	Inject step 1 Acceleration	Inject step 2 Velocity	Inject step 2 Acceleration	Inject step 3 Velocity	Inject step 3 Acceleration	Inject step 4 Velocity	Inject step 4 Acceleration	Packing Time (Set time)	Packing Pressure	Recovery Screw speed	Recovery Back Pressure
1	330	370	380	0.25	Normal	0.5	Normal	0.12	Normal	0.12	Soft	4	4000	120	200
2	330	370	380	0.25	Normal	0.5	Normal	0.25	Hard	0.25	Normal	12	10000	200	600
3	330	370	380	0.5	Hard	1	Hard	0.12	Normal	0.12	Soft	12	10000	200	600
4	330	370	380	0.5	Hard	1	Hard	0.25	Hard	0.25	Normal	4	4000	120	200
5	330	400	410	0.25	Normal	1	Hard	0.12	Normal	0.25	Normal	4	4000	200	600
6	330	400	410	0.25	Normal	1	Hard	0.25	Hard	0.12	Soft	12	10000	120	200
7	330	400	410	0.25	Normal	1	Hard	0.25	Hard	0.12	Soft	12	10000	120	200
8	330	400	410	0.5	Hard	0.5	Normal	0.25	Hard	0.12	Soft	4	4000	200	600
9	350	370	410	0.25	Hard	0.5	Hard	0.12	Hard	0.12	Normal	4	10000	120	600
10	350	370	410	0.25	Hard	0.5	Hard	0.25	Normal	0.25	Soft	12	4000	200	200
11	350	370	410	0.5	Normal	1	Normal	0.12	Hard	0.12	Normal	12	4000	200	200
12	350	370	410	0.5	Normal	1	Normal	0.25	Normal	0.25	Soft	4	10000	120	600
13	350	400	380	0.25	Hard	1	Normal	0.12	Hard	0.25	Soft	4	10000	200	200
14	350	400	380	0.25	Hard	1	Normal	0.25	Normal	0.12	Normal	12	4000	120	600
15	350	400	380	0.5	Normal	0.5	Hard	0.12	Hard	0.25	Soft	12	4000	120	600
16	350	400	380	0.5	Normal	0.5	Hard	0.25	Normal	0.12	Normal	4	10000	200	200

2.4 Results

The mechanical strength (flexural and tensile) results from the Taguchi design of experiment are summarized in Table 2.1. From the injection molding design of experiment, the maximum and minimum flexural strengths were 108.62 MPa and 78.09 MPa from experiments 1 and 15, respectively. The injection molding procedures represented in experiments 14 and 7 show a maximum tensile strength at 65.36 MPa and minimum flexural strength at 48.01 MPa. The average flexural strength and tensile strength reported by the manufacturer are 83 MPa and 48 MPa, respectively.

Figure 2.6 shows the influence of injection speeds and accelerations, packing pressure, screw recovery RPM, front temperature and nozzle temperatures—all affect the flexural and tensile strength of the final product. The largest effect was shown in injection molding speed and accelerations. The percentage contribution calculated is shown in Figure 2.7. The injection accelerations and speeds were the main contribution to flexural and tensile strength during processing showing a 97.1% contribution to flexural strength and 95.7 % contribution to tensile strength.

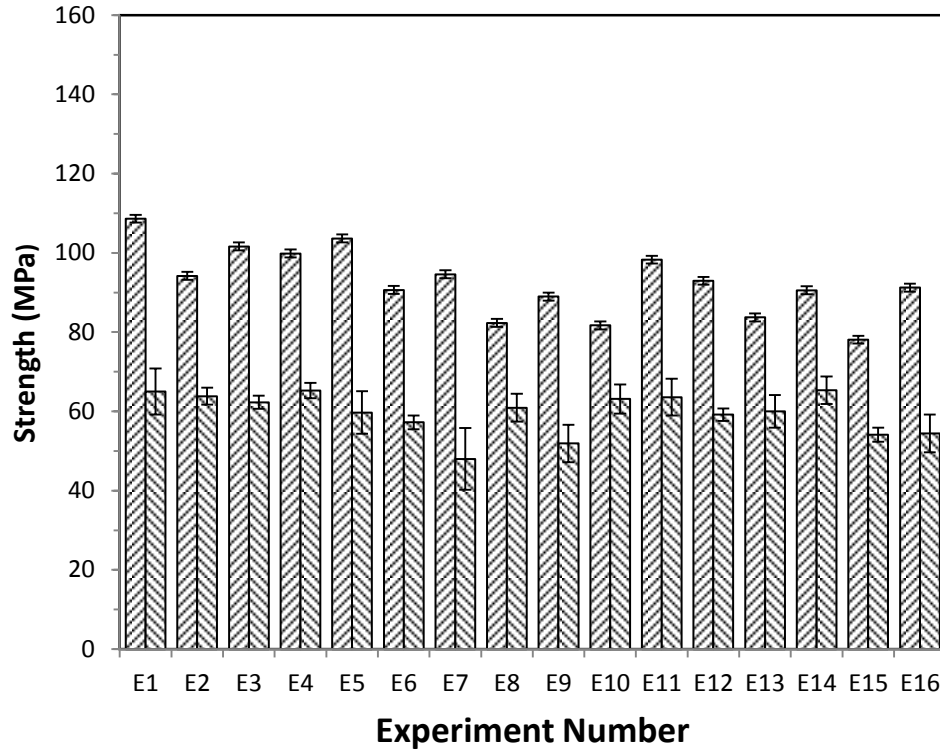


Figure 2.5. Mechanical strength from injection molding design of experiment average flexural strength (▨) and average tensile strength (▩) NatureWorks Ingeo 3251

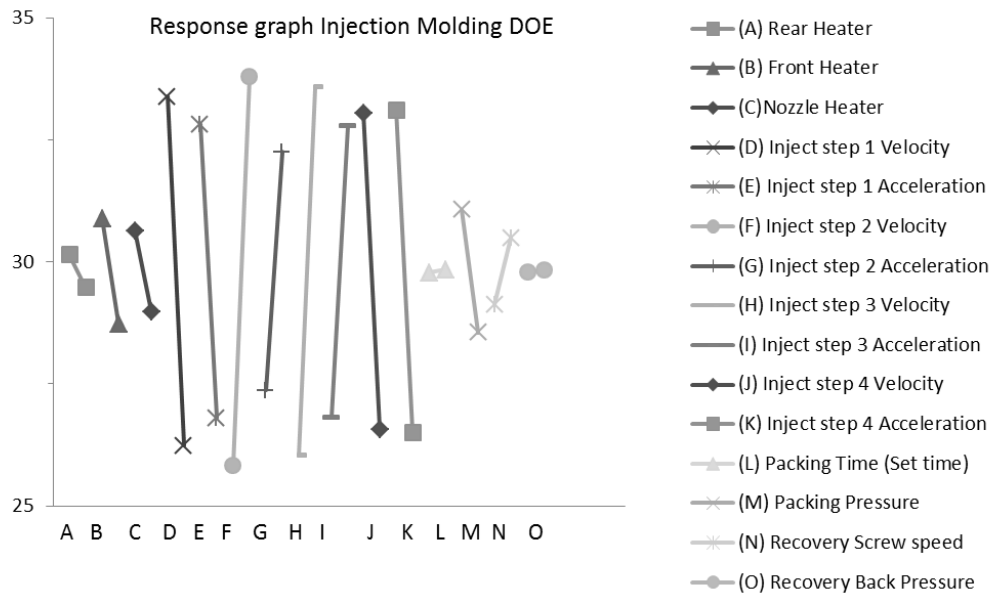


Figure 2.6. Response graph signal to noise ratio from injection molding design of experiment study.

Table 2.2. Percentage contribution from Taguchi design of experiment on injection molding

Parameter	Flexural Strength	Tensile Strength
Rear Heater	1.7	0.1
Front Heater	0.9	1.3
Nozzle Heater	0.1	0.8
Injection Velocity 1	12.7	13.4
Injection Acceleration 1	17.1	9.8
Injection Velocity 2	18.2	17.2
Injection Acceleration 2	11.1	6.5
Injection Velocity 3	8.2	15.4
Injection Acceleration 3	6.8	9.7
Injection Velocity 4	15.5	11.4
Injection Acceleration 4	7.5	11.8
Packing Time	0.2	0.0
Packing Pressure	0.0	1.7
Recovery Screw Speed	0.0	0.5
Recovery Back Pressure	0.1	0.0

2.5 Discussion

The main objective of the present study was to evaluate the influence of processing and fabrication techniques on the mechanical properties of PLA. Injection molding was chosen due to its high occurrence in industrial applications.

Control of the injection molding procedure for processing of polylactic acid has shown drastic increase in the flexural and tensile strength of the PLA. First, the temperature of the injection molding process was evaluated. This processing procedure revealed the sensitivity of the PLA to temperature as demonstrated by others. In this study, lower temperature was more desirable to enhance mechanical properties; however, low temperature can result in high pressure during injection cycle, which can result in flashing and poor part quality. Secondly, injection speeds and accelerations were studied and demonstrated a major contribution to the mechanical strength, i.e., 97.1% and 95.7%

for flexural and tensile, respectively. This was explained by velocity and accelerations that were used in this machine to control pressure in the injection cycle. Unlike controlling the pressure in conventional molding injection, speed and acceleration allow for good part quality from shot to shot where pressure was modified to maintain the speed or acceleration. Thirdly, the packing step was optimized in this processing procedure. This step was used to maintain a pressure following the injection cycle. In the present study, packing time suggested little impact on the mechanical properties. However, packing pressure data revealed that a lower packing pressure was desirable. Fourthly, a recovery step was used which replenishes the shot of polymer for the next shot. In the present study, limited impact was observed from the back pressure. However, the screw speed demonstrated a small impact on the strength. This is because the increased screw speed increases the rate at which the shot is recovered and decreases the time spent at elevated temperature. Additionally, higher screw speeds will facilitate further mixing of composites.

Many research methods for fabrication of PLA and PLA composites tend to have trouble with repeatability or iteration. The difficulty in getting consistent results may be explained by the sensitivity of the PLA to temperature in hot pressing applications, as observed by Ignjatovic et al. [13]. In Ignjatovic's study of PLA and HA, time and temperature data exhibited very different compressive strengths and moduli. Similarly, the variability in the bending and tensile strength using single screw injection molding with the NatureWorks Ingeo 3251 was observed. The variability in this experiment was from 78.1 MPa to 108.6 MPa in flexural strength and 48.6 MPa to 65.4 MPa in tensile strength based on experiments conducted in this study. This large variability in both

processing methods validated the need for processing optimization when using fabrication methods for PLA and other biodegradable polymer materials. The average strength from all experiments was 92.56 ± 8.52 MPa and 59.6 ± 5.2 MPa flexural and tensile, respectively. The small standard deviations over all the samples may show the reliability of injection molding process even with different processing parameters. Additionally, the optimal flexural strength recorded were 108.6 ± 6.0 , a 30.9 % increase from manufacture average value (83 MPa). Similarly, a 36.2 % increase was observed in tensile strength 65.4 ± 3.5 from manufacture average value (48 MPa). Though the values reported are averages, this information lends itself to the value of the Taguchi guidelines in developing the original research plan represented in this dissertation.

Furthermore, as expected, the injection molding processing parameter had a slight effect on the thermal transition temperatures, which was also observed by Mathieu et al. [14]. In the study by Mathieu, an observed decrease in both the T_g and T_m were seen with the incorporation of HA in PLA using higher temperature in the melt extrusion processing. The melt extrusion process used by Mathieu is similar to the injection molding screw portion in the current study, which displayed a decrease in melting temperature (T_m) and glass transition (T_g) temperature from 189.5 °C to 183.2 °C and 71.1 °C to 69.3 °C, respectively from previous work conducted by this investigator with a similar injection molding procedure.

The effect of thermal transition temperature can have an important effect on the adaptability of devices surgically placed in patients as indicated by the necessity to further control the preprocessing procedure as T_g has been shown to strongly influence the properties via in vivo testing as shown by Wong et al. [15].

2.6 Conclusion

PLA mechanical testing of specimens for bending and tensile strength tests were created using injection molding. This method was chosen as it is the most commonly used fabrication method and is considered repeatable and convenient. In the present study, the optimal processing condition revealed an increase of 30.9% and 36.2% in flexural and tensile strength, respectively, based on manufactured material properties. This success proved that optimizing the injection molding fabrication process is possible. With that in mind, the research plan for this project was to find a successful protocol. Additionally, the standard deviation from eight bending tested samples and six tensile tested samples was relatively low. This further supports the use of injection molding for medical implant materials to ensure product similarity between shots and parts. In the present study, the Taguchi Method[®] helped lay the foundation for design of experiments as we demonstrated how the injection molding speed and acceleration accounted for a 97.1% and a 95.7% increase in flexural and tensile strengths, respectively. PLA in this study demonstrated little sensitivity to temperatures used in the screw barrel and nozzle as predicted. Moreover, injection molding demonstrated its usefulness in this application by reducing the processing time substantially compared to other methods such as hot pressing. The combination of these benefits makes injection molding a near ideal processing method for fabrication of orthopedic fixation devices.

References

- [1] Feretis C, Benakis P, Dimopoulos C, Dailianas A, Filalithis P, Stamou KM, Manouras A, Apostolidis N: *Endoscopic implantation of Plexiglas (PMMA) microspheres for the treatment of GERD. Gastrointestinal Endoscopy* 2001, **53**(4):423-426.
- [2] Gilding DK, Reed AM: *Biodegradable polymers for use in surgery—polyglycolic/poly(actic acid) homo- and copolymers: 1. Polymer* 1979, **20**(12):1459-1464.
- [3] Middleton JC, Tipton AJ: *Synthetic biodegradable polymers as orthopedic devices. Biomaterials* 2000, **21**(23):2335-2346.
- [4] Standard Test Method for Tensile Properties of Plastics. *Annual Book of ASTM Standards* 2008.
- [5] *Standard Test Method for Determination of Modulus of Elasticity for Rigid and Semi-Rigid Plastic Specimens by Controlled Rate of Loading Using Three-Point Bending. Annual Book of ASTM Standards* 2002, **08**(01):4.
- [6] Altpeter H, Bevis MJ, Grijpma DW, Feijen J: *Non-conventional injection molding of poly(lactide) and poly(ϵ -caprolactone) intended for orthopedic applications. Journal of Materials Science: Materials in Medicine* 2004, **15**(2):175-184.
- [7] Menges G, Michaeli W, Mohren P: *How to make injection molds*, 3rd edn. Munich, Cincinnati: Hanser; Distributed in USA by Hanser Gardner Publications; 2001.
- [8] Isayev AI: *Modeling of polymer processing : recent developments*. Munich ; New York: Hanser Publishers ; Distributed in the United States of America and in Canada by Oxford University Press; 1991.
- [9] Malloy RA: *Plastic part design for injection molding : an introduction*. Munich ; New York Cincinnati: Hanser Publishers ; Hanser/Garnder Publications; 1994.
- [10] Taguchi GB, Chowdhury S, Wu Y: *Taguchi's quality engineering handbook*. Hoboken, N.J. Livonia, Mich.: John Wiley ; ASI Consulting Group; 2005.
- [11] Yang K, Teo E, Fuss F: *Application of Taguchi method in optimization of cervical ring cage. Journal of Biomechanics* 2007, **40**(14):3251-3256.
- [12] Fowlkes WY, Creveling CM: *Engineering methods for robust product design: using Taguchi methods in technology and product development*. Reading, Mass.: Addison-Wesley Pub. Co.; 1995.

- [13] Ignjatovic N, Suljovrujic E, Budinski-Simendic J, Krakovsky I, Uskokovic D: *Evaluation of hot-pressed hydroxyapatite/poly-L-lactide composite biomaterial characteristics. Journal of Biomedical Materials Research* 2004, **71B**(2):284-294.
- [14] Mathieu LM, Bourban PE, Månson JAE: *Processing of homogeneous ceramic/polymer blends for bioresorbable composites. Composites Science and Technology* 2006, **66**(11–12):1606-1614.
- [15] Wong S, Wu JS, Leng Y: *Mechanical Behavior of PLA/HA Composite in Simulated Physiological Environment. Key Engineering Materials* 2005, **288-289**:231-236.

CHAPTER 3: FABRICATION AND MECHANICAL EVALUATION OF POLYLACTIC ACID COMPOSITES CONTAINING HYDROXYAPATITE NANOFIBERS FOR ORTHOPEDIC APPLICATIONS

3.1 Chapter 3 Abstract

The objective of this research was to fabricate hydroxyapatite nanofiber (HANF) reinforced polylactic acid (PLA) orthopedic composites and investigate the influence of the HA nanofiber content on the mechanical properties of the resulting composites. An injection molding method was utilized to fabricate HANF/PLA composites with different mass fractions of HA nanofibers. The addition of very small mass fraction (1 wt%) of HA nanofibers into PLA matrix could effectively increase the bending strength by 37.8%. Compared to the pure PLA control, the bending strength, tensile strength and elastic modulus of 5 wt% HA/PLA composite were increased by 45.8%, 23.3% and 40.0%, respectively. Although scanning electron microscopy (SEM) revealed a generally well dispersed HA/PLA composite, some HA nanofiber bundles were not separated in processing and remained as bundles in the composite. Digital scanning calorimetry (DSC) revealed a decrease in transition temperatures following milling of PLA and injection molding of the composites with HA nanofibers. The substantial increases of the mechanical performance demonstrated in this study would encourage further device implementation study using HA nanofiber reinforced PLA composites for orthopedic fixation applications.

Keywords: *A. Nanocomposites, A. Polylactic Acid, A. Hydroxyapatite, B. Mechanical properties, E. Injection molding*

3.2 Introduction

Due to the advantages of less complicated revision surgeries, better postsurgical imaging, and avoiding removal operation [1-6], a variety of bioabsorbable polymer devices have been developed to replace metallic devices in the market [2, 7-10]. Most recently, polylactic acid (PLA) and other biodegradable polymers have demonstrated a great deal of success in reconstruction and repair of soft tissues in the knee and in the shoulder restoring a high-quality range of motion [7, 11-14]. Although PLA may be promising for future orthopedic fixation devices, it has demonstrated two critical flaws: 1) PLA exhibits low mechanical strength, which prevents its application on a high load bearing area or the PLA device has to be made with extra sizes to carry load as a sacrifice; 2) PLA alone has demonstrated poor biological response in clinical uses [15-17].

In order to compensate for these drawbacks, orthopedic devices have incorporated inorganic fillers such as β -Tricalcium phosphate (β -TCP) [18] and hydroxyapatite (HA) [19-22] to improve mechanical performance and biological response. Many studies have favored the use of hydroxyapatite because of its similarities to naturally occurring human bone, demonstrating increased bioactivity, biocompatibility and osteoconductivity [23-28]. *In vivo* studies on ovine models have revealed that significantly increased bone formation and decreased inflammatory response were achieved with HA micro particle reinforced PLA composite interference screws in comparison with the standard polymer interference screws [13, 29]. However, numerous attempts to increase mechanical performance experimentally via micro sized particles have presented limited improvement or even degradation in strength [23, 30-33]. Notable research in this area

includes the work by Kasuga et al. in which hydroxyapatite fibers (40-200 μm in length and 2-15 μm in diameter) demonstrated a maintained bending strength and an increased modulus [21]. Additionally, in the work performed by Shikinami and colleagues, bending strength was increased by 3.5% and modulus increased 89.2% with the addition of 50 wt% HA micro particles [10].

Aside from the critical disadvantage of HA/PLA composites continually displaying weak mechanical strength and toughness, the demand for bioabsorbable orthopedic implant composite materials is still growing. With an estimated 175,000 anterior cruciate ligament (ACL) reconstruction surgeries performed each year in the US [34], bioabsorbable polymers are fast becoming the most popular material for this ACL reconstruction procedure [7].

Furthermore, the majority of relevant studies have focused on the use of HA as micro sized particles and rods. PLA composites containing micro sized HA have demonstrated limited improvements in mechanical strength and toughness, but have shown increases in elastic modulus and biocompatibility at high filler loading [10, 21, 35, 36]. Hong et al. [33] used needle-like HA nanoparticles measuring 100 nm in length and 20-40 nm width thereby obtaining the sought after elastic modulus and biocompatibility in HA/PLA composites; however, they also observed decreases in tensile and bending strength with the addition of 10 wt% HA [33]. In the present study, HA nanofibers with a high aspect ratio were used and were made using a wet chemical method to reinforce the PLA matrix. The rationale for using 100 nm-long HA nanofibers is that ceramics reach their maximal/theoretical strength at the nanoscale size and the load transfer in composites is proportional to the fiber length or aspect ratio [37, 38]. This research

showed how the use of the nanosized fiber filler, as opposed to micro-sized particles and rods, can increase the load distribution between the hydroxyapatite nanofibers and polymer matrix, thereby increasing strength and toughness. Furthermore, biological properties and bioresorption may be improved due to increased surface area on HA nanofibers.

The objective of the present study was to evaluate the influence of HANF in a PLA matrix. HANF/PLA composites were prepared by injection molding without a controlled orientation. In the present study, HA nanofibers were first synthesized in a wet-chemical process and mixed with PLA resin. PLA resin and HANF were mixed, brought to a molten state with application of heat in an injection molding barrel, and shot with high pressure into tensile and bending molds where HANF/PLA composites solidified for mechanical testing. The addition of HA nanofibers was hypothesized to not only increase the mechanical strength, but also maintain the advantages of conventional HA/PLA composites.

3.3 Materials and Methods

3.3.1 Hydroxyapatite Nanofiber Synthesis

Hydroxyapatite nanofibers (HA NF) were fabricated in house by using a similar method reported by Liang Chen et al. [39]. In short, calcium nitrate (0.02 mol/L), sodium dihydrogen phosphate dihydrate (0.02 mol/L), gelatin (0.4 g/L), and urea (0.04 mol/L) (Sigma-Aldrich, St. Louis, MO, USA) were added into a glass beaker and dissolved in an aqueous solution at room temperature. Then, the solution was heated to 95 °C and maintained for 72 hours. Following this, the HA nanofibers were filtered, washed with

distilled water, and dried in an oven (Isotemp oven model 655f, Fisher Scientific, Agawam, MA, USA) at 100 °C for 12 hours.

3.3.2 HA/PLA Composite Fabrication

The commercial available Poly-L-lactic acid pellets (Purasorb, Purac Biomaterials, The Netherlands), approximately 1-4 mm in diameter, were milled at the highest setting for four three-minute intervals using a blender (Blendtec EZ-ES3, Blendtec, Orem, UT, USA). After that, the PLA powder was sieved by a sieve shaker model RX-29 (WS Tyler, Mentor, OH, USA) with USA standard test sieves mesh No. 35 (Hogentogler & Co, Columbia, MD, USA). This sieved powder was then mixed with HA nanofibers with different mass fractions such as 0, 1, 2, 5, and 10 wt% in a unitized jar mill model 755RMV (US Stoneware, East Palestine, OH, USA) to generate HA/PLA mixture. In the following step, the mixture was molded to bending test specimens with a 2.0 X 6.0 mm cross section (ASTM standard D5934) and tensile test specimens with a 3.2 X 3.2 mm cross section (ASTM standard D638) by injection molding machine (MiniJector model 45, Solon, OH, USA) at 190°C.

3.3.3 Characterization

3.3.3.1 Viscosity Measurement

The absolute viscosity of the original PLA pellets, milled PLA pellets and injected mold pure PLA was measured with Brookfield Model DV-II+ viscometer (Brookfield, Middleboro, MA, USA). PLA was firstly dissolved in chloroform at 6.8 wt% PLA. The viscometric studies were carried out at 20 RPM using spindle S25 at 30 °C

using a circulating bath (Cole-Palmer, Constant Temperature Circulator model 1267-62, Vernon Hills, IL, USA).

3.3.3.2 Mechanical Testing

The three-point bending (ASTM standard D5934) and tensile (ASTM standard D638) testing of pure PLA and HA/PLA composite samples was conducted using Instron 3367 universal testing equipment (Instron, Grove City, PA, USA) [40, 41]. The bending test was conducted using a 500 N load cell and three-point bending fixture with a 20 mm span length. In the tensile test, load was measured with a 5000 N load cell and strain was measured using a 7.62 mm strain gauge. All samples were tested to failure.

3.3.3.3 Morphology

Scanning electron microscopy (SEM) (FEI Quanta 600F environmental scanning electron microscope, FEI Co, Hillsboro, OR, USA) was employed to observe the HA nanofibers and the fracture surface of the bending samples of PLA and HA/PLA composites. Fractured samples were partially painted with silver conducting paint and platinum coated with sputter coater model EMS575X (Electron Microscopy Science, Hatfield, PA, USA) to resist charging effect, and a 5 kV acceleration voltage was used to image the fracture surface.

3.3.3.4 Differential Scanning Calorimetry (DSC)

Differential scanning calorimeter (DSC) Pyris™ 1 (Perkin-Elmer Corp., Norwalk, CT, USA), was used to determine the glass transition temperature (T_g), melt temperature (T_m), and degree of crystallinity (X_c) of the PLA and HA/PLA composite samples. The DSC specimens (10 to 12 mg) were placed in aluminum pans and run under

a flow of nitrogen (ASTM D7426) [42]. The following equation 4.1 was used to calculate the degree of crystallinity within the samples:

$$\% \text{ Crystallinity} = [\Delta H_m - \Delta H_c] / \Delta H_m^\circ \times 100\% \quad (4.1)$$

where ΔH_m is the measured endothermic enthalpy of melting and ΔH_c is the exothermic enthalpy that is absorbed by the crystals formed during the DSC heating scan. The theoretical melting enthalpy of 100% crystalline PLA was expressed as $\Delta H_m^\circ = 142 \text{ Jg}^{-1}$ as suggested by previous studies [43].

3.4 Results

Figure 4.1 shows the morphology and size of the HA nanofiber synthesized by the wet chemical method. As shown at low magnification SEM image (Figure 4.1a), the product consists of bundles of HA nanofiber with length ranging from 80-150 μm . The individual nanofiber width was observed at higher magnification (not shown here) to be about 100 nm similar to our previous results [39]. A relatively higher magnification image (Figure 4.1b) shows bundles of HA nanofiber composed of smaller HA nanofiber bundles.

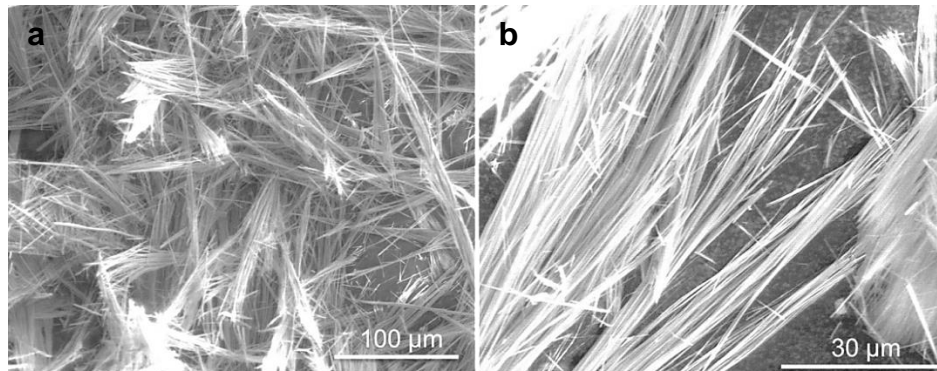


Figure 3.1. SEM images of Hydroxyapatite nanofibers synthesized by wet chemical method

Figure 3.2 shows the morphology and size of the original PLA pellets and milled PLA powders. It can be observed from the digital camera images that the size of as-

received PLA pellets (Figure 3.2a) ranges from 1 to 4 mm and much smaller PLA powders (Figure 3.2 b) are generated after the milling and sieving process. The optical microscope image (Figure 3.2c) with higher magnification (20X) shows the size of PLA powder, which ranges from 50 μm to 500 μm .

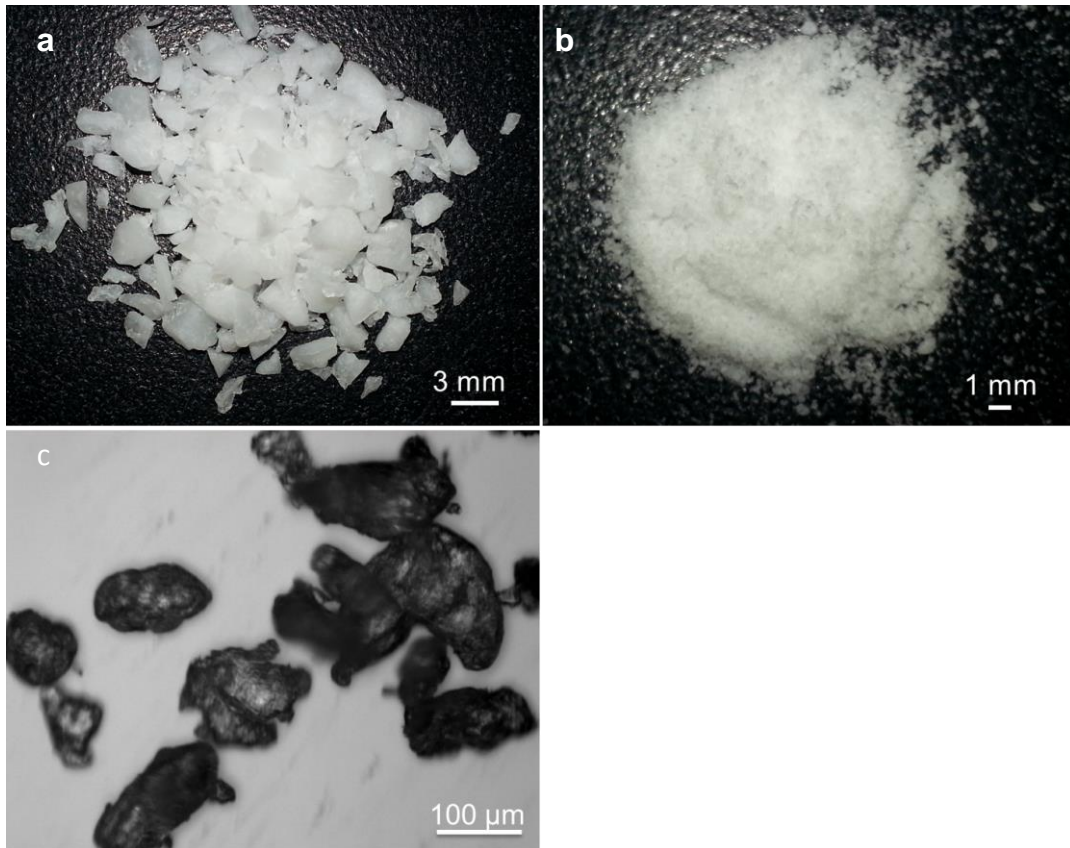


Figure 3.2. (a). Digital camera image of PLA pellets prior to milling; and (b) digital camera and (c) optical microscope images of PLA powders after milling and sieving procedure.

The viscometric studies of pure PLA following milling and injection molding are shown in Table 4.1. The control sample is pure PLA pellets prior to processing. As shown in Table 4.1, the absolute viscosity revealed a decrease in viscosity of 31.1% and 33.0% when PLA was milled and injection molded, respectively.

Table 3.1. Absolute viscosity measurements of PLA following milling and injection molding

Material	Viscosity (P)
PLA pellet	208.6 ± 4.0
Milled PLA	143.8 ± 43.5
Injection Molded PLA	139.8 ± 0.7

Figure 3.3 shows the influence of HA nanofiber content on the bending strength, bending modulus, tensile strength and tensile modulus compared to an unfilled PLA which was produced using the same process as the control.

The bending strength and modulus was increased compared to the Pure PLA control in every mass fraction. Figure 3.3a showed that the incorporation of 1 wt% HA nanofibers, a very small amount, into PLA matrix, which can significantly increase the bending strength from 96.5 ± 11.2 MPa to 132.9 ± 5.2 MPa, representing a 37.8% improvement. The bending strength peaks at 5 wt% HA to 140.7 ± 11.6 MPa (45.8%). Moreover, the bending strength at 10 wt% HA NF (130.9 ± 3.7 MPa) was only slightly lower than 5 wt% and still showed a 35.7% increase compared to the PLA control. The bending modulus (Figure 3.3a) increased greatly with every mass fraction from 3.1 ± 0.1 GPa for the PLA control to 4.8 ± 0.2 GPa for the samples with 10 wt% HA NF.

The tensile strength and modulus demonstrated similar improvements compare to the bending strength. The tensile strength (Figure 3.3b) showed that the incorporation of 2 wt% HA nanofibers, a very small amount, into PLA matrix could significantly increase the tensile strength from 54.0 ± 9.0 MPa to 70.0 ± 0.2 MPa (29.5%). However, increasing the mass fraction past 5 wt% HA did not further increase the mechanical strength.

Nevertheless, 10 wt% HA/PLA composite tensile strength still remained higher than the control by 7.7%. The tensile modulus displayed less drastic increases at 10 wt% loading from 3.8 ± 0.8 GPa to 4.21 GPa (12.0%) compared to the bending modulus.

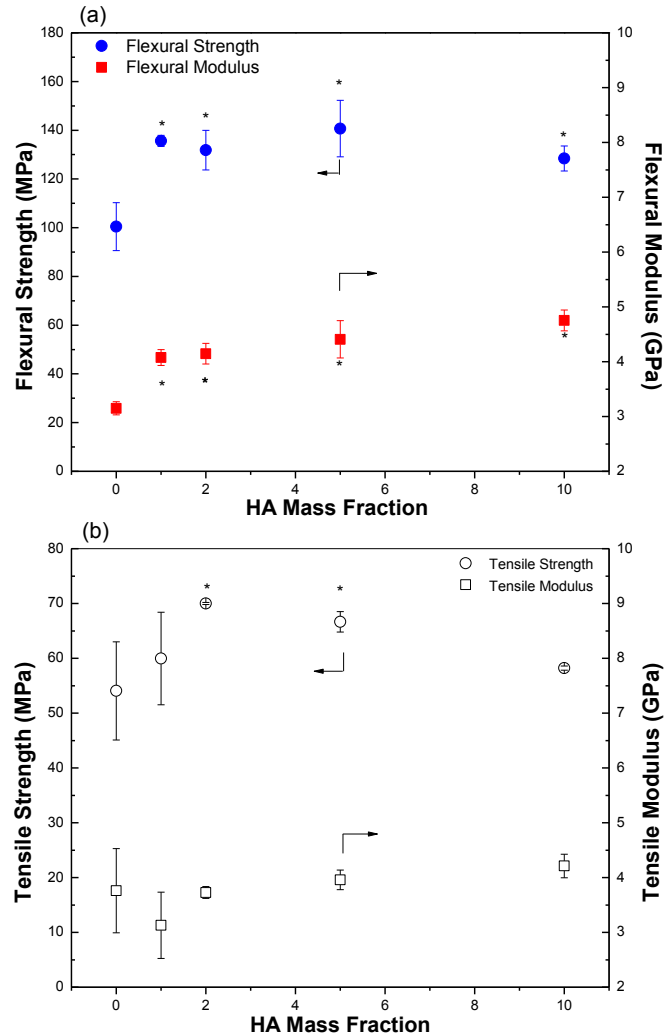


Figure 3.3 The bending strength, bending modulus (a) and tensile strength and tensile modulus (b) of the pure PLA and PLA/HA composites filled with different HA nanofiber mass fractions(*, $P < 0.05$).

Figure 3.4 depicts the typical stress versus strain relationship, calculated toughness energy, and strain to failure from tensile testing from each mass fraction HA NF. From the stress versus strain relationship an increase in strain at failure was observed, which is related to the material toughness and is shown in all samples up to 10

wt%. Additional correlation to material toughness can be drawn from a material toughness energy analysis, which is calculated from the area under the stress versus strain curve as the energy absorbed by the sample during mechanical testing. With the addition of low mass fraction of HA NF (1 wt% and 2 wt %), substantial increases in the toughness energy and strain at failure were observed. Particularly, the strain to failure of pure PLA ($1.7 \pm 0.6\%$) was increased by 64.7 % ($2.8 \pm 0.9\%$) and 94.1% ($3.3 \pm 0.6\%$) with 1 and 2 wt% HA NF, respectively. At 5 wt% HA NF the strain to failure and toughness energy are both lower than 2 wt% HA NF. However, a notable increase can be seen with 10 wt% HA NF, as strain at failure increased 535.3% ($10.8 \pm 5.6\%$) from pure PLA control. The toughness energy in every mass fraction was increased from 41.9 ± 20.0 mJ to 373.9 ± 196.0 mJ with 10 wt% HA NF.

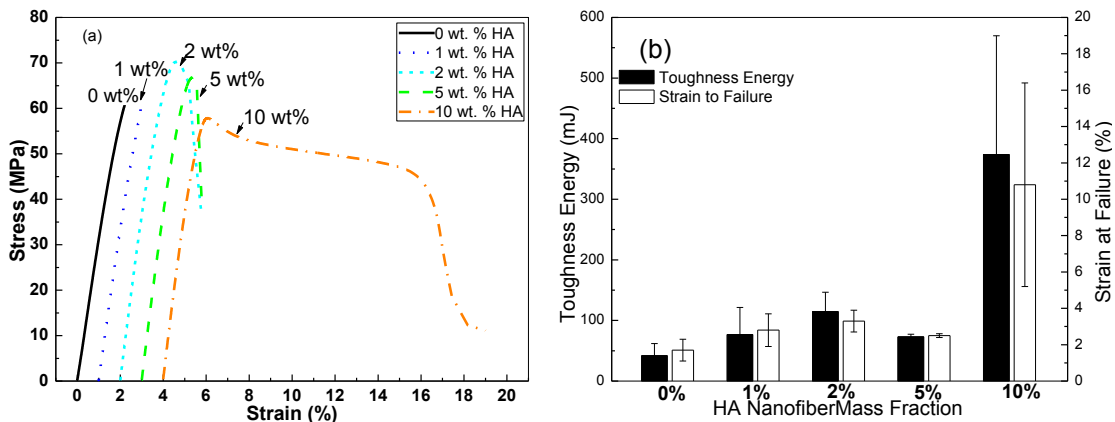


Figure 3.4. Stress versus strain relationship from tensile testing Pure PLA, 1 wt. % HA NF, 2 wt. % HA NF, 5 wt. % HA NF, 10 wt. % HA NF (a 1 percent strain is inserted for visualization purpose only) (a), and toughness energy and strain at failure of tensile tested HA nanofiber composites (b).

Figure 3.5 shows the SEM image of the HA NF/PLA fracture surface where single HA NF and HA NF bundles were observed in the PLA matrix. In addition to this dispersion of HA NF, some pullout of single nanofiber (short white arrow) and nanofiber bundles (long white arrow) were observed, also shown in Figure 3.5. As the mass fraction

of HA increases, the presence of HA nanofiber bundles also increases. Additionally, a pore artifact (Figures 3.5c and 3.5d) was only observed in composites with HA nanofibers (black arrows). Considering the similar size between the observed pore artifacts and HA nanofibers and related bundles, we speculated that the pore artifacts were generated by the fiber pullout. Similar phenomenon have also been reported by other researcher in cellulose/HDPE composites [44].

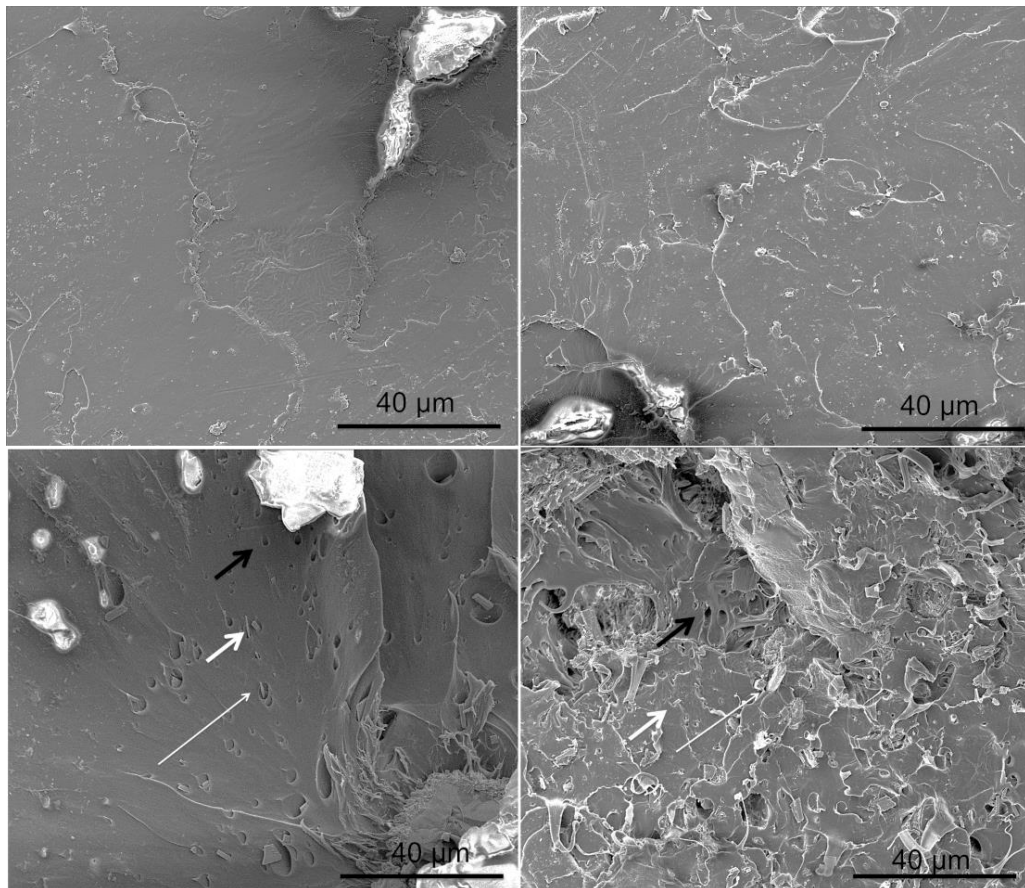


Figure 3.5. SEM fracture surface morphology HA/PLA composite 0 wt% (a), 2 wt% (b), 5 wt% (c), and 10 wt% (d) demonstrating single nanofiber pullout (short white arrows), nanofiber bundle pullout (long white arrow), and fracture artifact pores (black arrows).

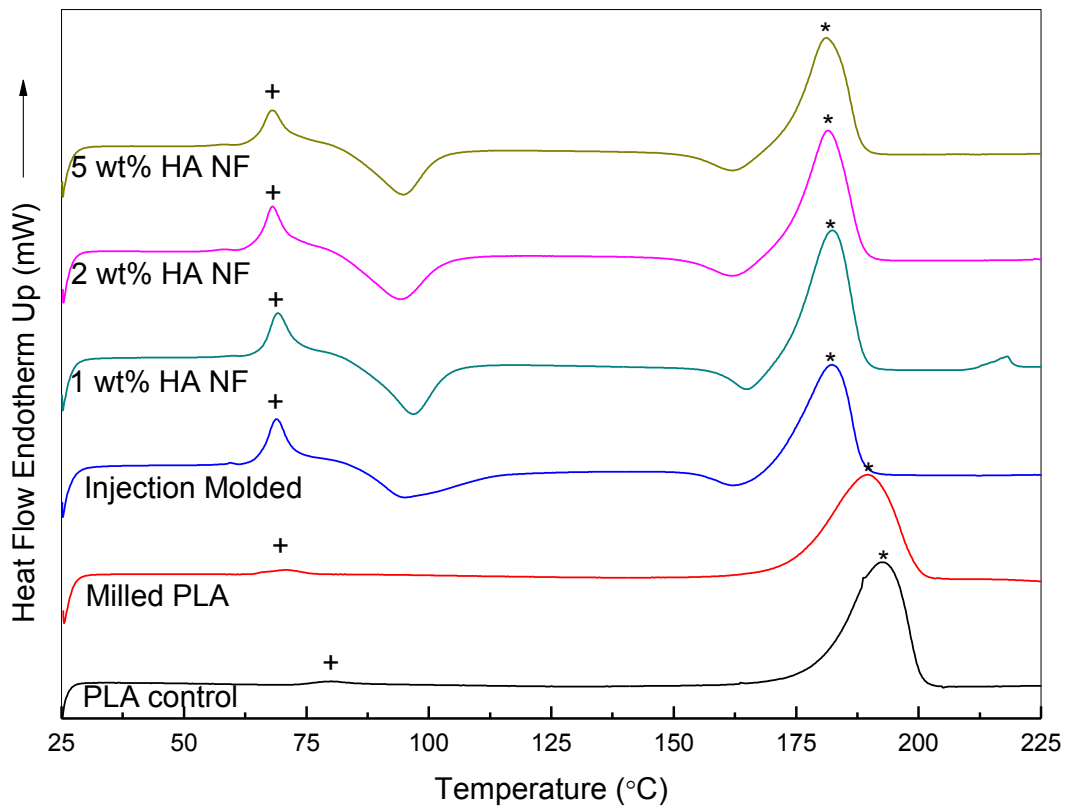


Figure 3.6. Differential scanning calorimetry (DSC) of PLA and HA/PLA composite following processing and fabrication (+ denotes the T_g, and * denotes the T_m)

Figure 3.6 shows the typical DSC thermographs of PLA and HA NF/PLA composite. The first observed peak denotes the glass transition temperature followed by the second peak denoting the melting temperature.

Table 3.2. Thermal characteristics melting temperature (T_m), glass transition temperature (T_g), and crystallinity (X_c) of PLA and HA/PLA composites

Material	T_m (°C)	T_g (°C)	X_c (%)
PLA pellet	193.8 ± 1.8	79.8 ± 0.3	47.0 ± 2.5
PLA milled	189.5 ± 0.1	71.1 ± 0.5	44.0 ± 0.1
PLA injection molded	183.2 ± 1.3	69.3 ± 0.5	49.1 ± 1.7
1 wt% HA injection molded	181.4 ± 1.3	68.2 ± 1.5	54.5 ± 0.3
2 wt% HA injection molded	181.9 ± 0.7	68.9 ± 1.2	52.0 ± 0.4
5 wt% HA injection molded	182.2 ± 1.6	68.6 ± 0.7	52.5 ± 0.4

Table 3.2 summarizes the result of DSC showing melting temperature (T_m), glass transition temperature (T_g), and crystallinity (X_c) of pure PLA and HA/PLA composites. As shown in Table 3.2, the primary influence in thermal transition temperature from processing was observed from the milling procedure, where the T_g was decreased from 79.8 °C to 71.1 °C. However, limited decrease was observed in the T_m following the milling procedure. Furthermore, the injection molding process further decreases the thermal transition temperatures T_g and T_m , as shown in Table 3.2 where injection molded PLA control T_m decreased from 189.5 °C to 183.2 °C from injection molding. Similarly, the T_g is decreased from 71.1 °C to 69.3 °C. The addition of HA to PLA demonstrated only small decreases in T_m and T_g .

The crystallinity as measured using Digital scanning calorimetry (DSC) was not substantially changed with processing or addition of HA nanofibers. The crystallinity of pure PLA pellets were $47.0 \pm 2.5\%$, milled 44.0 ± 0.1 , injection molded $49.1 \pm 1.7\%$, and with 5 wt% HA NF $52.5 \pm 0.4\%$.

3.5 Discussion

There are three main materials regions that make up any composite: the matrix, the reinforcement (filler), and the interfacial region. The matrix in the present study is the polylactic acid (PLA), and the reinforcement is the HA nanofiber. The interfacial region is between the matrix and the filler. The interfacial region is responsible for load transfer between the matrix and the filler. Polymer nanocomposites in contrast to conventional polymer composites differ due to increased number density making the processing and evaluation of polymer nanocomposites very important.

3.5.1 Polymer Nanocomposites Filler

The vast increase in mechanical strength, both bending (37.8%) and tensile (11.0%) with the addition of only 1 wt% HA nanofiber is an excellent indication of the advantages of HA nanofibers as opposed to micro-sized particles and rods which typically decrease the strength of the composites [10, 21, 35, 36]. We speculate that this is largely a result of the high strength HA nanofibers. At 100 nm diameter these nanofibers are estimated to have a strength of a few GPa as described by Yang [45] as the strength of ceramic fibers reaches their theoretical maximum at the nanoscale size. Additionally the high aspect ratio contributed to the reinforcement by carrying much of the load transfer through the polymer matrix. As the study of untreated HA nanoneedles with similar diameter by Hong could not demonstrate reinforcement due the very small length (100 nm). Furthermore, it is speculated that the quality dispersion at mass fractions as demonstrated in SEM likely contributed to the success of the composite reinforcement. Where, overall, the samples to 5 wt% HA NF demonstrated a good dispersion as observed through SEM (Figure 3.5) even though some bundles of nanofibers were not

separated in the milling procedure or preprocessing procedures. The dispersion of 5 wt% HA NF/PLA composite showed single HA nanofibers and nanofiber bundles that were similar compared to Kasuga et al. who demonstrated dispersion of micro sized HA rods via a solvent dispersion process using methylene chloride [21]. Without the use of solvents, the danger of residual toxic solvent was eliminated. Furthermore, HA NF/PLA composite dispersion followed a similar pattern as observed by Jonoobi et al. [46], who used micro-sized diameter cellulose fibers in a twin screw extrusion.

Additionally, this improvement in mechanical strength justified the milling procedure employed to fabricate this composite. The milling procedure of PLA pellets allowed for the good mixing of HA nanofibers likely due to the similarity in size between PLA powder and HA nanofibers and nanofiber bundles as shown in Figures 3.1 and 3.2. Without this preprocessing, large visible bundles of HANF were present in the composite. This non-uniform mixing in previous work (not shown here) was detrimental to the mechanical performance of the composite. Whereby, even small mass fractions of HA nanofiber could not achieve a reinforcement effect and even suffered from mechanical strength loss. In order to achieve similar dispersion of HA in the PLA matrix, solvent methods were required; however, replication of these methods could not match the reinforcement observed in the present study.

Non-uniform dispersion is a key problem in polymer nanocomposites specifically in the agglomeration of nano-sized fiber fillers which typically have a low percolation threshold (1-2%) [38]. As shown in Figure 1, the HA nanofibers as synthesized primarily form bundles. The processing of the PLA and HA NF composites has a critical importance to separate large bundles in order to achieve good mechanical strength. The

increases in strength were demonstrated to 5 wt% in the present study and could plateau between 5-10 wt%. From the present study, a plateau for mechanical strength between 5-10 wt% is an indication that the composite is near this threshold. Additionally the SEM of the 10 wt% showed a greater presence of HA NF bundles as pore artifact size and number increased. However, even at 10 wt% HA NF the strength increased from 0 wt% HA NF in both bending (35.7 %) and tensile (7.7 %).

In the present study, strain at failure increased by 87.7 % with only 2 wt% HA NF and increased more than five times (10.75 ± 5.64 %) with 10 wt% HA NF as shown in Figure 3.4. Increased strain at failure is a good indication of material toughness. This increase in strain at failure is uncharacteristic for ceramic composites using particles or microfibers as observed in literature [35, 36, 47-49]. Specifically, the use of 10 wt% micro fibrillated cellulose fiber by Suryanegara decreased the strain at failure by 71% in PLA [50]. Unfortunately, the high standard deviation with 10 wt% HANF in the present study suggests nonuniform dispersion at this mass fraction. Regardless of that, ceramic fillers typically result in decreased strain in response to failure and toughness tests; whereby ceramic composites typically demonstrate more brittleness as a strain response. Even at 10 wt% HA NF, a ductile response and substantial necking was observed. Furthermore, bending samples endured substantial displacement during the three point bending test and several were not broken. This was also observed by Shikinami et. al., however, the bending strength was not vastly improved [10]. The HA/PLA toughness, however, should be characterized further in impact loading environments to better understand HA/PLA composite toughness.

In addition to the improvements in bending and tensile strength, the bending modulus and tensile modulus were improved in every mass fraction reaching a peak of 10 wt% at HA nanofibers. Hong et al. demonstrated a 22% increase in modulus with the addition of 10 wt% HA nanoparticle needles [33]. Furthermore, Kasuga et al. observed a 21% increase in modulus with the addition of 10 wt% HA micro-sized fiber [21]. In the present study, the addition of 10 wt% HA nanofibers demonstrated a 50.1% increase in the bending modulus and 12.0% increase in the tensile modulus. However, the modulus of the composite at 5 wt% HA NF (4.4 ± 0.3 GPa) remained at the lower range of human cortical bone (3.5-18 GPa) [51] although when compared metal alternatives (100-200 GPa), the similarity to human cortical bone was definitely more pronounced and beneficial [8].

3.5.2 Polymer Matrix

DSC was primarily used to understand the changes in the PLA crystallinity through processing. The crystallinity (X_c) of the material after processing is very important to the device's final use. The values as calculated for pure PLA (47.0%) in the present study were similar to values calculated using DSC by Harris (41%), Shikinami (46%), Tasaka (55%), and others [10, 50, 52-54]. A polymer's crystallinity can not only have a strong impact on the mechanical strength of the composite, but it can also influence the polymer's degradation rate [55]. Additionally, increasing crystallinity has been used with success to improve mechanical strength such as the work by annealing PLA at elevated temperature for prolonged duration as shown in the research of Harris et al. [54]. However, with 40% increase in crystallinity, the bending strength increased 22%. In the present study, an increase in crystallinity of 5% or lower was observed from

milling and injection molding; hence, the increase in strength was more significant with 2 wt% HA NF (36.6 %), reinforcing the hypothesis that HANF/PLA composite is reinforced by nanofibers and not significantly influenced by crystallinity. Furthermore, the tensile strength was not significantly increased with crystallization of PLA, and the observed strain to failure was greatly decreased in pure PLA sample by 54% as observed by Suryanegara [50]. On the contrary, in the present study with every HANF mass fraction, the tensile strength and strain to failure was increased compared to PLA control.

The viscosity of PLA following milling and injection molding demonstrated a decrease of 31.1% and 33.0%, respectively which is similar to Garlotta's results following extrusion and injection molding [56]. With a correlation between viscosity of the polymer matrix the molecular weight and mechanical strength, it became clear that a substantial percentage of composites increased strength as a result of the nanofiber reinforcement and not as a result of processing. As with the decreased viscosity it was expected the strength would be similarly decreased.

In addition to crystallinity, DSC demonstrated the impact of processing procedures on glass transition temperature (T_g), and melting temperature (T_m). From the milling procedure alone, a decrease in the melting temperature and glass transition temperature was observed in a similar manner to Wong et. al. [57]. A drastic decrease in the T_g may impact the composite application in the human body at 37°C [57]. A decrease in the T_g to a similar level can make this composite more flexible depending on physiological conditions. This will dramatically impact the polymer's mechanical attributes in vivo and decrease the fatigue life. As noted by Wong et al., the ductility of HA/PLA composite (micro particles, 1 μm) is improved by immersion—not observed in

dry testing. HA/PLA composite tested by Wong was 43 °C [57]. Conversely, the preprocessing fabrication methods from pure pellet form to a 5 wt% HA NF composite injection molded specimen, the T_g decreased from 79.8°C to 68.6°C, which is still relatively higher than physiological temperature. However, the effect of the decrease in T_g from processing can be better characterized by immersion testing and mechanical testing in physiological conditions (37 °C).

Additionally, the melting temperature should also be monitored between the milling and molding procedure so that the injection molding processes can be tailored for specific compositions. In the present study, the melting temperature decreased 7.2 °C from processing with the addition of 5 wt% HA nanofibers.

3.5.3 Polymer Interfacial Region

The HA/PLA composite revealed not only a quality dispersion to 5 wt% HA nanofiber mass fraction, but also exhibited pullout which is an indication of the interfacial strength. In addition to nanofiber pullout, a pore artifact observed in the fracture surface (not present in the pure PLA control) is an indication of pullout as pores are similar in size in HA NF dispersion (as shown in nanofiber pullout areas of Figure 3.5) and in HA NF bundles. Similar observations were made by Daniella Mulinari using cellulose fibers in HDPE [44]. The limited pullout observed in the SEM fracture surface, however, demonstrates the need to improve the interface between PLA and HA NF. Coupling agents have been primarily employed to bridge the inorganic and organic components in the composite which should be investigated further [58-61].

3.5.4 Conclusions

Based on the promising result from the present study, a higher mass fraction HA NF may be considered. This higher mass fraction has demonstrated increased modulus as observed by Hasegawa and Ignatious et al. with micro sized HA [62, 63]. In addition to higher modulus, higher weight percentages of HA and/or β -TCP have proven crucial to the elimination of inflammatory responses and stimulation of bone growth in bioabsorbable implants [13, 64, 65]. In certain orthopedic fixation applications it may be beneficial to sacrifice superior mechanical strength for improved biological properties.

It is clear that new devices can have optimal performance with the given enhanced material properties. The results from the present study only considered the effect of fabrication on HA NF/PLA composites and not the effect of sterilization and shelf life. Beneficial and substantial increases in mechanical properties are demonstrated with the incorporation of hydroxyapatite nanofibers utilizing injection molding processing and fabrication.

3.6 Conclusion

The influence of HA nanofiber in PLA composite was found to provide excellent reinforcement. The 5 wt% HA NF/PLA composite displayed substantial increases in the bending strength (45.8 %), tensile strength (23.3%), and elastic modulus (40.0 %). This significant improvement helps to validate the hypothesis that high aspect ratio and high strength HA nanofibers can better facilitate load transfer in the polymer matrix. The strength of pure PLA was increased even with the addition of 10 wt% HA NF. However, SEM of the fracture surface revealed an increased presence of HA nanofiber bundles as the mass fractions was increased indicating a HA NF composite threshold. Furthermore,

in the present study HA NF/PLA composite experienced increased strain at failure and necking in the tensile samples which is typically not demonstrated on PLA or ceramic composite materials. This increase in toughness could lead to additional applications in the orthopedic fixation device field. Even with the increase in strength, the HA NF/PLA material is still not sufficient for fracture fixation applications in which bending strength similar to bone is required. It is with great optimism, however, that continued research in HA NF/PLA nanocomposites is planned as it represents a step toward continued use of PLA in orthopedic fixation devices to better facilitate uses in the soft tissue fixations where PLA is already used with success.

References

- [1] Zantop, T., *Graft Laceration and Pullout Strength of Soft-Tissue Anterior Cruciate Ligament Reconstruction: In Vitro Study Comparing Titanium, Poly-D,L-Lactide, and Poly-D,L-Lactide-Tricalcium Phosphate Screws*. *Arthroscopy: The Journal of Arthroscopic & Related Surgery*, 2006. **22**(11): p. 1204-1210.
- [2] Middleton, J.C. and A.J. Tipton, *Synthetic biodegradable polymers as orthopedic devices*. *Biomaterials*, 2000. **21**(23): p. 2335-2346.
- [3] Warden, W.H., D. Chooljian, and D.W. Jackson, *Ten-year magnetic resonance imaging follow-up of bioabsorbable poly-L-lactic acid interference screws after anterior cruciate ligament reconstruction*. *Arthroscopy: The Journal of Arthroscopic & Related Surgery*, 2008. **24**(3): p. 370. e1-370. e3.
- [4] Pihlajamäki, H., J. Kinnunen, and O. Böstman, *In vivo monitoring of the degradation process of bioresorbable polymeric implants using magnetic resonance imaging*. *Biomaterials*, 1997. **18**(19): p. 1311-1315.
- [5] Disegi, J. and H. Wyss, *Implant materials for fracture fixation: a clinical perspective*. *Orthopedics*, 1989. **12**(1): p. 75.
- [6] An Y., Woolf S., *IPre-clinical invivo evaluation of orthopedic bioabsorbable devices*. *Biomaterials*, 2000. **21**: p. 2635-2652.
- [7] Suchenski, M., *Material Properties and Composition of Soft-Tissue Fixation*. *Arthroscopy: The Journal of Arthroscopic & Related Surgery*, 2010. **26**(6): p. 821-831.
- [8] Daniels, A.U., *Mechanical properties of biodegradable polymers and composites proposed for internal fixation of bone*. *Journal of Applied Biomaterials*, 1990. **1**(1): p. 57-78.
- [9] Hanson, B., C. van der Werken, and D. Stengel, *Surgeons' beliefs and perceptions about removal of orthopaedic implants*. *BMC Musculoskeletal Disorders*, 2008. **9**(1): p. 73.
- [10] Shikinami, Y. and M. Okuno, *Bioresorbable devices made of forged composites of hydroxyapatite (HA) particles and poly-L-lactide (PLLA): Part I. Basic characteristics*. *Biomaterials*, 1999. **20**(9): p. 859-877.
- [11] Weiler, A., *Biodegradable interference screw fixation exhibits pull-out force and stiffness similar to titanium screws*. *The American Journal of Sports Medicine*, 1998. **26**(1): p. 119-128.

- [12] Andreas Weiler, *Biodegradable Implants in Sports Medicine: The Biological Base*. The Journal of Arthroscopic and Related Surgery, 2000. **16**(03).
- [13] Hunt, J. and J. Callaghan, *Polymer-hydroxyapatite composite versus polymer interference screws in anterior cruciate ligament reconstruction in a large animal model*. Knee Surgery, Sports Traumatology, Arthroscopy, 2008. **16**(7): p. 655-660.
- [14] Denard, P.J. and S.S. Burkhart, *The Evolution of Suture Anchors in Arthroscopic Rotator Cuff Repair*. Arthroscopy: The Journal of Arthroscopic & Related Surgery, 2013. **29**(9): p. 1589-1595.
- [15] Weiler, A., *Foreign-body reaction and the course of osteolysis after polyglycolide implants for fracture fixation experimental study in sheep*. Journal of Bone & Joint Surgery, British Volume, 1996. **78**(3): p. 369-376.
- [16] Busfield, B.T. and L.J. Anderson, *Sterile pretibial abscess after anterior cruciate reconstruction from bioabsorbable interference screws: a report of 2 cases*. Arthroscopy: The Journal of Arthroscopic & Related Surgery, 2007. **23**(8): p. 911.e1-911.e4.
- [17] Konan, S. and F. Haddad, *A clinical review of bioabsorbable interference screws and their adverse effects in anterior cruciate ligament reconstruction surgery*. The Knee, 2009. **16**(1): p. 6-13.
- [18] Stephane Aunoble, *Biological performance of a new beta-TCP/PLLA composite material for applications in spine surgery: In vitro and in vivo studies*. Journal of Biomedical Materials Research Part A, 2006. **78A**(2): p. 416-422.
- [19] Takayama, T., M. Todo, and A. Takano, *The effect of bimodal distribution on the mechanical properties of hydroxyapatite particle filled poly(L-lactide) composites*. Journal of the Mechanical Behavior of Biomedical Materials, 2009. **2**(1): p. 105-112.
- [20] Macarini, L., *Poly-L-lactic acid — hydroxyapatite (PLLA-HA) bioabsorbable interference screws for tibial graft fixation in anterior cruciate ligament (ACL) reconstruction surgery: MR evaluation of osteointegration and degradation features*. La Radiologia Medica, 2008. **113**(8): p. 1185-1197.
- [21] Kasuga, T., *Preparation and mechanical properties of polylactic acid composites containing hydroxyapatite fibers*. Biomaterials, 2001. **22**(1): p. 19-23.
- [22] Mathieu, L.M., P.E. Bourban, and J.A.E. Mason, *Processing of homogeneous ceramic/polymer blends for bioresorbable composites*. Composites Science and Technology, 2006. **66**(11-12): p. 1606-1614.

- [23] Furukawa, T., *Biodegradation behavior of ultra-high-strength hydroxyapatite/poly (l-lactide) composite rods for internal fixation of bone fractures*. *Biomaterials*, 2000. **21**(9): p. 889-898.
- [24] Calandrelli, L., *Biocompatibility studies on biodegradable polyester-based composites of human osteoblasts: A preliminary screening*. *Journal of Biomedical Materials Research*, 2002. **59**(4): p. 611-617.
- [25] Agrawal, C.M. and K.A. Athanasiou, *Technique to control pH in vicinity of biodegrading PLA-PGA implants*. *Journal of Biomedical Materials Research*, 1997. **38**(2): p. 105-114.
- [26] Rizzi, S.C., *Biodegradable polymer/hydroxyapatite composites: Surface analysis and initial attachment of human osteoblasts*. *Journal of Biomedical Materials Research*, 2001. **55**(4): p. 475-486.
- [27] Shikinami, Y., Y. Matsusue, and T. Nakamura, *The complete process of bioresorption and bone replacement using devices made of forged composites of raw hydroxyapatite particles/poly -lactide (F-u-HA/PLLA)*. *Biomaterials*, 2005. **26**(27): p. 5542-5551.
- [28] Ylinen, P., *Use of hydroxylapatite/polymer-composite in facial bone augmentation. An experimental study*. *International Journal of Oral and Maxillofacial Surgery*, 2002. **31**(4): p. 405-409.
- [29] *Arthex BioComposite Interference Screws for ACL and PCL Reconstruction*.
- [30] Wright-Charlesworth, D.D., *In vitro flexural properties of hydroxyapatite and self-reinforced poly(L-lactic acid)*. *Journal of Biomedical Materials Research Part A*, 2006. **78A**(3): p. 541-549.
- [31] Deng, X., J. Hao, and C. Wang, *Preparation and mechanical properties of nanocomposites of poly(d,l-lactide) with Ca-deficient hydroxyapatite nanocrystals*. *Biomaterials*, 2001. **22**(21): p. 2867-2873.
- [32] Liu, F., *Properties and morphology of bioceramics/poly(D,L-lactide) composites modified by in situ compatibilizing extrusion*. *Journal of Applied Polymer Science*, 2006. **102**(5): p. 4085-4091.
- [33] Hong, Z., *Nano-composite of poly(-lactide) and surface grafted hydroxyapatite: Mechanical properties and biocompatibility*. *Biomaterials*, 2005. **26**(32): p. 6296-6304.
- [34] Wasserstein, D., *Risk Factors for Recurrent Anterior Cruciate Ligament Reconstruction: A Population Study in Ontario, Canada, With 5-Year Follow-up*. *Am J Sports Med*, 2013. **41**(9): p. 2099-107.

- [35] Roeder, R.K., M.M. Sproul, and C.H. Turner, *Hydroxyapatite whiskers provide improved mechanical properties in reinforced polymer composites*. Journal of Biomedical Materials Research Part A, 2003. **67A**(3): p. 801-812.
- [36] Converse, G.L., W. Yue, and R.K. Roeder, *Processing and tensile properties of hydroxyapatite-whisker-reinforced polyetheretherketone*. Biomaterials, 2007. **28**(6): p. 927-935.
- [37] Gao, H., *Materials become insensitive to flaws at nanoscale: lessons from nature*. Proc Natl Acad Sci U S A, 2003. **100**(10): p. 5597-600.
- [38] Vaia, R.A. and H.D. Wagner, *Framework for nanocomposites*. Materials Today, 2004. **7**(11): p. 32-37.
- [39] Chen, L., *BisGMA/TEGDMA dental composite containing high aspect-ratio hydroxyapatite nanofibers*. Dental Materials, 2011. **27**(11): p. 1187-1195.
- [40] ASTM, *Standard Test Method for Determination of Modulus of Elasticity for Rigid and Semi-Rigid Plastic Specimens by Controlled Rate of Loading Using Three-Point Bending*. Annual Book of ASTM Standards, 2002. **08**(01): p. 4.
- [41] ASTM *Standard Test Method for Tensile Properties of Plastics*. Annual Book of ASTM Standards, 2008.
- [42] ASTM *D7426-08: Standard test method for assignment of the DSC procedure for determining TG of a polymer or an elastomeric compound*. ASTM book of standards 2008.
- [43] Tsuji, H., *Poly(lactide) stereocomplexes: formation, structure, properties, degradation, and applications*. Macromol Biosci, 2005. **5**(7): p. 569-97.
- [44] Mulinari, D.R., *Sugarcane bagasse cellulose/HDPE composites obtained by extrusion*. Composites Science and Technology, 2009. **69**(2): p. 214-219.
- [45] Yang, W., *Single-Crystal SiC Nanowires with a Thin Carbon Coating for Stronger and Tougher Ceramic Composites*. Advanced Materials, 2005. **17**(12): p. 1519-1523.
- [46] Jonoobi, M., *Mechanical properties of cellulose nanofiber (CNF) reinforced polylactic acid (PLA) prepared by twin screw extrusion*. Composites Science and Technology, 2010. **70**(12): p. 1742-1747.
- [47] Abu Bakar, M.S., *Tensile properties, tension–tension fatigue and biological response of polyetheretherketone–hydroxyapatite composites for load-bearing orthopedic implants*. Biomaterials, 2003. **24**(13): p. 2245-2250.

- [48] Kasuga, T., *Preparation of poly(lactic acid) composites containing calcium carbonate (vaterite)*. *Biomaterials*, 2003. **24**(19): p. 3247-3253.
- [49] Kasuga, T., *Preparation and mechanical properties of polylactic acid composites containing hydroxyapatite fibers*. *Biomaterials*, 2000. **22**(1): p. 19-23.
- [50] Suryanegara, L., A.N. Nakagaito, and H. Yano, *The effect of crystallization of PLA on the thermal and mechanical properties of microfibrillated cellulose-reinforced PLA composites*. *Composites Science and Technology*, 2009. **69**(7–8): p. 1187-1192.
- [51] Bayraktar, H.H., et al., *Comparison of the elastic and yield properties of human femoral trabecular and cortical bone tissue*. *Journal of Biomechanics*, 2004. **37**(1): p. 27-35.
- [52] Nam, J.Y., S. Sinha Ray, and M. Okamoto, *Crystallization Behavior and Morphology of Biodegradable Polylactide/Layered Silicate Nanocomposite*. *Macromolecules*, 2003. **36**(19): p. 7126-7131.
- [53] Tasaka, F., *Synthesis of comb-type biodegradable polylactide through depsipeptide-lactide copolymer containing serine residues*. *Macromolecules*, 1999. **32**(19): p. 6386-6389.
- [54] Harris, A.M. and E.C. Lee, *Improving mechanical performance of injection molded PLA by controlling crystallinity*. *Journal of Applied Polymer Science*, 2008. **107**(4): p. 2246-2255.
- [55] Pantani, R. and A. Sorrentino, *Influence of crystallinity on the biodegradation rate of injection-moulded poly(lactic acid) samples in controlled composting conditions, in Polymer Degradation and Stability*. 2012.
- [56] Garlotta, D., *A Literature Review of Poly(Lactic Acid)*. *Journal of Polymers and the Environment*, 2001. **9**(2): p. 63-84.
- [57] Wong, S., J.S. Wu, and Y. Leng, *Mechanical Behavior of PLA/HA Composite in Simulated Physiological Environment*. *Key Engineering Materials*, 2005. **288-289**: p. 231-236.
- [58] Šupová, M., *Problem of hydroxyapatite dispersion in polymer matrices: a review*. *Journal of Materials Science: Materials in Medicine*, 2009. **20**(6): p. 1201-1213.
- [59] Rakmae, S., *Physical properties and cytotoxicity of surface-modified bovine bone-based hydroxyapatite/poly(lactic acid) composites*. *Journal of Composite Materials*, 2010. **45**(12): p. 1259-1269.

- [60] Zhang, H.-p., *Molecular dynamics simulations on the interaction between polymers and hydroxyapatite with and without coupling agents*. Acta Biomaterialia, 2009. **5**(4): p. 1169-1181.
- [61] Zhang, S.M., *Molecular Modification of Hydroxyapatite to Introduce Interfacial Bonding with Poly (Lactic Acid) in Biodegradable Composites*. Key Engineering Materials, 2005. **288-289**: p. 227-230.
- [62] Hasegawa, S., *A 5–7 year in vivo study of high-strength hydroxyapatite/poly(L-lactide) composite rods for the internal fixation of bone fractures*. Biomaterials, 2006. **27**(8): p. 1327-1332.
- [63] Ignatius, A.A., *In vivo investigations on composites made of resorbable ceramics and poly(lactide) used as bone graft substitutes*. Journal of Biomedical Materials Research, 2001. **58**(6): p. 701-709.
- [64] Macarini, L., *Poly-L-lactic acid — hydroxyapatite (PLLA-HA) bioabsorbable interference screws for tibial graft fixation in anterior cruciate ligament (ACL) reconstruction surgery: MR evaluation of osteointegration and degradation features*. La Radiologia Medica, 2008. **113**(8): p. 1185-1197.
- [65] Tecklenburg, K., *Prospective evaluation of patellar tendon graft fixation in anterior cruciate ligament reconstruction comparing composite bioabsorbable and allograft interference screws*. Arthroscopy: The Journal of Arthroscopic & Related Surgery, 2006. **22**(9): p. 993-999.

CHAPTER 4: MECHANICAL EVALUATION OF POLYLACTIC ACID AND HYDROXYAPATITE COMPOSITES FOLLOWING 24-HOUR IMMERSION IN SIMULATED PHYSIOLOGICAL ENVIRONMENT

4.1 Chapter 4 Abstract

The motivation of the present study was to develop a stronger polymer composite to allow for more flexibility in the design of orthopedic interference screws. Current orthopedic fixation interference screws are prone to failure during insertion due to high initial loading. In order to develop a superior fixation device, an understanding of the composite's mechanical performance when dry and after immersion is vital. Hydroxyapatite (HA) was mixed with polylactic acid (PLA), in an injection molding process to create specimens for mechanical testing. Mechanical properties were evaluated through flexural and tensile tests. The specimens were tested both dry and after 24-hour immersion in phosphate buffered saline (PBS) at 37 °C in order to mimic body conditions. The fracture surfaces of the flexural samples were then evaluated using scanning electron microscopy (SEM) to evaluate dispersion and filler matrix interaction. With samples of 25 wt% HA, the flexural strength increased to 109.3 MPa, a 14.8% increase from the pure specimen; the tensile strength decreased to 60.0 MPa, an 8.3% decrease; and the elastic modulus increased to 5.3 GPa, a 44.2% increase. After the 24-hour immersion, the flexural strength of the 25 wt% sample remained stronger than the pure sample of PLA but decreased 10.6% from the dry state. SEM revealed well-dispersed HA throughout the polymer matrix at all mass fractions. The results indicate the potential for further use of hydroxyapatite in orthopedic soft tissue applications.

Keywords: *Polylactic acid, Hydroxyapatite, Mechanical evaluation, In vitro, immersion*

4.2 Introduction

Conventional metal orthopedic fixation devices have been used successfully to provide bone healing and union. Although metal implants exhibit superior mechanical strength, they often cause a mismatch in mechanical properties between healing bone and implant. One reason for this is the elastic modulus of bone ranges between 3-20 GPa, and the bending strength ranges between 140-270 MPa, while the elastic modulus for metal implants is 100-200 GPa, and 500-700 MPa, respectively [1]. This variation in mechanical properties can account for micro-motion and stress shielding effects which can lead to osteoporosis and nonunion. Consequently, there is a critical need for orthopedic biomaterials which more accurately resemble human bone mineral.

Since 1960, polylactic acid has been used as a bioabsorbable polymer implant material. Due to its superior biological properties, non-obstructive imaging, and elimination of surgical removal due to bioabsorption of anchors and screws PLA and other bioabsorbable materials have become a popular implant alternative. Kulkarni and colleagues were among the first to demonstrate nontoxic, non-tissue reactive, and slowly degrading PLA implants demonstrating their use in guinea pigs and rats in 1966 [2]. Presently in the orthopedic soft tissue fixation market, 55% of bioabsorbable suture anchors and 74% of interference screws are composed of PLA [3]. Unfortunately, these bioabsorbable polymer implants have suffered from implant fracture, fibrous defect after resorption, and well-documented inflammatory response resulting from rapid degradation [4-10]. Additionally, late foreign body reactions have been demonstrated as in the case observed by Bergsma [11].

In order to address the critical needs for bioabsorbable implants, research has recently focused on the fabrication and development of PLA composites incorporated with bioactive ceramics such as hydroxyapatite (HA) [12-15], calcium sulfate (CS) [16, 17], or β -Tricalcium phosphate (β -TCP) [18]. Hydroxyapatite (HA) has been widely used to reinforce orthopedic biomaterials in order to mimic the mechanical and biological properties of bone mineral [19]. HA is useful because it has the closest synthetic resemblance to the inorganic component of hard tissues, which composes 70% of human bone mineral and is made up of calcium-deficient and hydroxyl-deficient carbonate apatite [20, 21]. For this reason, composites containing HA typically exhibit high biocompatibility, bioactivity, and osteoconductivity [22-25]. Furthermore, HA is commonly used to reinforce polymer matrixes such as polyethylene, poly acrylics, polyesters, and polyether ether ketone (PEEK). Of these polymer biomaterials, the most commonly used in orthopedic soft tissue fixation applications is polylactic acid (PLA), which is a thermoplastic aliphatic polyester.

With the addition of HA to PLA, improved biocompatibility and osteogenic properties have been demonstrated by Calandrelli via the human osteoblast cell [26]. Additionally, this combination has been shown to buffer pH during material degradation and maintain physiological pH [27]. To supplement the biological advantages of the HA/PLA composition, additional research is required to develop a composite which also possesses mechanical properties similar to human bone for use in orthopedic biomaterials [8].

Relatively small increases in mechanical strength have been observed with the addition of HA and tricalcium phosphates, but are only demonstrated at low composite

mass fractions. A relatively high mass fraction of HA and/or TCP has proven crucial to eliminate the inflammatory responses and stimulate bone growth (improve osteoconductivity) [25, 28, 29]. Higher mass fractions of HA fillers near 30 wt% exhibit enhanced biological properties and increased elastic modulus, reaching similar levels noted within human cortical bone as demonstrated by Russias et al., but researchers have failed to increase the mechanical strength of the composite [30]. For this reason, ceramic composites with 25-30 wt% calcium phosphate mass fractions are the most popular in the orthopedic fixation market [3]. However, a critical problem arises for composites using high mass fraction HA due to non-homogeneous mixing and agglomerations. These dispersion issues result in poor mechanical strength due to void formation and large areas without the presence of ceramics [31, 32]. Another disadvantage of current orthopedic implant devices is the high rate of device failures during insertion [4, 33-36]. Biodegradation studies often omit a dry test in lieu of the 24-hour immersion test; however, both conditions are critical in the implant process. It is important to have a full understanding of the material properties at time of insertion as well as 24 hours after immersion when the patient is told he or she can stand or bear the initial loading.

It is critical that studies of mechanical evaluation use a method most similar to the industrial fabrication process. The fabrication method of HA/PLA composite in literature for mechanical evaluation are extrusion followed by machining, hot pressing [37, 38], cast forging [30], and injection molding[39]. Though the majority of commercial products are fabricated with a screw type injection molding, availability of research in the processing is limited. While researchers have made important developments in

fabrication methods, many contain flaws that make them unusable in medical devices such as the use of toxic solvent, methods which are infeasible for production rate, or methods where geometry may not precisely be controlled.

In the present study, HA whisker (HA-w) structure was prepared using a molten salt fabrication method with aspect ratio between 5-10 (length divided by width) in which stable whiskers were produced with a Ca/P ratio greater than 1.67 using a similar fabrication method described by Tas et al. [40]. The prepared whiskers were then dispersed in mass fractions between 0 and 30 wt% HA, and were injection molded to form bending and tensile specimens. To improve the dispersion of HA whiskers, additional mixing was performed during the injection molding setup.

4.3 Materials and Methods

4.3.1 HA whiskers and polylactic acid composite

In order to prepare hydroxyapatite polylactic acid composites, commercially available polylactic acid Ingeo™ 3251 (NatureWorks LLC ©, Minnetonka, MN, USA) was first milled in a cryogenic milling procedure. This was done by first immersing the PLA pellets into liquid nitrogen in a stainless steel blender. Following this the pellets were milled at the highest setting for four three-minute intervals, adding more liquid nitrogen between intervals. After milling, the produced powder was collected under 500 µm using USA standard test sieve (size No. 35) made by Hogentogler & Co, Columbia, MD, USA) in a sieve shaker model RX-29 (WS Tyler, Mentor, OH, USA). Following the milling PLA powder was stored at 4°C to reduce the amount of moisture in the PLA powder.

Hydroxyapatite nanoparticles were first synthesized in a wet precipitation method using calcium nitrate, sodium phosphate and ammonium hydroxide [41, 42]. A molten salt synthesis (MSS) similar to that used by Tas et al. produced whiskers with a length and width of 10-20 μm and 2-5 μm , respectively. The HA nanoparticles and potassium sulfate salt was well mixed and combined in a combustion boat. The boat was placed in furnace ST-1600C-888 (Sentro Tech, Strongsville, OH, USA) at 1190 °C. The salt and HA were removed from the combustion boat and washed six times with DI water to remove all salt.

HA whiskers from 0 to 30 wt% and PLA powder were combined in a unitized jar mill model 755RMV (US Stonewares, East Palestine, OH, USA) and injection molded into tensile and flexural samples for mechanical evaluation (MiniJector model 55E, Solon, OH, USA). Bending plates were produced with width, thickness and length of 6.0 mm, 2.0 mm and 25.0 mm, respectively. Additionally, tensile dumbbell specimens were produced with a gauge length cross section of 3.2 mm by 3.2 mm.

4.3.2 Mechanical testing

The mechanical properties of polylactic acid and hydroxyapatite polylactic acid composites were evaluated dry and after 24 hours of immersion in phosphate buffered saline (PBS) (Sigma-Aldrich, St. Louis, MO, USA). Dry samples were stored in a desiccator for 24 hours before mechanical testing. Following the initial 24 hours in the desiccator, immersion samples were fully immersed in PBS with a pH level of 7.4 and placed in an incubator at 37°C to mimic physiological conditions. To evaluate the strength of the composites, tensile and bending tests were conducted using Instron 3367 universal testing equipment (Instron, Grove City, PA, USA). Bending strength was

evaluated using a 3-point bending fixture equipment with a 20 mm span length. Tensile strength was conducted with manual tensile grips with a 7.62 mm strain gauge. All samples were tested at a constant cross head rate of 5 mm/min to failure. Load, displacement, and strain data were collected to assess the ultimate bending strength, ultimate tensile strength, and elastic modulus.

4.3.3 Characterization

HA whisker length width and aspect ratio were evaluated using optical microscopy. Following the final washing procedure, the HA whiskers were placed on a microscope slide and dispersed in a droplet of DI water. The sample was dried in an oven. General images were taken at random at 10X and 20 X magnifications to calculate average length, width, and aspect ratio.

Following mechanical evaluation, the microstructure of the flexural fracture surface was examined using scanning electron microscopy (SEM) by an FEI Quanta 600F environmental SEM (FEI Co, Hillsboro, OR, USA). A thin layer of platinum was deposited on the fractured surface with a sputter coater model EMS575X (Electron Microscopy Science, Hatfield, PA, USA) to decrease charging effect and increase image quality. An acceleration voltage of 5 kV was used to image the fracture surface of each mass fraction of HA (0 wt% to 30 wt %).

4.4 Results

Mechanical properties of the PLA/HA-w composites were evaluated by flexural three-point bending, and tensile mechanical testing. In Figure 1, the relationship between the Young's modulus and HA-w content was demonstrated. It is clear that the modulus of the composites is strongly dependent on the mass fraction of HA-w in composite. In

Figure 4.1, a near linear increase is demonstrated up to 30 wt% HA-w content. PLA/HA-w composite with 30wt% HA-w demonstrated the highest Young's modulus peaking at 5.9 GPa, a 61.3% increase from pure PLA at 3.7 GPa.

The mechanical strength, both flexural and tensile, of the PLA/HA-w composites was evaluated in both the dry state and after 24 hours of immersion in PBS at 37 °C. In Figure 4.2, the relationship between HA-w content and tensile and flexural strength is demonstrated. As shown in Figure 4.2, the flexural samples that were tested demonstrated no loss in strength up to 30 wt% HA-w mass fraction. Specifically, 25wt% PLA/HA-w revealed a 14.8% increase in strength in the dry state. Additionally, the samples tested with HA-w following immersion retained their mechanical strength overall from dry testing, unlike the pure PLA sample which demonstrated a 7.7% decrease. Tensile strength decreased slightly at a 30 wt% mass fraction by 9.5% in the dry state and 15.3% overall following immersion in PBS.

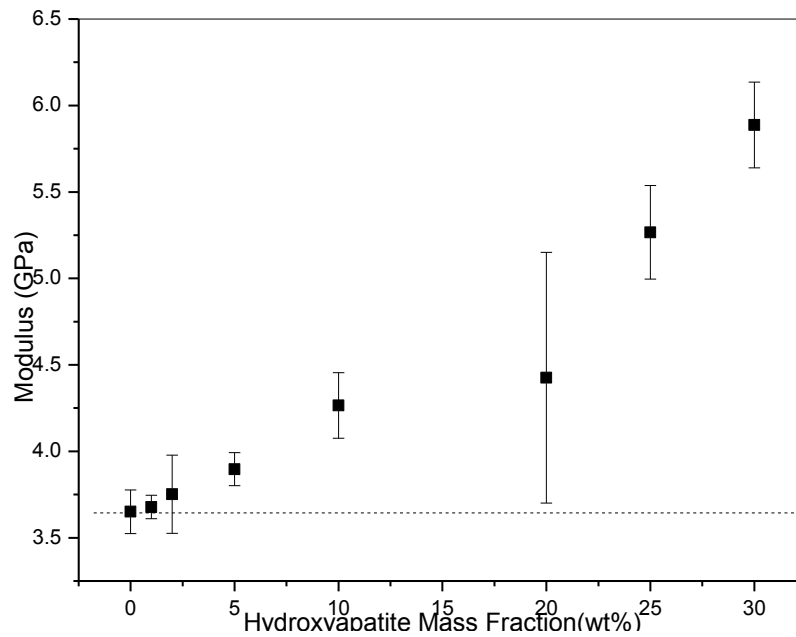


Figure 4.1. Young's modulus (tensile) values of polylactic acid/hydroxyapatite composite containing 0 to 30 wt. % HA-w. Dashed line represents Young's modulus of pure PLA.

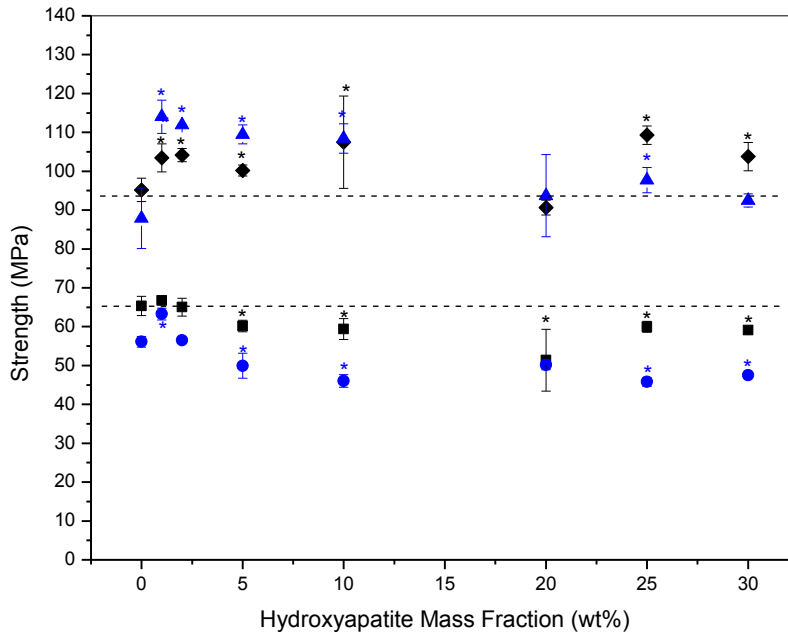


Figure 4.2. The dependence of flexural strength and tensile strength on hydroxyapatite whisker (HA-w) mass fraction, flexural strength dry (♦), 24-hour immersion flexural strength (▲), dry tensile strength (■), and 24-hour immersion strength (●). Dashed line represents flexural and tensile strength of pure PLA in the dry state (*, * $P=0.05$).

SEM micrographs of the fracture surface of the PLA and HA-w composite are presented in Figure 4.3. As displayed in Figure 4.3, aggregation or bundles of HA-w are not present even in 30 wt% samples. Furthermore HA-w pull-out and breakage were observed as shown in Figure 4.3(A-D). The presence of whisker pull-out and breakage is an indication of positive interaction between the PLA matrix and HA-w filler.

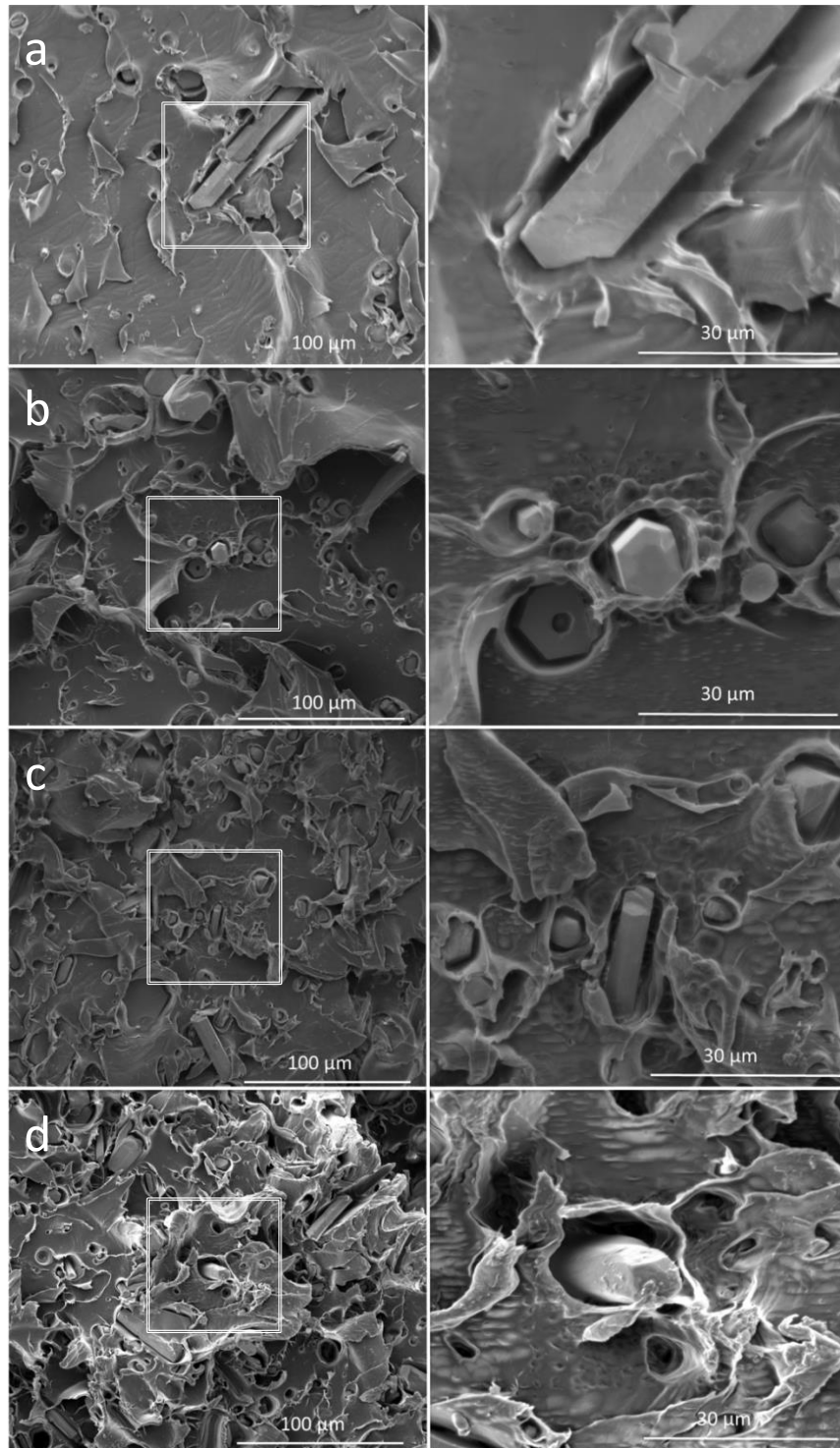


Figure 4.3. SEM micrographs of poly(lactic acid)/hydroxyapatite whisker composites and fracture surface from three-point bending test. (a) 5 wt% HA-w, (b) 10 wt% HA-w, (c) 20 wt% HA-w, and (d) 30 wt% HA-w.

4.5 Discussion

The fabrication method chosen for PLA composites significantly impacts application and mechanical properties. Commonly used fabrication methods in current research include hot pressing, extrusion and machining, and casting [30, 37-39]. These methods allow for more straightforward manufacturing; however, they often limit the final application in the orthopedic medical device field. The present study justified the use of injection molding based on various concerns with other processing methods.

Typically, hot pressing and casting of PLA composite involve the use of solvents to initially mix the filler in the polymer matrix. This method is convenient, but a residual toxic solvent remains which is hard to detect and fully remove.

Furthermore, hot pressing and extrusion fabrication techniques use high temperatures which can be detrimental to the mechanical properties of composites [38]. Additionally, hot pressing temperatures are above melting and are held for longer periods often causing thermal degradation of the polymer matrix.

Though extrusion methods can eliminate the need for extended periods above melting temperature, the need for secondary processing to form devices and test specimen can raise the polymer temperatures and cause further mechanical degradation. The use of elevated temperatures mainly affects the polymer molecular weight which directly impacts the final materials properties as described by von Oepen et al. [39, 43, 44].

Additionally, the methods described above have limited geometric possibilities and may be inconvenient in industrial medical device fabrication. An attractive alternative to these described methods is injection molding. In this procedure polymer

and filler are mixed with a screw, heated in a barrel, and shot into a mold to form a mechanical test specimen which can be directly used without additional processing. The described fabrication method allows near limitless geometric possibilities and requires short cycle times when compared to hot pressing and extrusion. Additionally, injection molding is the most commonly used fabrication method in industry application, making the results from preliminary mechanical evaluation applicable in medical device design and optimization. The injection molding equipment used in the present study is a single screw type. The processing parameter was chosen based on a previously used design of experiment optimization approach proven effective in recent research.

Immersion testing of bioabsorbable composites is critical in the development of new materials for implantation in the human body. PLA and HA are commonly combined in soft tissue fixation applications to increase both mechanical properties and biological response. Recent research results show bioabsorbable materials experiencing a high rate of failure during insertion in ligament reconstruction surgeries [35, 36]. An original solution to this problem is the use of taps in operations; while the screw is still self-tapping, a pilot hole and tap are first used to reduce the occurrence of screw failure during insertion. Another solution is to further increase the composite's mechanical strength, specifically strain to failure. Unfortunately, increasing the mechanical strength has reached a plateau with the addition of ceramic fillers to date [14, 24, 39, 45-48].

Insertion failure can be detrimental to the outcome of surgeries as time is critical for operation success, and the time spent finding debris and fragments from failure has been reported to take up to 1 hour based on data available from the manufacturer and user facility device experience (MAUDE)

(<http://www.accessdata.fda.gov/scripts/cdrh/cfdocs/cfmaude/TextSearch.cfm>) using keywords interference screw provided by the FDA accessed on October 15th 2013. Therefore, analyses of both dry state and immersion testing are useful in understanding the mechanical performance of materials in use. In the present study, flexural and tensile tests are the only tests used to evaluate these properties. However, device-specific testing should be utilized to fully understand device installation such as shear testing, insertion torque, and pull-out as described in ASTM standard F2502-09 [49]. The dry state test would demonstrate the mechanical properties during installation. The wet test results would be analyzed after 24 hours of immersion in PBS at 37 °C to simulate body conditions, which more closely reveals mechanical properties of a device's screws and anchors at patient's first use.

The mechanical evaluation of PLA/HA composites revealed a strong dependence on the mass fraction HA. As demonstrated, elastic modulus is highly dependent on the mass fraction HA in composite. This result is similar to many research studies, specifically that of Russia et al, in which an increase in the modulus of a PLA/HA composite was demonstrated to be over 10 GPa with HA whiskers [30]. Similarly, the modulus was drastically increased as high as 5.88 GPa. The increase in modulus for orthopedic fixation application is very important to reduce stress shield and device migration. Even small mass fractions (1 wt %) caused bending strength and tensile strength to increase by 8.7% and 2.1% respectively. Furthermore, three-point bending dry state evaluation revealed an increase in flexural strength by 14.83% with 25 wt% HA in common soft tissue composite material. The present state of research has shown limited positive increases, especially at high weight percentage composites. This has been

demonstrated by Hong et al. with low aspect ratio nanoparticles where bending strength is increased at 5 wt%; however, bending strength has been observed to sharply decrease at 7.5 wt% with a near 50% strength loss at 20 wt% HA [48]. In the present study, HA/PLA composite with 25 wt% HA-w following immersion still remained 2.6% higher than pure PLA dry state and 11.1% higher than the immersed PLA sample. As seen in similar studies conducted by Bakar et al. [50] among others, the tensile test post-immersion exhibited little loss in strength from the dry state. The 25 wt% HA specimens displayed an 8.3% loss relative to the dry pure PLA and an 18.4% decrease after immersion compared to the immersed pure PLA [50, 51].

The increase in strength in flexural testing after immersion could be an indication of increased interface and was also observed by Wright-Charles et al. [46]. After immersion in PBS at 37 °C, the PLA matrix may become weaker, and HA whiskers with a high aspect ratio may become more entangled and form stronger bonds with PLA to better transfer load. This is apparent in the three-point bending specimen and the extension at break in tensile testing up to 10 wt%. However, this is not demonstrated in the tensile strength. This could be a result of the tensile test's sensitivity to flaws, where HA/PLA composite were fabricated without methods to control orientation of HA-w as used in self-reinforced PLA [52]. In tensile testing, HA specimens which are orientated normal to the test force will act as a void, thus decreasing the composite's strength in this testing method. A further indication of increased interface is the increase in extension at break up to 10 wt% HA-w resulting in a more ductile failure where a small necking was observed before failure. Typically the addition of ceramic filler decreases the ductility and facilitates a more brittle failure demonstrated by Kasuga et al. [14]. At 10 wt%

HA/PLA composite, the extension at break is increased from 0.7 mm to 0.9 mm, a 32.2% increase. Furthermore, tensile strain in 5 wt% HA samples was increased from 2.3% tensile strain to 4.4%. Unlike the decreased strain at failure observed by Roeder et al. in polyether ether ketone (PEEK) HA-w composites [53], this tensile strain increase may also help reduce the risk of brittle failure during insertion.

Finally, SEM analysis revealed a desirable dispersion of HA in PLA polymer matrix. Multiple areas were observed to determine the dispersion, and there were not any agglomerations or regions void of HA found. This was also observed in the author's previous work using hot pressing, but only to 10 wt% HA NF. This dispersion is an indication of the benefit of the processing and fabrication methods used. The dispersion observed is similar to that of the solvent casting method [54]. Additionally, HA and PLA dispersion is similar to twin-screw extrusion of cellulose fiber in PLA as shown by Jonoobi et al. [55]. Twin-screw extrusion is the most repeatable and convenient method for processing polymer composites. However, due to the fact that the PLA would be required to undergo extended periods at a higher temperature, which has been shown to be detrimental to material properties, the twin-screw method was avoided. Similar results were shown by Ignjatovic in a hot pressing study in terms of molecular weight and compressive strength degradation [38]. The low standard deviation of the tensile strain at break is an indication of effective mixing since a higher standard deviation can often indicate poor filler dispersion. Additionally, the SEM micrograph revealed many areas of fiber pull-out, which is representative of a desirable interface between organic and inorganic phases. The SEM analysis provided key information for further composite

study such as the morphology of HA which can most positively impact HA/PLA material properties.

4.6 Conclusion

The aim of this chapter was to evaluate the mechanical properties of HA/PLA composites for soft tissue fixation applications. An HA/PLA composite with 30 wt% HA-w was accomplished via an injection molding processing method. Both tensile specimen and bending specimens were produced for mechanical evaluation. Specimens were subjected to mechanical assessment in the dry state and 24 hours after immersion in PBS at 37 °C (wet), which is the temperature used to simulate the human body's temperature. HA/PLA composites up to 30 wt% demonstrated increased modulus from 3.7 GPa to 5.9 GPa, a 61.3% increase, and flexural strength from 95.2 MPa to 103.8 MPa, a 9.0% increase. A peak in flexural strength was demonstrated at 25 wt%, a 14.8% increase. Furthermore, the testing from the dry state to wet state demonstrated no significant mechanical decrease up to 20 wt% HA-w. The tensile strength of the composite was decreased for all samples except 1 and 2 wt% HA. However, increases in tensile strain and extension at break were seen as an indication of a desirable interface between HA and PLA. The immersion of HA/PLA composites in PBS was critical to understanding the mechanical behavior, which demonstrated an excellent maintenance of strength. Additionally, the processing method utilized in the present study achieved a well-dispersed composite to the highest mass fraction studied (30 wt %). This dispersion was critical for the success of HA/PLA composites and indicates the benefit of using injection molding as opposed to other composite fabrication methods.

Though promising, the results of the present study can only account for early immersion behavior of HA/PLA composite materials. Further investigation into HA/PLA composites' degradation profile is required to better understand their possible applications. Additionally, the use of actual orthopedic soft tissue devices should be considered in future studies relating to mechanical performance and degradation.

The implications presented in this chapter's review of research results have various positive impacts on the orthopedic device market. Injection molding in the present study proved to be a valuable and reliable method for HA/PLA composite fabrication and should be considered for future manufacturing of orthopedic devices. Additionally, immersion in phosphate buffered saline (PBS) revealed maintenance of strength, which reinforced confidence in the material properties of HA/PLA composites after insertion. Furthermore, the increase in modulus and flexural strength demonstrated progress; however, in order to extend these biomaterials to load bearing orthopedic fixation applications, further investigation is required.

References

- [1] Daniels, A.U., *Mechanical properties of biodegradable polymers and composites proposed for internal fixation of bone*. Journal of Applied Biomaterials, 1990. **1**(1): p. 57-78.
- [2] Kulkarni Rk, Pani K.C, Leonard F., *Polylactic acid for surgical implants*. Archives of Surgery, 1966. **93**(5): p. 839-843.
- [3] Suchenski, M., *Material Properties and Composition of Soft-Tissue Fixation*. Arthroscopy: The Journal of Arthroscopic & Related Surgery, 2010. **26**(6): p. 821-831.
- [4] Andreas Weiler, *Biodegradable Implants in Sports Medicine: The Biological Base*. The Journal of Arthroscopic and Related Surgery, 2000. **16**(03).
- [5] Ma, C.B., *Hamstring anterior cruciate ligament reconstruction: a comparison of bioabsorbable interference screw and endobutton-post fixation*. Arthroscopy: The Journal of Arthroscopic & Related Surgery, 2004. **20**(2): p. 122-128.
- [6] Bostman, O., *Foreign-body reactions to fracture fixation implants of biodegradable synthetic polymers*. Journal of Bone & Joint Surgery, British Volume, 1990. **72**(4): p. 592-596.
- [7] Weiler, A., et al., *Foreign-body reaction and the course of osteolysis after polyglycolide implants for fracture fixation experimental study in sheep*. Journal of Bone & Joint Surgery, British Volume, 1996. **78**(3): p. 369-376.
- [8] Busfield, B.T. and L.J. Anderson, *Sterile pretibial abscess after anterior cruciate reconstruction from bioabsorbable interference screws: a report of 2 cases*. Arthroscopy: The Journal of Arthroscopic & Related Surgery, 2007. **23**(8): p. 911. e1-911. e4.
- [9] Kwak, J.H., *Delayed intra-articular inflammatory reaction due to poly-L-lactide bioabsorbable interference screw used in anterior cruciate ligament reconstruction*. Arthroscopy: The Journal of Arthroscopic & Related Surgery, 2008. **24**(2): p. 243-246.
- [10] Konan, S. and F. Haddad, *A clinical review of bioabsorbable interference screws and their adverse effects in anterior cruciate ligament reconstruction surgery*. The Knee, 2009. **16**(1): p. 6-13.
- [11] Bergsma, J.E., *Late degradation tissue response to poly(l-lactide) bone plates and screws*. Biomaterials, 1995. **16**(1): p. 25-31.

- [12] Takayama, T., M. Todo, and A. Takano, *The effect of bimodal distribution on the mechanical properties of hydroxyapatite particle filled poly(L-lactide) composites*. Journal of the Mechanical Behavior of Biomedical Materials, 2009. **2**(1): p. 105-112.
- [13] Macarini, L., *Poly-L-lactic acid — hydroxyapatite (PLLA-HA) bioabsorbable interference screws for tibial graft fixation in anterior cruciate ligament (ACL) reconstruction surgery: MR evaluation of osteointegration and degradation features*. La Radiologia Medica, 2008. **113**(8): p. 1185-1197.
- [14] Kasuga, T., *Preparation and mechanical properties of polylactic acid composites containing hydroxyapatite fibers*. Biomaterials, 2001. **22**(1): p. 19-23.
- [15] Mathieu, L.M., P.E. Bourban, and J.A.E. Mason, *Processing of homogeneous ceramic/polymer blends for bioresorbable composites*. Composites Science and Technology, 2006. **66**(11-12): p. 1606-1614.
- [16] Murariu, M., *Polylactide compositions. Part 1: Effect of filler content and size on mechanical properties of PLA/calcium sulfate composites*. Polymer, 2007. **48**(9): p. 2613-2618.
- [17] Mirosław Pluta, *Polylactide compositions. II. Correlation between morphology and main properties of PLA/calcium sulfate composites*. Journal of Polymer Science Part B: Polymer Physics, 2007. **45**(19): p. 2770-2780.
- [18] Stephane Aunoble, *Biological performance of a new beta-TCP/PLLA composite material for applications in spine surgery: In vitro and in vivo studies*. Journal of Biomedical Materials Research Part A, 2006. **78A**(2): p. 416-422.
- [19] Roeder, R., *Hydroxyapatite-reinforced polymer biocomposites for synthetic bone substitutes*. JOM, 2008. **60**(3): p. 38-45.
- [20] Best, S.M., *Bioceramics: Past, present and for the future*. Journal of the European Ceramic Society, 2008. **28**(7): p. 1319-1327.
- [21] Hench, L.L., *Bioceramics: From Concept to Clinic*. Journal of the American Ceramic Society, 1991. **74**(7): p. 1487-1510.
- [22] Oguchi, H., *Long-term histological evaluation of hydroxyapatite ceramics in humans*. Biomaterials, 1995. **16**(1): p. 33-38.
- [23] Rizzi, S.C., et al., *Biodegradable polymer/hydroxyapatite composites: Surface analysis and initial attachment of human osteoblasts*. Journal of Biomedical Materials Research, 2001. **55**(4): p. 475-486.

- [24] Shikinami, Y., Y. Matsusue, and T. Nakamura, *The complete process of bioresorption and bone replacement using devices made of forged composites of raw hydroxyapatite particles/poly -lactide (F-u-HA/PLLA)*. *Biomaterials*, 2005. **26**(27): p. 5542-5551.
- [25] Hunt, J. and J. Callaghan, *Polymer-hydroxyapatite composite versus polymer interference screws in anterior cruciate ligament reconstruction in a large animal model*. *Knee Surgery, Sports Traumatology, Arthroscopy*, 2008. **16**(7): p. 655-660.
- [26] Calandrelli, L., *Biocompatibility studies on biodegradable polyester-based composites of human osteoblasts: A preliminary screening*. *Journal of Biomedical Materials Research*, 2002. **59**(4): p. 611-617.
- [27] Agrawal, C.M. and K.A. Athanasiou, *Technique to control pH in vicinity of biodegrading PLA-PGA implants*. *Journal of Biomedical Materials Research*, 1997. **38**(2): p. 105-114.
- [28] Macarini, L., *Poly-L-lactic acid — hydroxyapatite (PLLA-HA) bioabsorbable interference screws for tibial graft fixation in anterior cruciate ligament (ACL) reconstruction surgery: MR evaluation of osteointegration and degradation features*. *La Radiologia Medica*, 2008. **113**(8): p. 1185-1197.
- [29] Tecklenburg, K., *Prospective evaluation of patellar tendon graft fixation in anterior cruciate ligament reconstruction comparing composite bioabsorbable and allograft interference screws*. *Arthroscopy: The Journal of Arthroscopic & Related Surgery*, 2006. **22**(9): p. 993-999.
- [30] Russias, J., *Fabrication and mechanical properties of PLA/HA composites: A study of in vitro degradation*. *Materials Science and Engineering: C*, 2006. **26**(8): p. 1289-1295.
- [31] Šupová, M., *Problem of hydroxyapatite dispersion in polymer matrices: a review*. *Journal of Materials Science: Materials in Medicine*, 2009. **20**(6): p. 1201-1213.
- [32] Vaia, R.A. and H.D. Wagner, *Framework for nanocomposites*. *Materials Today*, 2004. **7**(11): p. 32-37.
- [33] Weiler, A., *The influence of screw geometry on hamstring tendon interference fit fixation*. *The American Journal of Sports Medicine*, 2000. **28**(3): p. 356-359.
- [34] Weiler, A., *Biodegradable interference screw fixation exhibits pull-out force and stiffness similar to titanium screws*. *The American Journal of Sports Medicine*, 1998. **26**(1): p. 119-128.

- [35] Purcell, D.B., J.R. Rudzki, and R.W. Wright, *Bioabsorbable interference screws in ACL reconstruction*. Operative Techniques in Sports Medicine, 2004. **12**(3): p. 180-187.
- [36] Weiler, A., *The Influence of Screw Geometry on Hamstring Tendon Interference Fit Fixation*. The American Journal of Sports Medicine, 2000. **28**(3): p. 356-359.
- [37] Charles, L.F., *Fabrication and mechanical properties of PLLA/PCL/HA composites via a biomimetic, dip coating, and hot compression procedure*. Journal of Materials Science: Materials in Medicine, 2010. **21**(6): p. 1845-1854.
- [38] Ignjatovic, N., *Evaluation of hot-pressed hydroxyapatite/poly-L-lactide composite biomaterial characteristics*. Journal of Biomedical Materials Research, 2004. **71B**(2): p. 284-294.
- [39] Deng, X., J. Hao, and C. Wang, *Preparation and mechanical properties of nanocomposites of poly(d,l-lactide) with Ca-deficient hydroxyapatite nanocrystals*. Biomaterials, 2001. **22**(21): p. 2867-2873.
- [40] Taş, A.C., *Molten Salt Synthesis of Calcium Hydroxyapatite Whiskers*. Journal of the American Ceramic Society, 2001. **84**(2): p. 295-300.
- [41] Jarcho, M., *Tissue, cellular and subcellular events at a bone-ceramic hydroxylapatite interface*. J Bioeng, 1977. **1**(2): p. 79-92.
- [42] Ferraz, M.P., F.J. Monteiro, and C.M. Manuel, *Hydroxyapatite nanoparticles: A review of preparation methodologies*. J Appl Biomater Biomech, 2004. **2**(2): p. 74-80.
- [43] Middleton, J.C. and A.J. Tipton, *Synthetic biodegradable polymers as orthopedic devices*. Biomaterials, 2000. **21**(23): p. 2335-2346.
- [44] von Oepen, R. and W. Michaeli, *Injection moulding of biodegradable implants*. Clinical Materials, 1992. **10**(1-2): p. 21-28.
- [45] Liu, F., *Properties and morphology of bioceramics/poly(D,L-lactide) composites modified by in situ compatibilizing extrusion*. Journal of Applied Polymer Science, 2006. **102**(5): p. 4085-4091.
- [46] Wright-Charlesworth, D.D., *In vitro flexural properties of hydroxyapatite and self-reinforced poly(L-lactic acid)*. Journal of Biomedical Materials Research Part A, 2006. **78A**(3): p. 541-549.
- [47] Furukawa, T., *Biodegradation behavior of ultra-high-strength hydroxyapatite/poly (l-lactide) composite rods for internal fixation of bone fractures*. Biomaterials, 2000. **21**(9): p. 889-898.

- [48] Hong, Z., *Nano-composite of poly(-lactide) and surface grafted hydroxyapatite: Mechanical properties and biocompatibility*. *Biomaterials*, 2005. **26**(32): p. 6296-6304.
- [49] ASTM, *Standard Specification and Test Methods for Bioabsorbable Plates and Screws for Internal Fixation Implants*. ASTM International, 2009.
- [50] Abu Bakar, M.S., *Tensile properties, tension–tension fatigue and biological response of polyetheretherketone–hydroxyapatite composites for load-bearing orthopedic implants*. *Biomaterials*, 2003. **24**(13): p. 2245-2250.
- [51] Aydin, E., J.A. Planell, and V. Hasirci, *Hydroxyapatite nanorod-reinforced biodegradable poly(l-lactic acid) composites for bone plate applications*. *Journal of Materials Science: Materials in Medicine*, 2011. **22**(11): p. 2413-2427.
- [52] Altpeter, H., *Non-conventional injection molding of poly(lactide) and poly(ϵ -caprolactone) intended for orthopedic applications*. *Journal of Materials Science: Materials in Medicine*, 2004. **15**(2): p. 175-184.
- [53] Roeder, R.K., M.M. Sproul, and C.H. Turner, *Hydroxyapatite whiskers provide improved mechanical properties in reinforced polymer composites*. *Journal of Biomedical Materials Research Part A*, 2003. **67A**(3): p. 801-812.
- [54] Kasuga, T., *Preparation and mechanical properties of polylactic acid composites containing hydroxyapatite fibers*. *Biomaterials*, 2000. **22**(1): p. 19-23.
- [55] Jonoobi, M., *Mechanical properties of cellulose nanofiber (CNF) reinforced polylactic acid (PLA) prepared by twin screw extrusion*. *Composites Science and Technology*, 2010. **70**(12): p. 1742-1747.

CHAPTER 5: MECHANICAL EVALUATION OF HYBRID POLYLACTIC ACID HYDROXYAPATITE MICRO- AND NANO-COMPOSITE FOR ORTHOPEDIC FIXATION APPLICATIONS

5.1 Chapter 5 Abstract

Biological ceramic/polymer composites for fixation in orthopedic sports medicine, which focus specifically on knee and shoulder injuries, are largely replacing existing metal products. However, polymer-based implants have suffered from a history of problems with negative biological responses and mechanical strength. The objective of this research was to fabricate a hybrid Polylactic acid (PLA) composite containing hydroxyapatite (HA) nanofibers and micro-sized HA whiskers (short single-crystal fibers) and investigate the influence of such a composite on mechanical properties. The increase in the bending strength from 0 wt% (107.9 ± 4.1 MPa) HA to 30 wt% HA (119.4 ± 2.7 MPa) was 17.5%. Even with 60 wt% HA the strength of the composite was 93.0 ± 2.4 MPa a decrease of only 13.8%. The bending modulus at 60 wt% was greatly increased to 9.1 ± 0.4 GPa (165%) from 3.4 ± 0.1 GPa (pure PLA control). Additionally, the hybrid composite fracture surface evaluation under SEM revealed excellent dispersion. Though the mechanical strength could not be improved past 40 wt% HA, the dispersion and limited loss of flexural strength is a promising advance to the improvement of biological ceramic/polymer composites for orthopedic fixation application.

Keywords: Bioabsorbable, Hydroxyapatite, Polylactic acid, Injection molding

5.2 Introduction

Interference screws and suture anchors have been widely used for reconstruction and repair of soft tissue in arthroscopic surgery and sports medicine for repair to the knee and shoulder. It is estimated that there are as many as 400,000 cases of anterior cruciate ligament fixation [1-3] and 250,000 shoulder repairs [4] each year in the United States. Due to the advantages of no obstruction in revision surgeries, better postsurgical imaging, avoiding removal operation and less risk of graft damage [5-9], a variety of bioabsorbable polymer interference screws and suture anchors made from polylactic acid (PLA), polyglycolic acid (PGA), and their copolymers have been developed, which have largely replaced metallic devices in the orthopedic soft tissue fixation market. These bioabsorbable polymer implants, however, have suffered from implant fracture, fibrous defect after resorption, and well-documented inflammatory response during degradation [10-16].

In order to address the aforementioned drawbacks, great efforts have recently been focused on the fabrication and development of bioresorbable composites incorporated with bioactive ceramics such as hydroxyapatite (HA) [17-20], calcium sulfate (CS) [21, 22] or β -Tricalcium phosphate (β -TCP) [23].

In vitro degradation tests have revealed that the addition of HA into PLA can reduce the incidence of foreign body response and inflammation reaction [24], while *in vivo* studies on small animal models have shown HA-PLA composites to have excellent biodegradability and osteoconductivity [25]. Additionally, large animal models have demonstrated significantly increased bone formation and decreased inflammatory

response with HA-PLA composite interference screws in comparison with the standard polymer interference screws [26-28].

The greatest challenge for ceramic bioabsorbable polymer composites is that the mechanical strength of composites containing HA, CS or β -TCP particles or short crystal whiskers generally decreases after addition of the ceramic phase, especially with filler mass fraction around 20-40%. Even worse, the addition of HA, CS or β -TCP particles or whiskers to PLA or other polymers have resulted in a more brittle composite [29-31], which have led to catastrophic failures during insertion [32, 33].

Preliminary experimental results have indicated that small mass fractions (5-10 wt%) of HA nanofibers (HANF), have great potential to improve the composites' mechanical strength (bending and tensile), tensile strain at failure (toughness), and elastic modulus (rigidity) of PLA. Additionally, previous research conducted by this author has demonstrated how HA whiskers fabricated via a molten salt synthesis procedure at elevated temperatures (1190 °C) can maintain the strength (bending and tensile) with a high loading rate (30 wt%) in hydroxyapatite whisker (HA-w) composites.

Compared to bioceramic particles and short whiskers used in existing bioresorbable composites, HA nanofibers, which are several times stronger than stainless steel, with HA microfibers can provide a much better reinforcing effect and have the potential to provide the composites' with ideal biological properties.

The use of nanofibers as opposed to nanoparticles, micro particles, or microfibers is due to the mechanical strength of ceramic nanofibers, which can reach the maximum/theoretical value with nanoscale diameter and a load transfer capability that is roughly proportional to the length (aspect ratio) up to a maximum value. The hypothesis

is that the ultra-long and super strong HA nanofibers with small mass fractions such as 5 wt% can significantly improve the mechanical strength and toughness of the new composites. Additionally, the HA nanofibers, made with a biomimetic method inspired by bone mineralization and with very large surface areas (for surface reactions) and some defects, can significantly improve the composite biocompatibility and osteoconductivity.

Unfortunately, HA nanofibers alone cannot reach the high mass fraction (>30 wt%) of HA, which has proven to be crucial to the elimination of inflammatory responses and stimulation of bone growth (improved osteoconductivity) in bioabsorbable implants [26, 28, 34]. Due to the very small percolation threshold for nanomaterials in polymer composites, beyond which the addition of more nanomaterials inevitably degrades the mechanical strength of the polymer composites [35, 36], the combination of HA nanofibers (5 wt%) and microfibers (25-55 wt%) may lead to a composite with high HA mass fraction for better biocompatibility and a modulus closer to cortical bone. This combination also has superior toughness and strength for fewer catastrophic failures. Additionally, when different sized HA microfibers are used, the maximum loading rate without mechanical property degradation can be higher as the void space around large fillers can be filled with smaller fillers [37, 38].

HA nanofibers in the present study were fabricated using a biomimetic approach at low temperature (95 °C). The HA whisker was fabricated using a molten salt synthesis approach at elevated temperature (1190 °C). The most popular method of fabrication for HA whiskers is the hydrothermal (wet chemical) method, which can generate microfibers of $2.3 \pm 0.8 \mu\text{m}$ in diameter and $18.0 \pm 8.9 \mu\text{m}$ in length [29]. Nanofibers made with the hydrothermal method at low temperatures are very strong because their strength is not

sensitive to defects, but microfibers made under such conditions may have many defects and much lower strength [39]. As an example, hydrothermal HA whiskers (30 vol%) in polyether ether ketone (PEEK) led to a 25.9% loss in tensile strength and an 80.8% loss in strain to failure [30], while HA-w composite (30 wt%) demonstrated a 9.0% increase in flexural strength, a 9.4% loss in tensile strength, and no loss in strain to failure.

In the present study, a hybrid HA/PLA composite was formed using injection molding containing HA-w and HA-NF. The new composite is evaluated using bending tests for mechanical evaluation. It is the hope that this hybrid composite may both increase the mass fraction of HA without negatively influencing mechanical strength.

5.3 Methodology

5.3.1 Materials

Commercially available polylactic acid by Ingeo (3251) was acquired from NatureWorks as the matrix in the present study (NatureWorks, MN, USA). Hydroxyapatite nanofibers (HA NF) were fabricated in a similar manner as presented by Chen et al. using a hydrothermal method [40]. HA whiskers (HA-w) were synthesized using a molten salt synthesis procedure at high temperatures similar to that described by Tas et al. [41]. The synthesized HA nanofibers were approximately 50-100 nm in width and 100 μm in length, and HA whiskers were 2-5 μm in width and as well as 7-12 μm in length.

5.3.2 Fabrication

PLA and HA were combined in an injection mold fabrication process. First PLA pellets as received were first milled under 500 μm in a cryogenic milling process. HA nanofibers and whiskers in appropriate mass fractions were combined in a mortar and

pestle, and milled to separated large visible bundles. The HA and PLA were mixed in a unitized jar mixer prior to injection molding. Weight fraction evaluated in the present study contained 5 wt% HA NF and the subsequent weight fraction HA-w. Bending specimens produced using injection molding were 6.0 mm in width, 2.0 mm in thickness, and 25 mm in length. In this process HA/PLA composite was further mixed with the application of heat at 190 °C and a mixing screw. Samples were then stored at least 24 hours prior to mechanical testing. This ensured the polymer reached room temperature.

5.3.3 Testing

HA/PLA hybrid composites were mechanically evaluated via a three-point bending procedure using an Instron universal testing equipment (Instron, PA, USA). A constant cross head rate of 5 mm/min. was used with a 20 mm support span.

Following the mechanical evaluation, the flexural samples were examined using scanning electron microscopy (SEM) to evaluate the dispersion of HA-w and HA NF on the fracture surface. A thin film of platinum was sputtered onto the surface to reduce the charging effect. A 5 kV accelerating voltage was used to image the surface using an FEI Quanta 600F environmental SEM (FEI Co, Hillsboro, OR, USA).

5.4 Results & Discussion

5.4.1 Mechanical Evaluation

The flexural strength of the HA/PLA composites is summarized in Figure 5.1, where each datum point provides the mean value of four measurements with standard deviation. The flexural strength of pure PLA without filler was 107.9 ± 4.1 MPa. A 30 wt% composite increased the strength to 119.4 ± 2.7 MPa (10.6%). Maintenance in strength was shown to 40 wt% HA where the flexural strength was 110.8 ± 2.5 MPa.

Following this mass fraction the bending strength began to degrade, at the highest mass fraction (60 wt%) the strength decreased by 13.8% to 93.0 ± 2.4 MPa. The modulus was increased with every loading rate in the present study from 3.4 ± 0.1 GPa pure PLA to 5.0 ± 0.2 GPa (44.9%) with 30 wt% HA, and 6.1 ± 0.4 GPa (78. %) with 40 wt% HA, which peaked to 9.1 ± 0.4 GPa (165.3%) at 60 wt% HA. At 60 wt% the modulus is similar to human cortical bone.

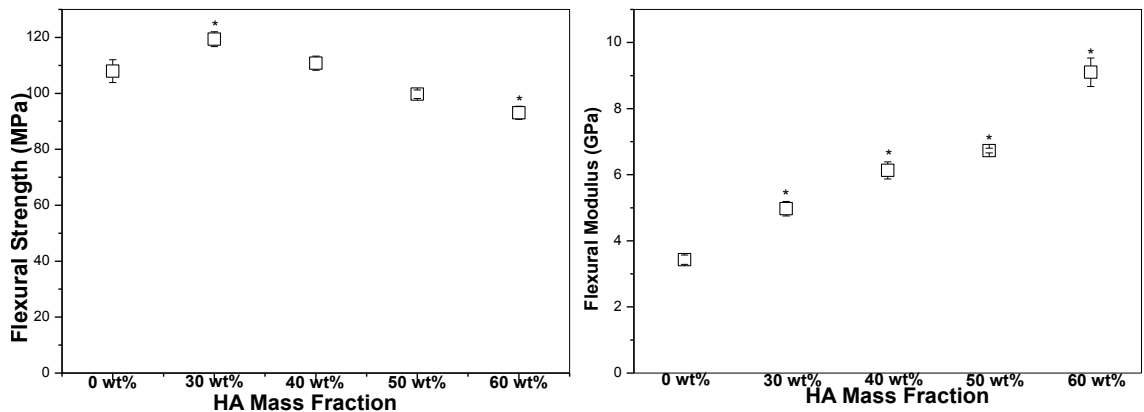


Figure 5.1 Flexural strength and modulus from 3-point bending HA/PLA composites containing various weight fractions of HA whiskers and nanofibers (*, $P < 0.05$).

Commercially available interference screws' highest loading rate is 60 wt% in the CompositTCP screw (Biomet, 40% PLDLA/60% β -TCP), and the most common loading rate is 30 wt% [42]. Similar composites described by Murariu with 50 wt% calcium sulfate particles demonstrated a substantial loss in strength (43%) [21], and Converse et al. observed a decrease in strength by 57.8% with HA whiskers in polyether ether ketone (PEEK) [30]. The present study only exhibited a 7.6% loss at 50 wt% loading and 13.8% with 60 wt% HA whiskers. Typically substantially large losses in strength are observed with ultra-high mass fractions of ceramic filler. In the present study, loss of strength due to these high mass fractions is minimal which has great potential for future orthopedic fixation applications.

5.4.2 Scanning Electron Microscopy

Scanning electron microscopy was used to evaluate the fracture surface of flexural samples tested to failure. Figure 5.2 shows the SEM Fractography of HA/PLA composite to 60 wt% the highest loading rate evaluated in the present study. A lower magnification SEM image first shows the quality of the HA dispersion on the fracture surface without visible agglomerations. The second image at higher magnification shows individual HA whiskers and nanofibers without any visible agglomerations.

Additionally pullout of both HA nanofiber and whiskers is visible in the higher magnification images in Figure 5.2. This excellent dispersion as shown in the SEM images may be related to the hybrid composite as described by Uddin [43] whereby improved dispersion and mass fractions were observed with carbon nanofibers, silica nanoparticles, and alumina nanoparticles. Though it was not directly studied in the present work, limited agglomerations of the HA nanofiber may be influenced by the presence of the microsized HA whisker filler since nanofibers have shown a high propensity to form agglomerates in polymer nanocomposites [36]. Similar dispersion of whiskers was observed by Kasuga et al. [19]. However, in the present study the pullout of whisker is enhanced, which is demonstrated by the noticeable pullout of whiskers and the presence of holes formed where whiskers were removed. This pullout indicates the interface between the matrix and filler.

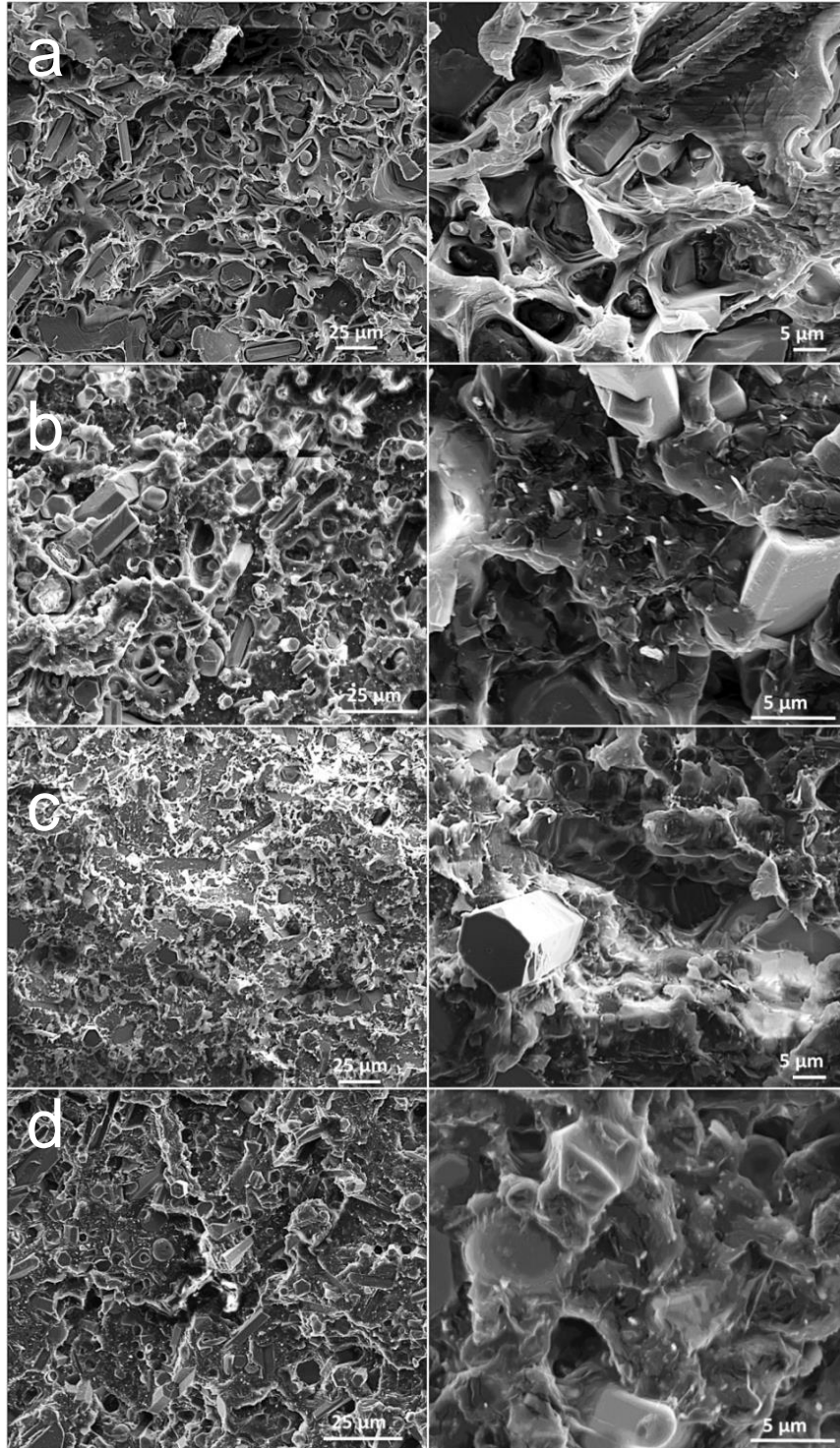


Figure 5.2 Scanning electron microscopy of flexural fracture surface containing Hydroxyapatite whiskers and nanofibers a.) 30 wt% HA, b.) 40 wt% HA, c.) 50 wt% HA, d.) 60 wt% HA.

5.5 Conclusions

The aim of the present study to fabricate a hybrid nano and microsized composite was accomplished through injection molding from 0 to 60 wt% HA content. In the present study, 30 wt% HA hybrid composite demonstrated an enhanced strength and modulus compared to pure PLA control. Additionally, the typical polymer ceramic composite with such a mass fraction (30 wt%) exhibit losses in strength. Though the strength could not be increased past a loading rate of 40 wt%, the minimal loss at 60 wt% (13.8%) is a promising result and justifies further research for implementation of hybrid composites in the manufacturing orthopedic fixation applications. Specifically, the dispersion observed in the present study without clear agglomerations of nanofibers or large voids containing pure polymer is an excellent indication of the potential application of this material. The conventional benefit of adding ceramic to increase the modulus was confirmed in the present study as a 165% increase with 60 wt% to 9.1 GPa was achieved, which is similar to that of human cortical bone. The result in the present study is very promising for future orthopedic fixation applications; however, more research is required before its implementation in actual device. Future research methods should include additional immersion testing, tensile testing, and impact toughness measurement in the development of hybrid HA fiber composite material to assure success.

References

- [1] Murray, M.M., P. Vavken, and B. Fleming, *The ACL Handbook: Knee Biology, Mechanics, and Treatment*. 2013: Springer.
- [2] Arendt, E.A., *OKU orthopaedic knowledge update: Sports medicine 2*. Vol. 2. 1999: Amer Academy of Orthopaedic.
- [3] Vavken, P. and M.M. Murray, *Translational studies in anterior cruciate ligament repair*. Tissue Engineering Part B: Reviews, 2009. **16**(1): p. 5-11.
- [4] Kuhn, J.E., *Effectiveness of physical therapy in treating atraumatic full-thickness rotator cuff tears: a multicenter prospective cohort study*. Journal of Shoulder and Elbow Surgery, 2013.
- [5] Zantop, T., Weimann A., Schmidtko, R., Herbort, M., Raschke, M. J., Petersen, W. *Graft laceration and pullout strength of soft-tissue anterior cruciate ligament reconstruction: In vitro study comparing titanium, poly-d,l-lactide, and poly-d, l-lactide-tricalcium phosphate screws*. Arthroscopy, 2006. **22**(11): p. 1204-1210.
- [6] Middleton, J.C. and A.J. Tipton, *Synthetic biodegradable polymers as orthopedic devices*. Biomaterials, 2000. **21**(23): p. 2335-2346.
- [7] Warden, W.H., D. Chooljian, and D.W. Jackson, *Ten-year magnetic resonance imaging follow-up of bioabsorbable poly-L-lactic acid interference screws after anterior cruciate ligament reconstruction*. Arthroscopy: The Journal of Arthroscopic & Related Surgery, 2008. **24**(3): p. 370. e1-370. e3.
- [8] Pihlajamäki, H., J. Kinnunen, and O. Böstman, *In vivo monitoring of the degradation process of bioresorbable polymeric implants using magnetic resonance imaging*. Biomaterials, 1997. **18**(19): p. 1311-1315.
- [9] Disegi, J. and H. Wyss, *Implant materials for fracture fixation: a clinical perspective*. Orthopedics, 1989. **12**(1): p. 75.
- [10] AndreasWeiler, *Biodegradable Implants in Sports Medicine: The Biological Base*. The Journal of Arthroscopic and Related Surgery, 2000. **16**(03).

- [11] Ma, C.B., *Hamstring anterior cruciate ligament reconstruction: a comparison of bioabsorbable interference screw and endobutton-post fixation*. *Arthroscopy: The Journal of Arthroscopic & Related Surgery*, 2004. **20**(2): p. 122-128.
- [12] Bostman, O., *Foreign-body reactions to fracture fixation implants of biodegradable synthetic polymers*. *Journal of Bone & Joint Surgery, British Volume*, 1990. **72**(4): p. 592-596.
- [13] Weiler, A., *Foreign-Body Reaction and The Course of Osteolysis After Polyglycolide Implants for Fracture Fixation Experimental Study in Sheep*. *Journal of Bone & Joint Surgery, British Volume*, 1996. **78**(3): p. 369-376.
- [14] Busfield, B.T. and L.J. Anderson, *Sterile pretibial abscess after anterior cruciate reconstruction from bioabsorbable interference screws: a report of 2 cases*. *Arthroscopy: The Journal of Arthroscopic & Related Surgery*, 2007. **23**(8): p. 911. e1-911. e4.
- [15] Kwak, J.H., *Delayed intra-articular inflammatory reaction due to poly-L-lactide bioabsorbable interference screw used in anterior cruciate ligament reconstruction*. *Arthroscopy: The Journal of Arthroscopic & Related Surgery*, 2008. **24**(2): p. 243-246.
- [16] Konan, S. and F. Haddad, *A clinical review of bioabsorbable interference screws and their adverse effects in anterior cruciate ligament reconstruction surgery*. *The Knee*, 2009. **16**(1): p. 6-13
- [17] Takayama, T., M. Todo, and A. Takano, *The effect of bimodal distribution on the mechanical properties of hydroxyapatite particle filled poly(L-lactide) composites*. *Journal of the Mechanical Behavior of Biomedical Materials*, 2009. **2**(1): p. 105-112.
- [18] Macarini, L., *Poly-L-lactic acid — hydroxyapatite (PLLA-HA) bioabsorbable interference screws for tibial graft fixation in anterior cruciate ligament (ACL) reconstruction surgery: MR evaluation of osteointegration and degradation features*. *La Radiologia Medica*, 2008. **113**(8): p. 1185-1197.
- [19] Kasuga, T., *Preparation and mechanical properties of polylactic acid composites containing hydroxyapatite fibers*. *Biomaterials*, 2001. **22**(1): p. 19-23.

- [20] Mathieu, L.M., P.E. Bourban, and J.A.E. Mason, *Processing of homogeneous ceramic/polymer blends for bioresorbable composites*. Composites Science and Technology, 2006. **66**(11-12): p. 1606-1614.
- [21] Murariu, M., *Polylactide compositions. Part 1: Effect of filler content and size on mechanical properties of PLA/calcium sulfate composites*. Polymer, 2007. **48**(9): p. 2613-2618.
- [22] Mirosław Pluta, *Polylactide compositions. II. Correlation between morphology and main properties of PLA/calcium sulfate composites*. Journal of Polymer Science Part B: Polymer Physics, 2007. **45**(19): p. 2770-2780.
- [23] Stephane Aunoble, *Biological performance of a new beta-TCP/PLLA composite material for applications in spine surgery: In vitro and in vivo studies*. Journal of Biomedical Materials Research Part A, 2006. **78A**(2): p. 416-422.
- [24] David D. Hile, Stephen A. Doherty, and Debra J. Trantolo, *Prediction of resorption rates for composite polylactide/hydroxylapatite internal fixation devices based on initial degradation profiles*. Journal of Biomedical Materials Research Part B: Applied Biomaterials, 2004. **71B**(1): p. 201-205.
- [25] Hasegawa, S., *A 5-7 year in vivo study of high-strength hydroxyapatite/poly(L-lactide) composite rods for the internal fixation of bone fractures*. Biomaterials, 2006. **27**(8): p. 1327-1332.
- [26] Suchenski M., *Polymer interference screws in anterior cruciate ligament reconstruction in a large animal model*. Knee Surgery, Sports Traumatology, Arthroscopy, 2008. **16**(7): p. 655-660.
- [27] *Arthex BioComposite Interference Screws for ACL and PCL Reconstruction*.
- [28] Tecklenburg, K., *Prospective evaluation of patellar tendon graft fixation in anterior cruciate ligament reconstruction comparing composite bioabsorbable and allograft interference screws*. Arthroscopy: The Journal of Arthroscopic & Related Surgery, 2006. **22**(9): p. 993-999.
- [29] Roeder, R.K., M.M. Sproul, and C.H. Turner, *Hydroxyapatite whiskers provide improved mechanical properties in reinforced polymer composites*. Journal of Biomedical Materials Research Part A, 2003. **67A**(3): p. 801-812.

- [30] Converse, G.L., W. Yue, and R.K. Roeder, *Processing and tensile properties of hydroxyapatite-whisker-reinforced polyetheretherketone*. *Biomaterials*, 2007. **28**(6): p. 927-935.
- [31] Wright-Charlesworth, D.D., *In vitro flexural properties of hydroxyapatite and self-reinforced poly(L-lactic acid)*. *Journal of Biomedical Materials Research Part A*, 2006. **78A**(3): p. 541-549.
- [32] Weiler, A., *The influence of screw geometry on hamstring tendon interference fit fixation*. *The American Journal of Sports Medicine*, 2000. **28**(3): p. 356-359.
- [33] Weiler, A., *Biodegradable interference screw fixation exhibits pull-out force and stiffness similar to titanium screws*. *The American Journal of Sports Medicine*, 1998. **26**(1): p. 119-128.
- [34] Macarini, L., *Poly-L-lactic acid — hydroxyapatite (PLLA-HA) bioabsorbable interference screws for tibial graft fixation in anterior cruciate ligament (ACL) reconstruction surgery: MR evaluation of osteointegration and degradation features*. *La Radiologia Medica*, 2008. **113**(8): p. 1185-1197.
- [35] Rong, M.Z., *Improvement of tensile properties of nano-SiO₂/PP composites in relation to percolation mechanism*. *Polymer*, 2001. **42**(7): p. 3301-3304.
- [36] Vaia, R.A. and H.D. Wagner, *Framework for nanocomposites*. *Materials Today*, 2004. **7**(11): p. 32-37.
- [37] Vlasveld, D.P.N., H.E.N. Bersee, and S.J. Picken, *Nanocomposite matrix for increased fibre composite strength*. *Polymer*, 2005. **46**(23): p. 10269-10278.
- [38] Zhao, Z.G., *The growth of multi-walled carbon nanotubes with different morphologies on carbon fibers*. *Carbon*, 2005. **43**(3): p. 663-665.
- [39] Gao, H., *Materials become insensitive to flaws at nanoscale: lessons from nature*. *Proc Natl Acad Sci U S A*, 2003. **100**(10): p. 5597-600.

- [40] Chen, L., *BisGMA/TEGDMA dental composite containing high aspect-ratio hydroxyapatite nanofibers*. Dental Materials, 2011. **27**(11): p. 1187-1195.
- [41] Taş, A.C., *Molten Salt Synthesis of Calcium Hydroxyapatite Whiskers*. Journal of the American Ceramic Society, 2001. **84**(2): p. 295-300.
- [42] Suchenski, M., *Material Properties and Composition of Soft-Tissue Fixation*. Arthroscopy: The Journal of Arthroscopic & Related Surgery, 2010. **26**(6): p. 821-831.
- [43] Uddin, M.F. and C.T. Sun, *Improved dispersion and mechanical properties of hybrid nanocomposites*. Composites Science and Technology, 2010. **70**(2): p. 223-230.

CHAPTER 6: POLYLACTIC ACID COMPOSITES CONTAINING HYDROXYAPATITE IN SIMULATED BODY ENVIRONMENT FOR ORTHOPEDIC FIXATION APPLICATION: A 24 WEEK STUDY

6.1 Chapter 6 Abstract

A new polylactic acid (PLA) composite containing hydroxyapatite (HA) nanofibers and short single-crystal HA whiskers has been developed with promising improvements in mechanical performance. Consequently, it is important to understand its behavior in a physiological environment. Injection molded mechanical testing specimens were fully immersed in a phosphate buffered saline (PBS) solution as a simulated body fluid, and mechanical strength was evaluated at 0, 8, 16, and 24 weeks. The *in vitro* changes to the HA/PLA composites were evaluated using scanning electron microscopy (SEM) to evaluate the fracture surface morphology. Simulated body fluid (PBS) pH measurements were recorded of the fluid in the vicinity of degrading composites. The results indicated that with the addition of 5 wt% HA nanofibers, the flexural strength was maintained and 81.5% of the tensile strength was retained *in vitro* through 16 weeks. SEM of the fracture surface revealed a well-dispersed HA composite free of voids and large agglomerations. Furthermore, the pH of the fluid in the vicinity of HA/PLA composite was maintained throughout the 24 weeks in all samples excluding the 50 wt%. The results from the present study, therefore, suggest the use of HA nanofibers and whiskers may have a strong impact on future orthopedic fixation devices.

Keywords: *Hydroxyapatite, Polylactic acid, in vitro degradation, Mechanical Evaluation*

6.2 Introduction

Bioresorbable implants used in fracture fixation are an attractive alternative to conventional metal devices for two main reasons: 1) they require no secondary surgery for removal and 2) their modulus is more similar to that of human bone, eliminating a stress shielding effect [1, 2]. Unfortunately, bioresorbable materials have demeritorious properties which have limited their use in the orthopedic fixation field, such as lower mechanical properties compared to metal and degradation byproducts which have been shown to cause a decrease in pH leading to an inflammatory response and other adverse effects [3, 4]. Additionally, early micro movements of implant devices have been reported clinically [5]. Many of the potential problems associated with biological response have been solved with the use of hydroxyapatite (HA). However, there is still a need to increase the mechanical strength and to develop a more perfect implantable material.

Polylactic acid/hydroxyapatite (HA/PLA) composites have gained increasing interest mainly due to their biocompatibility, bioresorbability, and bioactivity. The effects of HA on the composite's material properties have been well studied, in which a limited increase is typically observed in flexural or tensile strength, while the modulus can be drastically improved with HA rods as shown by Kasuga et al. [6]. Although limited improvements in flexural and tensile properties were demonstrated, research continues with HA/PLA and other calcium phosphate composites, which have become the most popular degradable polymer in soft tissue orthopedic fixation applications.

Recently, a new HA/PLA composite has been developed with improved mechanical properties. This HA/PLA composite has demonstrated increases in both

flexural and tensile strength as well as Young's modulus and elongation in the dry state. In order to fully understand the applications of this composite, an understanding of the degradation behavior is needed to justify final application in orthopedic implanted devices. A common method to understand degradation behavior is an *in vitro* immersion test. In this test HA/PLA composites are held in a simulated body fluid (PBS) for a period of time after which samples are removed and tested. This method has been proven to show a good relationship to *in vivo* results as presented by Shikinami with the complete bioresorption of PLA and HA composite [7].

The aim of the present study was to investigate the degradation behavior of HA/PLA composite with HA weight fractions of 0, 5, 30, and 50 wt%. It is hypothesized that the HA nanofiber with a diameter around 100 nm and length of 100 μm should increase the tensile and flexural strength by providing high load transfer with high aspect ratio fiber. Furthermore, the HA whisker will allow the composite to maintain this strength with an increased HA loading rate up to 50 wt%. HA/PLA mechanical testing specimens (flexural and tensile) were placed in PBS for a period of 24 weeks. Scanning electron microscopy (SEM) of the fractured surface was used to observe HA/PLA morphology. Degradation was analyzed according to mechanical evaluation and pH change of PBS in the vicinity of degrading HA/PLA composites.

6.3 Materials and Methods

6.3.1 Polylactic acid/hydroxyapatite composite fabrication

Polylactic acid (PLA) resin received from Purac Biomaterials (Purac Biomaterials, Netherlands) was first milled using a cryogenic milling procedure, and the polymer pellet size was reduced to under 500 μm with the use of a sieve (Hogentogler &

Co, Columbia, MD, USA) and sieve shaker model RX-29 (WS Tyler, Mentor, OH, USA). Hydroxyapatite (HA) nanofibers and whiskers were produced with wet precipitation and molten salt synthesis, respectively. HA and PLA powder was combined in a unitized jar mill (US Stoneware, East Palestine, OH, USA) at a mass fraction of 0, 5, 30, and 50 percent by weight. Other than the 0 wt% sample, each sample contained 5wt% HA nanofibers, and the subsequent higher percentage was comprised of HA whiskers. Following this, mechanical testing specimens were created using injection molding where the composite was further mixed above melting temperature of PLA matrix (190 °C) and made at high pressure in bending and tensile molds.

6.3.2 Degradation *in vitro*

In vitro behavior of HA/PLA composites 0, 5, 30, and 50 wt% were studied in PBS purchased from Sigma-Aldrich (Sigma-Aldrich, St. Louis, MO, USA). Flexural and tensile specimens were immersed fully in PBS at 37 °C, and 7.4 pH. Mechanical specimens were removed at 8, 16, and 24 weeks for mechanical evaluation. Mechanical testing specimens' PBS pH was monitored for changes greater than 0.2 pH, at which point the PBS would be replaced; otherwise the PBS was changed every 2 weeks regardless of pH change. Separate specimens were prepared to study changes in pH in the vicinity of degrading composite over the 24-week period.

6.3.3 Mechanical evaluation

Mechanical evaluation was conducted immediately after removal from the incubated PBS. Both flexural and tensile specimens were evaluated using Instron 3367 universal testing equipment (Instron, Grove City, PA, USA). Flexural specimens were tested using three-point bending conforming to ASTM standard D5934. Tensile

specimens were tested in uniaxial tensile test conforming to ASTM standard D638. Five samples were tested to generate a mean and standard deviation from each interval test.

6.3.4 Weight loss and water absorption

Water absorption and weight loss were calculated as percentages. Samples were weighed dry before immersion, wet following immersion and dry after immersion. Weight loss and water absorption were calculated using equations 6.1 and 6.2 where W_w is the wet weight, W_d is the dry weight, and W_i initial weight.

$$\text{Percentage weight loss} = \frac{W_i - W_d}{W_i} \times 100\% \quad (6.1)$$

$$\text{Percentage absorption} = \frac{W_w - W_d}{W_d} \times 100\% \quad (6.2)$$

6.3.5 Scanning electron microscopy (SEM)

Fractured surfaces from flexural samples at each weight percent sample were evaluated under SEM. Fractured samples were first coated with a thin layer of platinum using sputter coater model EMS575X (Electron Microscopy Science, Hatfield, PA, USA). Following this, a FEI Quanta 600F environmental scanning electron microscope (FEI Co, Hillsboro, OR, USA) using a 5 kV accelerating voltage was used to image the fractured surfaces.

6.4 Results & discussion

6.4.1 Mechanical properties

The mechanical strength of bending and tensile samples was recorded at intervals of 0, 8, 16, and 24 weeks as shown in Figure 6.1. Flexural testing in the dry state exhibited maintenance in strength at 5 wt% HA, however, 30 and 50 wt% HA were slightly lowered by 10.1% and 17.9%, respectively. This maintenance in strength was also demonstrated by Kasuga with up to 70 % HA [8]. Unlike the research by Kasuga,

however, the tensile testing (dry) of 5 wt% HA/PLA composites revealed a 14.8% (73.2 ± 2.0 MPa) increase in strength compared to the 0 wt% (63.8 ± 13.3 MPa) samples, and no loss in strength even at 50 wt% HA. The samples' maintained strength during tensile testing is a strong indication of quality dispersion as this uniaxial test is the most sensitive to flaws. Following immersion, the tensile strength of the 30 and 50 wt% HA/PLA composites decreased with 8-week strength retention of $93.6 \pm 12.7\%$ (43.3 ± 3.4 MPa) and $72.9 \pm 21.8\%$ (31.8 ± 2.8 MPa), respectively. Alternatively, the 0 wt% and 5 wt% specimen both retained their strength after 8 weeks of immersion. Moreover, the 5 wt% specimen specifically exhibited an increase in flexural strength to 150.3 ± 16.0 MPa after 8 weeks immersion and maintained 88.1% (106.3 ± 17.8 MPa) of its original strength after 24 weeks of immersion. Immersed 30 and 50 wt% HA composites tested at week 8 and week 24 only had minor decreases in tensile strength 6.7% and 2.5% respectively. Similarly, flexural strength at higher mass fractions of HA 30 wt% and 50 wt% was decreased, but after 24 weeks of immersion still retained 62.7% and 61.5% flexural strength, respectively. The positive results in the current study were unlike the findings by Wright-Charlesworth et al. [9] where the observed flexural strength of pure PLA and Self-Reinforced PLA (SR-PLA) were found to be stronger than HA/PLA composite initially. However, at 40 wt% HA/PLA composite after 12 weeks of immersion, Wright-Charlesworth samples were untestable [9]. The fact that in the present study samples were not only testable after 12 weeks, but were also testable after 24 weeks and showed improved flexural and tensile strength is noteworthy (see Figure 6.1).

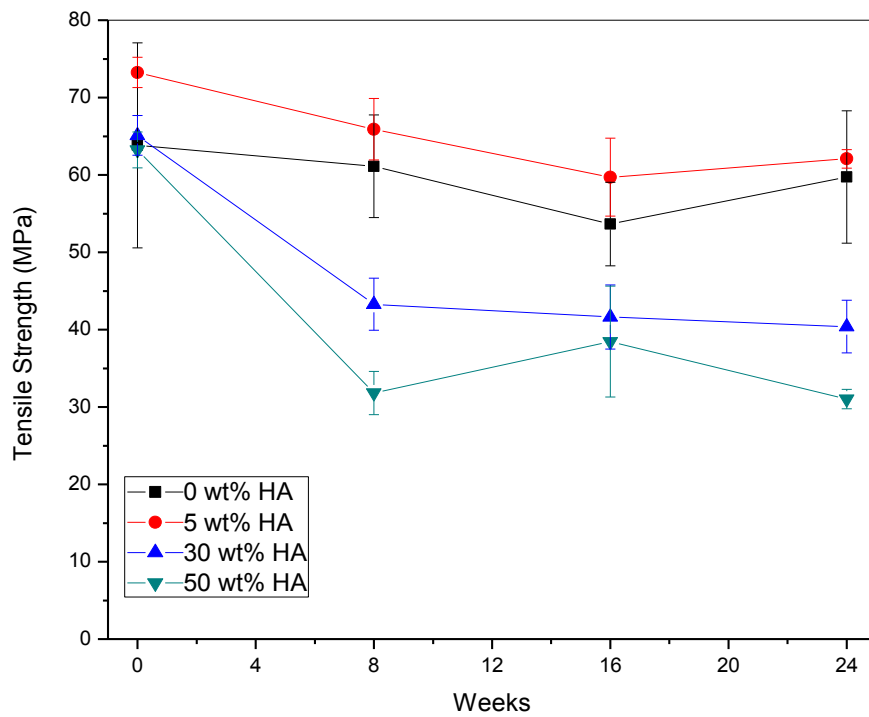
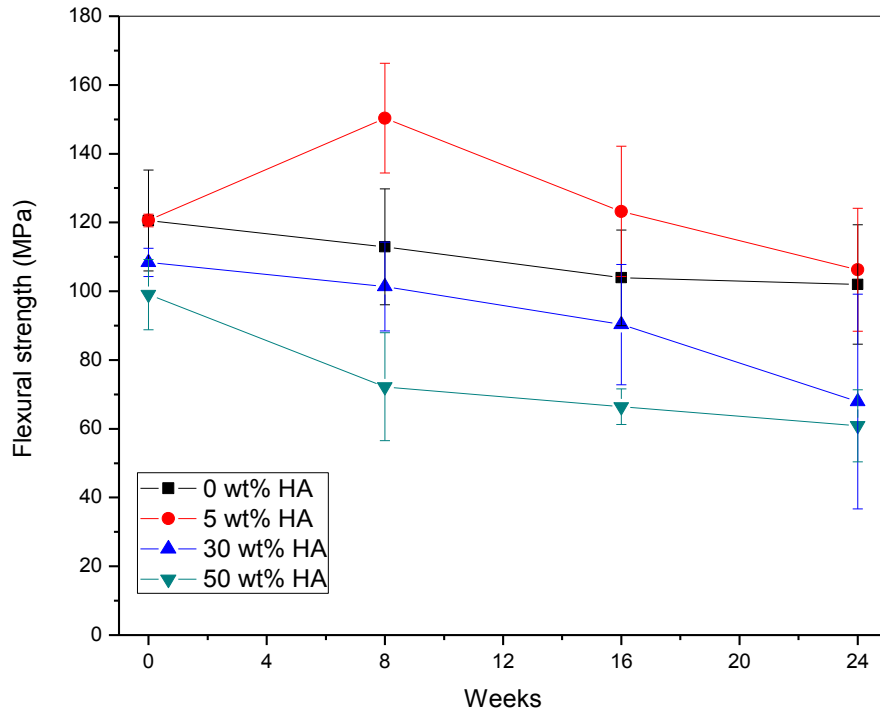


Figure 6.1. Mechanical evaluation (Flexural and Tensile) with varying loading rates of HA through 24-week immersion in simulated body fluid 0 wt% HA, 5 wt% HA, 30 wt% HA, 50 wt% HA

In the tensile evaluation, strain was recorded using a 7.62 mm strain gauge. The strain at the failure of tensile specimens is summarized in Table 1. Unlike traditional ceramic based composites, 5 wt% HA/PLA composite demonstrated significant elongation before its failure in the dry state prior to immersion. Behaving as a tough material, it exhibited necking following yielding and then broke. In the dry state, the strain to failure was $22.2 \pm 6.3\%$, while the pure PLA sample was $6.4 \pm 8.6\%$. Similarly, Hong et. al. in a grafting polymerization process demonstrated an increase in strain at failure [10]. However, the largest elongation to failure observed in the study by Hong et al was 10-13%, and in the present study a strain to failure was nearly doubled (22%). The strain to failure of higher mass fractions of HA was lower compared to pure PLA and 5 wt% HA/PLA composites at $2.2 \pm 0.5\%$ at 30 wt% HA and $1.1 \pm 0.2\%$ at 50 wt% HA. However, following immersion the strain at failure rose to $12.0 \pm 2.3\%$ and $8.9 \pm 1.9\%$, respectively, after the 24-week immersion. The strain to failure of 30 and 50 wt% HA demonstrated this rise immediately following immersion between 0 and 8 weeks where strain increased to $11.3 \pm 6.2\%$ and $8.8 \pm 4.3\%$, respectively. A stress strain relationship following 24 weeks immersion is displayed in Figure 6.2.

The result from the present study is an attractive improvement as the composite is tougher, and may bend before it is broken *in vivo*. Furthermore, it is common for the strain at failure to be decreased following immersion which was observed by Wright-Charlesworth [9]. As shown in Figure 6.2, the 5 wt% HA specimens demonstrated a very ductile response to tensile testing. After 8 weeks immersion 5 wt% HA and higher mass fractions of HA (30 wt% and 50 wt%) demonstrated this ductile response. Moreover, the strain is much closer to the yield strength shown in Figure 6.2B (8 weeks) unlike the

sharp decrease as shown in Figure 6.2A (0 weeks). In addition as observed in Figure 6.2 A-D and Table 6.1, strain at failure of pure PLA is nearly unchanged with immersion. The strain at failure observed in the present study lends the materials to previously unconsidered uses. This property could give doctors and patients an *in vivo* response to understand rehab schedule and device failure prevention.

Table 6.1. Dependence of strain to failure of HA/PLA composite filled with various mass fraction of hydroxyapatite

Strain at failure (%)	0 Weeks		8 Weeks		16 Weeks		24 Weeks	
	Mean	± SD	Mean	± SD	Mean	± SD	Mean	± SD
0 wt% HA	6.4	± 8.6	3.0	± 2.0	2.4	± 1.3	2.5	± 1.3
5 wt% HA	22.2	± 6.3	15.8	± 8.2	17.6	± 7.0	13.8	± 4.5
30 wt% HA	2.2	± 0.5	11.3	± 6.2	14.5	± 5.0	12.0	± 2.3
50 wt% HA	1.1	± 0.2	8.8	± 4.3	6.9	± 3.0	8.9	± 1.9

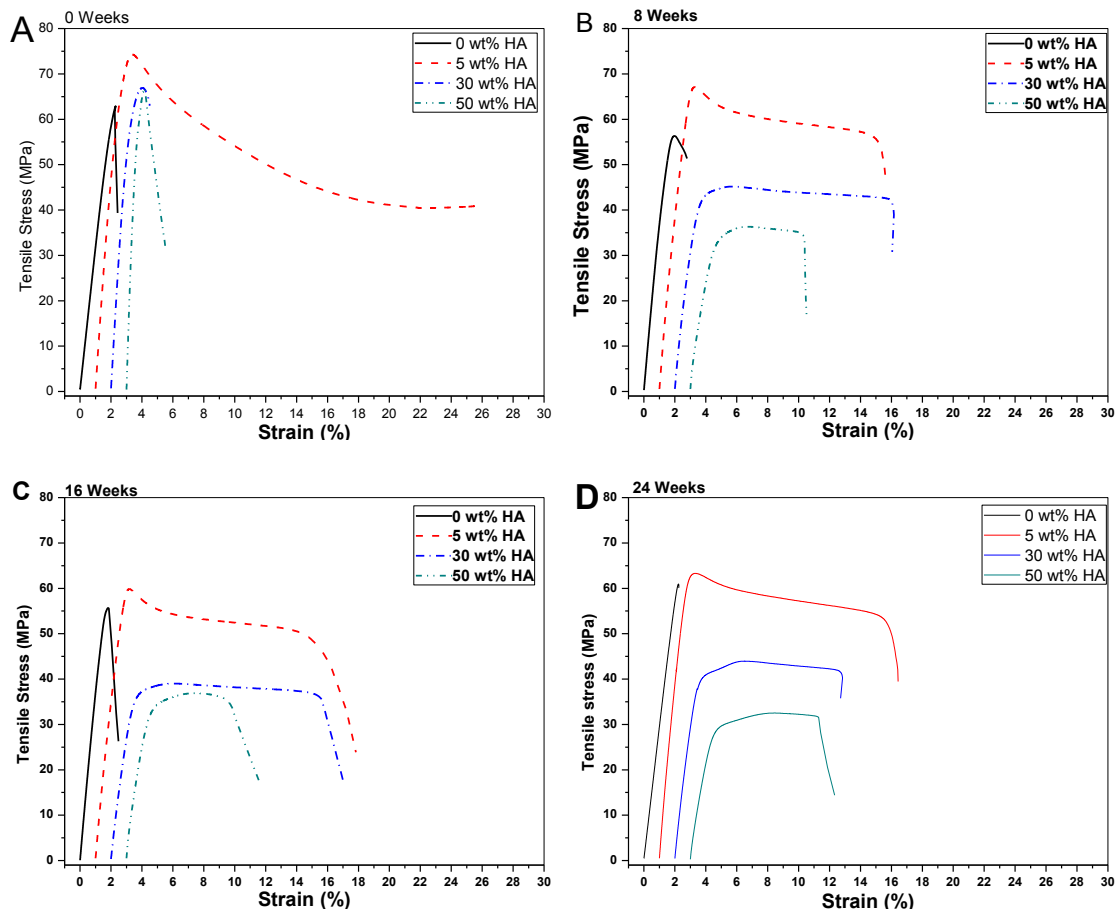


Figure 6.2. Stress versus strain relationship following immersion 0 wt% HA, 5 wt%, 30 wt%, 50 wt% HA (1% separation added for visualization purpose): A. represents results at 0 weeks, B. at 8 weeks, C. at 16 weeks, and D. at 24 weeks.

Additionally, a shelf life of the HA/PLA composite was tested to simulate storage of device before its end use and indicate expiration of material. Specimens in this experiment were vacuum sealed and stored in a desiccator for a period of 24 weeks following fabrication. In the present study, shelf life samples presented no degradation in mechanical strength, visual changes, changes in ductility, or geometric changes following this storage period. As explained by Middleton and Tipton, shelf life and shelf stability is a key factor in the application of absorbable materials for medical applications [11]. This can give an idea of the time the device may be stored prior to expiration and gives confidence in the use of this material.

6.4.2 Physiological evaluations

The cross section of tested samples were measured before and following immersion to observe changes to cross sectional areas during *in vitro* degradation and is presented in Figure 6.3. Samples with higher content of HA exhibited a greater increase in cross sectional area or swelling. The changes in cross sectional area with 0 wt% and 5 wt% HA were similar and had no discernible change over the 24-week period. HA/PLA composite with 30 wt% HA initially reached $2.4 \pm 1.8\%$ at 8 weeks immersion, but did not rise above this following the 24-week immersion. The 50 wt% HA samples experienced a steady growth to $5.4 \pm 2.0\%$ increase in the cross sectional area, while 0 wt% remained the same $0.05 \pm 1.1\%$ in the same time interval. The cross section increase is similar to the results observed by Hile et al. in flexural and screw testing [12]. In the Hile et al. study, HA/PLA specimens experienced a $4.27 \pm 0.95\%$ increase in thread diameter and $0.58 \pm 0.12\%$ increase in length at 24 weeks, while pure screws increased $0.68 \pm 0.34\%$ and $0.46 \pm 0.38\%$, respectively [12]. The swelling of the HA/PLA composite may be a result of the diffusion of water into the matrix due to the presence of HA resulting in a porous matrix as explained by Proikakis et al. [13]. Furthermore, increased cross sectional areas with high loading rates of HA may be a result of increased hydrophilicity when using HA. The limited increase in cross sectional areas with 5 wt% HA nanofibers may be explained by the low loading rate of HA, the surface modification treatment to the HA nanofiber surface or a combination of the two.

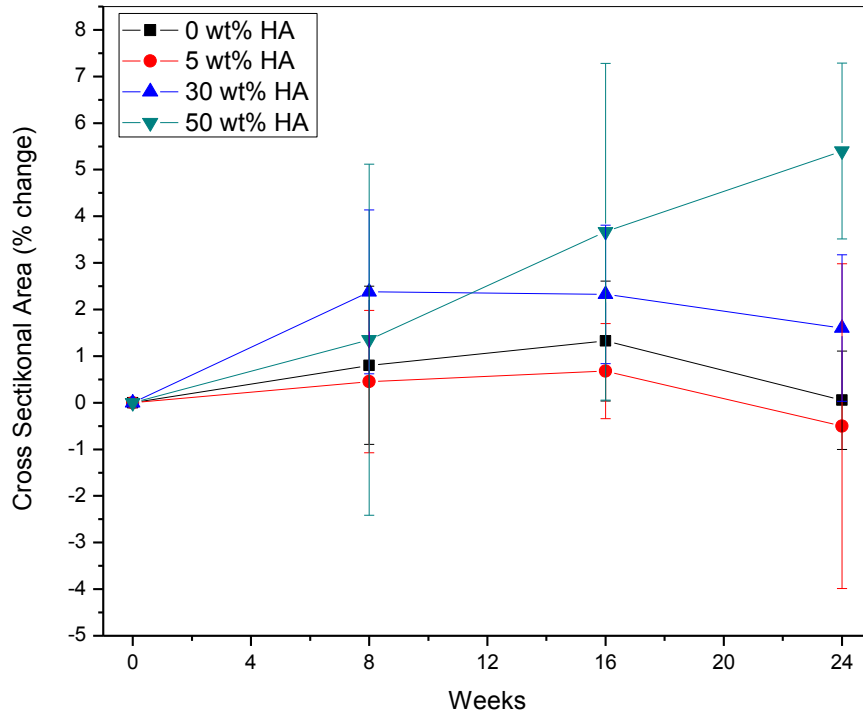


Figure 6.3. Cross-sectional area variations following immersion in simulated body fluid with various loading rates of HA 0 wt% HA, 5 wt% HA, 30 wt% HA, 50 wt% HA

Additionally, water absorption was measured through the 24-week trial. The largest water absorption was demonstrated by 30 wt% and 50 wt% HA/PLA composite samples at $4.0 \pm 0.4\%$ and $3.2 \pm 0.2\%$, respectively, as displayed in Figure 6.4. In the same way, PLGA and HA composites experienced similar increases with the addition of HA in a study by Li et al. [14]. However, 5 wt% HA samples only experienced a $2.2 \pm 0.2\%$ increase, while the pure sample increased to $1.3 \pm 0.3\%$. This may be explained by the silane surface modification used on the HA nanofibers, which may influence water absorption. The HA nanofiber surface is hydrophilic, while the PLA is hydrophobic based on the methyl groups ($-\text{CH}_3$) [15]. The surface treatment to the HA nanofibers makes it slightly more hydrophobic as discussed by Rakmae [16] and resulted in less

water absorption compared to 30 and 50 wt% HA, which contained untreated HA whiskers.

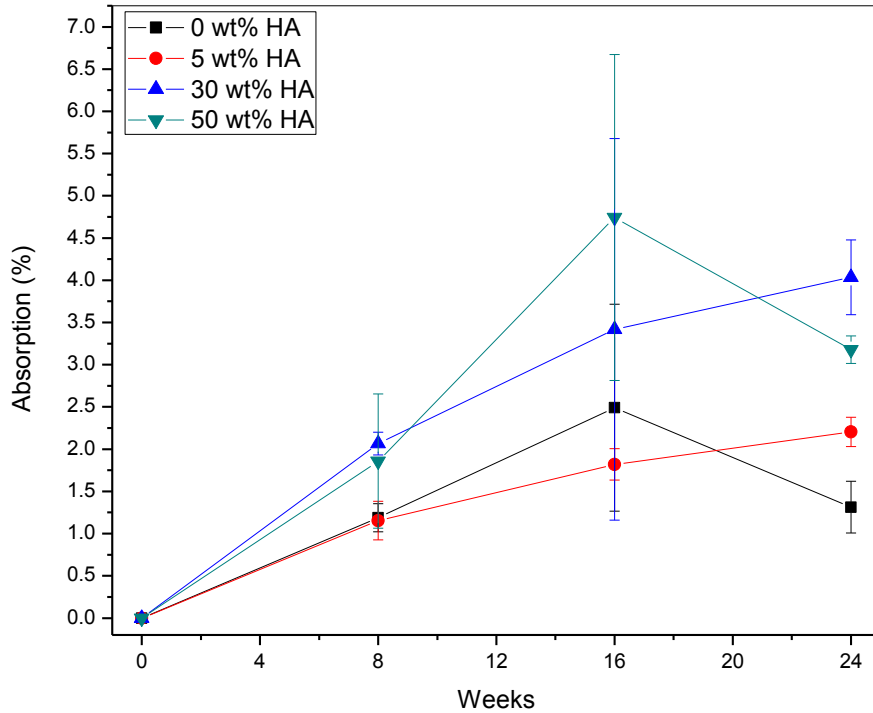


Figure 6.4. Percentage water absorption of flexural bending specimens with varying loading rates of HA immersed in simulated body fluid after 24 weeks at 0 wt% HA, 5 wt% HA, 30 wt% HA, and 50 wt% HA

Furthermore, mass retention was measured following immersion intervals as shown in Figure 6.5. The mean mass loss during the first 16 weeks of immersion in PBS was minimal. However, between week 16 and 24 mass loss was initiated. Following 24 weeks of immersion, samples with HA demonstrated the largest mass loss. Vast mass loss up to 24 weeks was not expected as mass loss in PLA does not typically occur until after 24 weeks as shown by Shikinami et al. [7]. Similarly, physiological degradation can occur *in vitro* and *in vivo* as shown by Weir, where PLA indicated no visual changes or mass loss until the 32nd week [17].

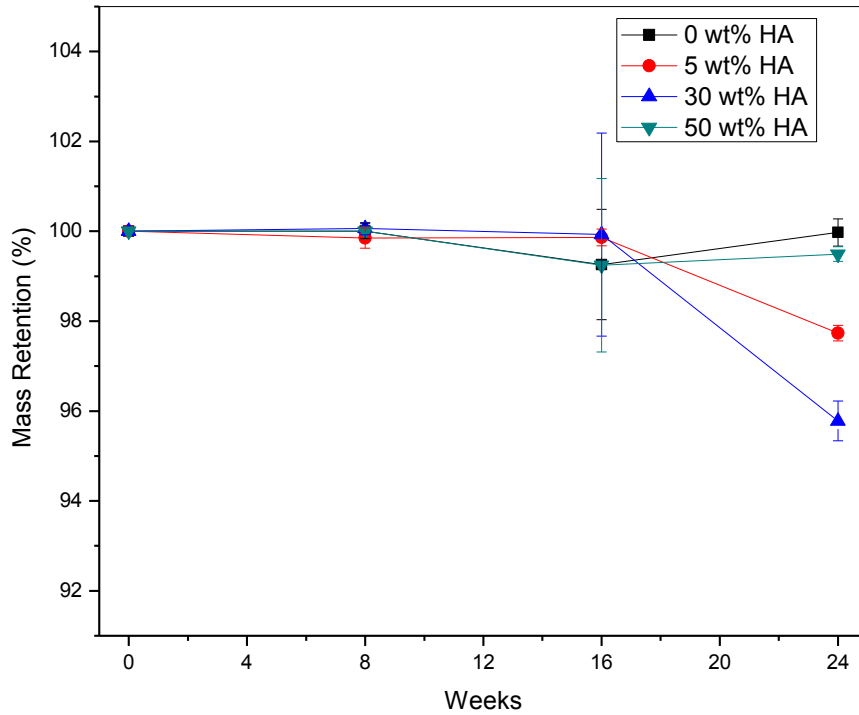


Figure 6.5. The dependence of mass retention on immersion time in PBS with various loading rates of HA filler: 0 wt%, 5 wt%, 30 wt%, and 50 wt%

The pH in the vicinity of degrading PLA and HA/PLA composite was evaluated. In the present study extending to 24 weeks, little effect was observed in the 0, 5, and 30 wt% HA composites. However, 50 wt% composites experience a decreased pH from PBS buffered to 7.4 to 6.6 ± 0.3 following 24 weeks immersion as shown in Figure 6.6. PLA is degraded by hydrolysis and produced lactic acid causing the decrease in the pH of the PBS. The decrease in pH of 50 wt% HA composite was unexpected as HA is hypothesized to help buffer the acid response in the body [14]. However, the HA nanofibers and whisker may begin to dissolve at a lower pH, which may contribute to the pH increase later in the degradation process which will not be present in Pure samples. Additionally, the higher mass fraction absorbed the most water and subsequently may have a higher release of acidic products.

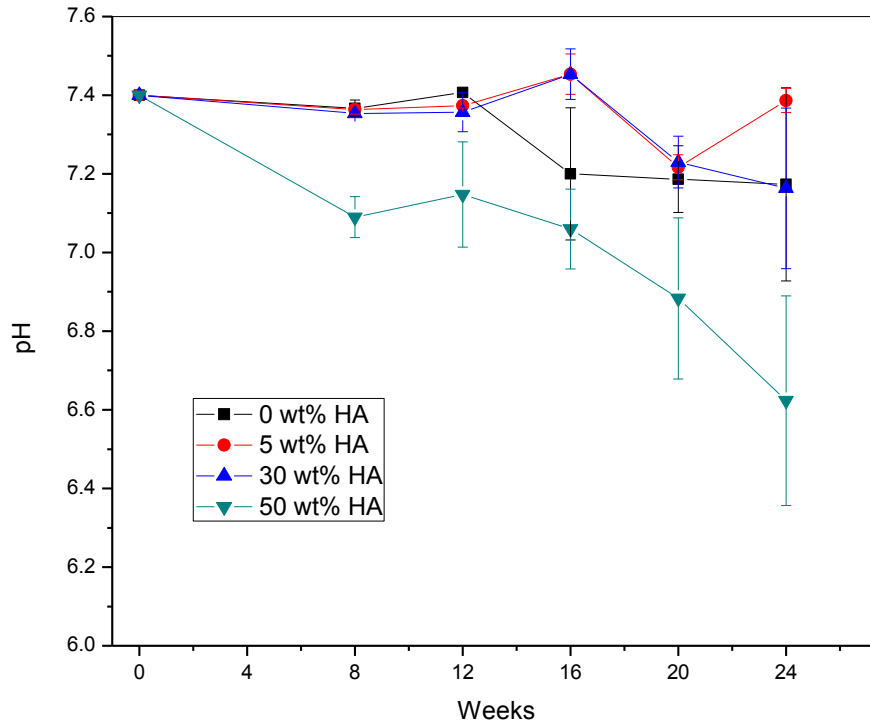


Figure 6.6. The dependence of pH in the vicinity of degrading HA/PLA composites as they relate to immersion times at 0 wt% HA, 5 wt% HA, 30 wt% HA, and 50 wt% HA

The experimental procedure neglects the effect of the buffering performed by the body fluid recirculation, but gives an understanding of how HA/PLA may perform in areas which have limited body fluid replenishment.

Additionally, visual changes in the color of the pure PLA samples were observed as the pure PLA began clear and transparent and slowly changed to white in color over the progression of the study as displayed in Figure 6.7. In addition to this color change, a distinct fiber like structure (arrows) formed on the inside of the PLA sample beginning after week 8 which can be seen in Figure 6.7 at weeks 16 and 24. This change was not observed in the samples with HA since the original color in the dry state was white in color. This color change was also observed in various immersion studies such by Weir et al. in the degradation of pure PLA [18].

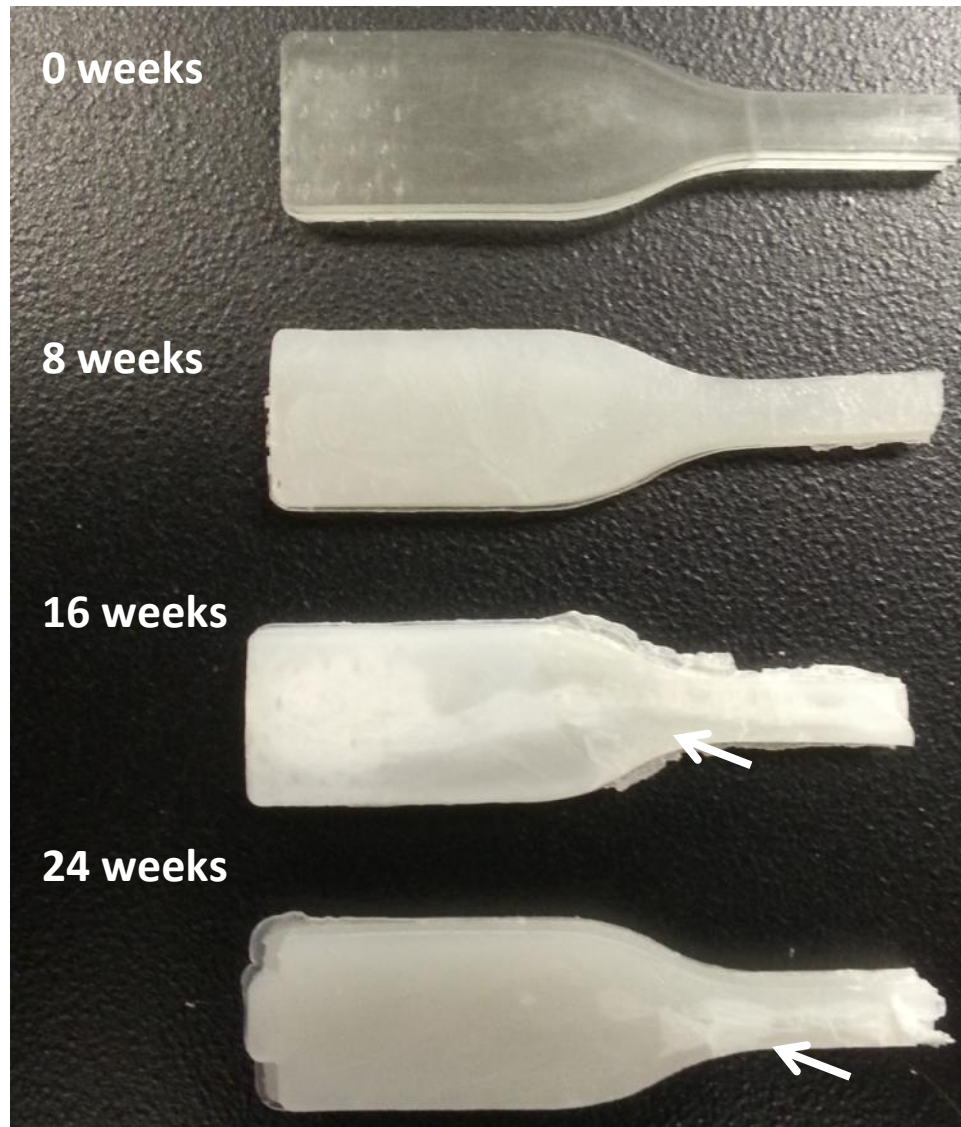


Figure 6.7 Pure PLA tensile specimens degraded in PBS at 37 °C

6.4.3 Scanning electron microscopy of fracture surface

Scanning electron microscopy (SEM) of the fractured surface of flexural samples is presented in Figures 6.8 and 6.9. The SEM fracture surface revealed an excellent dispersion of HA whiskers and nanofibers in the PLA matrix which was similar to that found in Russias and Aydin et al. [19, 20]. Additionally, the HA nanofibers demonstrated limited agglomerations or bundles, which is a common problem attributed to

nanocomposites, as reviewed by Supova [21]. Figure 6.8 represents the dispersion of both HA nanofibers and whiskers. This superior mixing can be attributed to processing using injection molding as previously studied and used throughout this study. The dispersion of HA whiskers and nanofibers observed under SEM clearly showed the benefit of using injection molding and preprocessing treatments used in the present study. The observed pull-out of a single HA nanofiber and nanofiber bundles were an indication of the presence of an interface between HA filler and PLA matrix. Figures 6.9 A and B depict the fracture surface of 5 wt% HA composite following three point bending. From this SEM, the fracture surface demonstrated not only a well dispersed single nanofiber (arrow) and bundled nanofibers (circled), but also shows pull-out of both nanofiber and nanofiber bundles an indication of the interface between the nanofiber and PLA matrix. The combination of HA nanofibers and HA whiskers shown in Figure 6.8 C and D depict 30 wt% HA, and Figures 6.8E and F depict 50 wt% HA. In the fracture surface of both 30 wt% and 50 wt% HA nanofibers and whiskers, HA composites demonstrated an excellent dispersion, where limited agglomerations were present. Even at 50 wt% HA, the presence of agglomerated HA whiskers were not present. In addition to the pull-out of HA whiskers shown, some breaking of whiskers can be easily observed in image F of Figure 6.8 as highlighted, where the facet of the HA whiskers (highlighted) and broken whiskers (arrows) was observed. This breakage of whiskers was an indication of the strength of the interface between the whiskers and PLA matrix since the HA whisker are very strong. Additionally, large holes in the matrix could be seen from pull-out during testing and had a larger diameter than the whiskers, which indicated the force in shear which it took to be removed. The excellent dispersion of both HA nanofibers and HA

whiskers is shown in Figure 6.9. In this fractured surface of 30 wt% HA broken whiskers (dashed arrows) and unbroken facets (highlighted) of HA whiskers, single nanofiber pull-outs (arrows), and voids can be seen where HA pull-out in testing occurred.

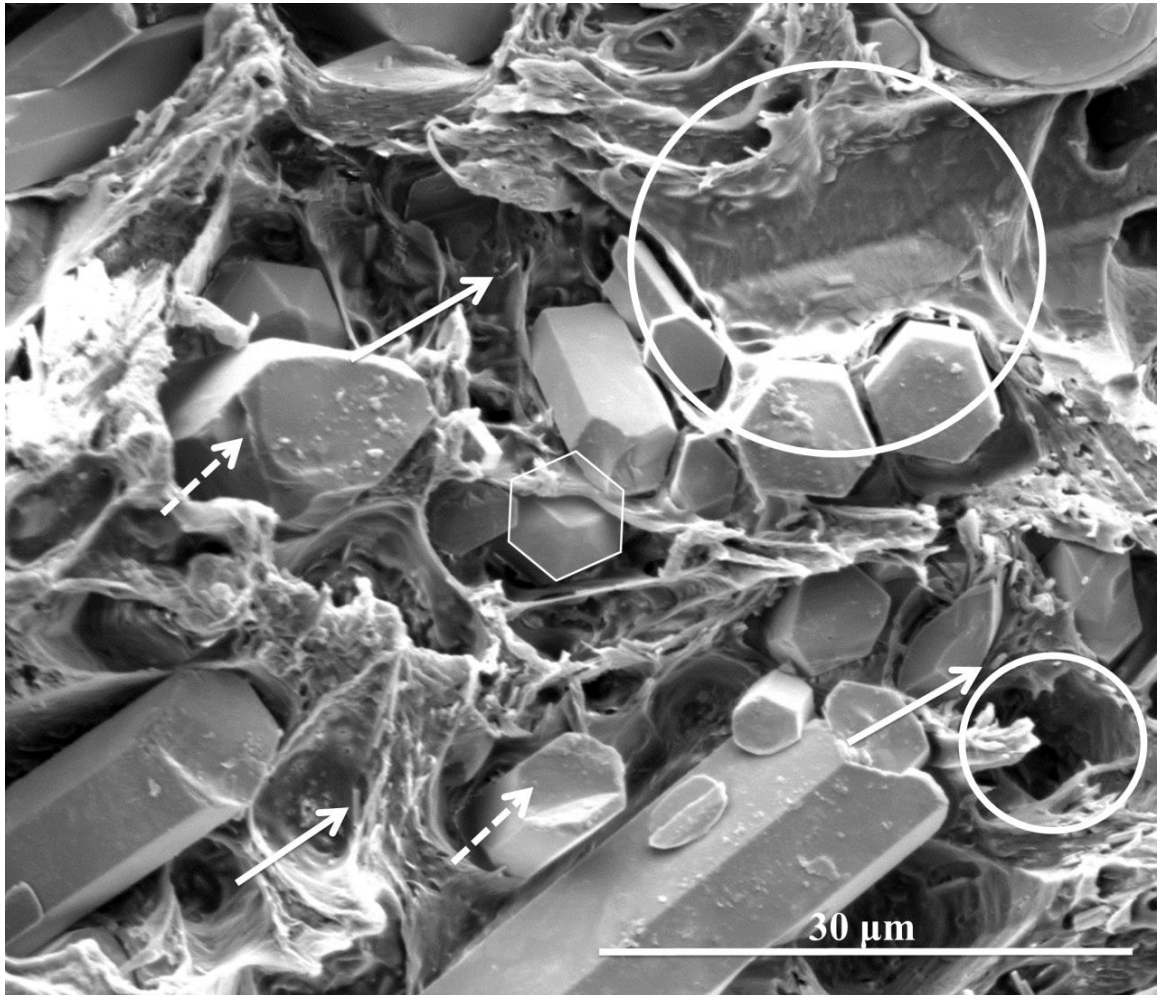


Figure 6.8. SEM fracture surface of 30 wt% HA whisker and nanofiber/polylactic acid composite. (Arrows refer to fiber, dashed arrows represent broken HA whisker, encircled areas represent holes from whisker pull-out, and hexagons highlight HA whisker facet unbroken).

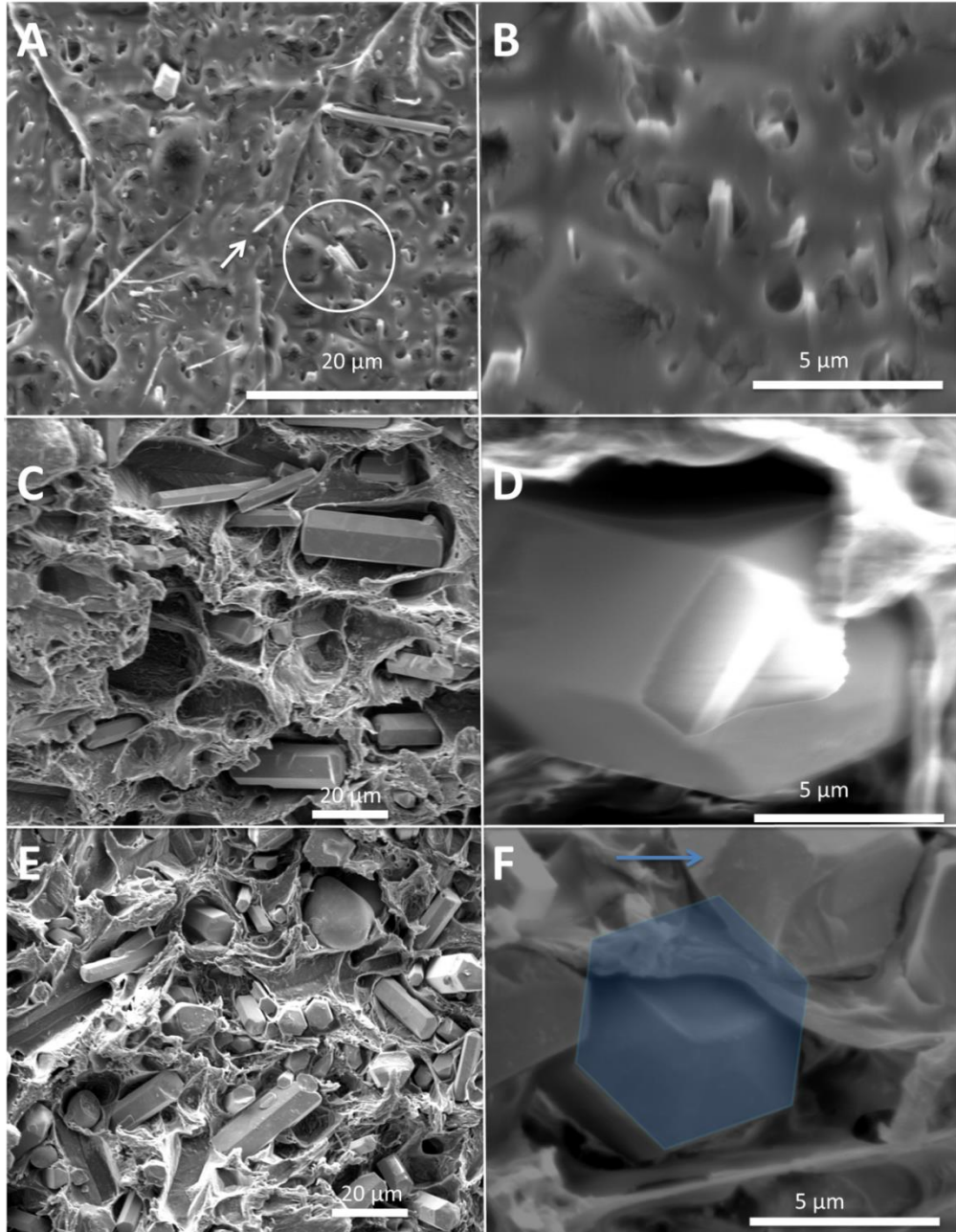


Figure 6.9. Scanning electron microscopy of the fractured surface of bending specimens following mechanical evaluation A) 5 wt% HA–NF B) 30 wt% HA (5 wt% HA–NF/25 wt% HA-w), and C) 50 wt% HA (5 wt% HA–NF/45 wt% HA-w). Arrows depict single fiber pull-out, and circle show HA nanofiber bundles.

6.5 Conclusions

The biodegradation of HA/PLA composite in a simulated body fluid was evaluated mechanically and physiologically. Flexural strength of 5 wt% HA/PLA

composite was maintained at 16 weeks at 123.2 ± 19.0 MPa, 18.6% higher than the pure PLA at the same immersion interval. Furthermore, tensile strength was increased to 73.3 ± 2.0 MPa, a 14.8% increase from the pure PLA. Additionally the strength of the 5 wt% HA composite following 24 weeks immersion retained 84.8% of its dry strength and is only 2.7% lower than the pure PLA in the dry state. The SEM fracture surface demonstrated the positive effect from the preprocessing treatment and fabrication methods revealing an excellent dispersion of HA in the PLA matrix. Additionally, the presence of nanofiber and whisker pull-out, and whisker breakage represented the interface formed between the filler and matrix as a promising step and crucial enhancement. Physiological changes in the PLA such as swelling and water absorption at higher loading of HA from the present study suggest that surface modification may play a significant role in the degradation of HA/PLA composites. It would be of great value to further explore different surface modification techniques and coupling agents in degradation environments. The present study has resulted in a better understanding of the behavior of polylactic acid and hydroxyapatite whiskers and nanofibers composites. However, further continued work with packaging, sterilization, and long-term *in vitro* and *in vivo* response is necessary to fully understand the material's potential.

References

- [1] Hanafusa, S., *Biodegradable Plate Fixation of Rabbit Femoral Shaft Osteotomies: A Comparative Study*. Clinical Orthopaedics and Related Research, 1995. **315**: p. 262-271.
- [2] Akeson, W.H., *The effects of rigidity of internal fixation plates on long bone remodeling. A biomechanical and quantitative histological study*. Acta orthopaedica Scandinavica, 1976. **47**(3): p. 241-249.
- [3] Martin, C., H. Winet, and J.Y. Bao, *Acidity near eroding polylactide-polyglycolide in vitro and in vivo in rabbit tibial bone chambers*. Biomaterials, 1996. **17**(24): p. 2373-2380.
- [4] Heidemann, W., *pH-stabilization of predegraded PDLA by an admixture of water-soluble sodiumhydrogenphosphate—results of an in vitro- and in vivo-study*. Biomaterials, 2002. **23**(17): p. 3567-3574.
- [5] Ahl, T., *Biodegradable fixation of ankle fractures: A roentgen stereophotogrammetric study of 32 cases*. Acta Orthopaedica, 1994. **65**(2): p. 166-170.
- [6] Kasuga, T., *Preparation of poly(lactic acid) composites containing calcium carbonate (vaterite)*. Biomaterials, 2003. **24**(19): p. 3247-3253.
- [7] Shikinami, Y., Y. Matsusue, and T. Nakamura, *The complete process of bioresorption and bone replacement using devices made of forged composites of raw hydroxyapatite particles/poly -lactide (F-u-HA/PLLA)*. Biomaterials, 2005. **26**(27): p. 5542-5551.
- [8] Kasuga, T., *Preparation and mechanical properties of polylactic acid composites containing hydroxyapatite fibers*. Biomaterials, 2000. **22**(1): p. 19-23.
- [9] Wright-Charlesworth, D.D., *In vitro flexural properties of hydroxyapatite and self-reinforced poly(L-lactic acid)*. Journal of Biomedical Materials Research Part A, 2006. **78A**(3): p. 541-549.
- [10] Hong, Z., *Nano-composite of poly(-lactide) and surface grafted hydroxyapatite: Mechanical properties and biocompatibility*. Biomaterials, 2005. **26**(32): p. 6296-6304.
- [11] Middleton, J.C. and A. Tipton, *Synthetic biodegradable polymers as medical devices*. Medical Plastic and Biomaterials, 1998. **5**: p. 30-39.
- [12] David D. Hile, Stephen A. Doherty, and Debra J. Trantolo, *Prediction of resorption rates for composite polylactide/hydroxylapatite internal fixation devices based on*

- initial degradation profiles*. Journal of Biomedical Materials Research Part B: Applied Biomaterials, 2004. **71B**(1): p. 201-205.
- [13] Proikakis, C.S., P.A. Tarantili, and A.G. Andreopoulos, *The role of polymer/drug interactions on the sustained release from poly(dl-lactic acid) tablets*. European Polymer Journal, 2006. **42**(12): p. 3269-3276.
- [14] Li, H. and J. Chang, *pH-compensation effect of bioactive inorganic fillers on the degradation of PLGA*. Composites Science and Technology, 2005. **65**(14): p. 2226-2232.
- [15] Shikinami, Y. and M. Okuno, *Bioresorbable devices made of forged composites of hydroxyapatite (HA) particles and poly L-lactide (PLLA). Part II: practical properties of miniscrews and miniplates*. Biomaterials, 2001. **22**(23): p. 3197-3211.
- [16] Rakmae, S., *Physical properties and cytotoxicity of surface-modified bovine bone-based hydroxyapatite/poly(lactic acid) composites*. Journal of Composite Materials, 2010. **45**(12): p. 1259-1269.
- [17] Weir, N.A., *Processing, annealing and sterilisation of poly-l-lactide*. Biomaterials, 2004. **25**(18): p. 3939-3949.
- [18] Weir, N.A., *Degradation of poly-L-lactide. Part 2: Increased temperature accelerated degradation*. Proceedings of the Institution of Mechanical Engineers, Part H: Journal of Engineering in Medicine, 2004. **218**(5): p. 321-330.
- [19] Aydin, E., J.A. Planell, and V. Hasirci, *Hydroxyapatite nanorod-reinforced biodegradable poly(l-lactic acid) composites for bone plate applications*. Journal of Materials Science: Materials in Medicine, 2011. **22**(11): p. 2413-2427.
- [20] Russias, J., *Fabrication and mechanical properties of HA/PLA composites: A study of in vitro degradation*. Materials Science and Engineering: C, 2006. **26**(8): p. 1289-1295.
- [21] Šupová, M., *Problem of hydroxyapatite dispersion in polymer matrices: a review*. Journal of Materials Science: Materials in Medicine, 2009. **20**(6): p. 1201-1213.

CHAPTER 7: ACCELERATED *IN VITRO* STUDY OF SURFACE MODIFIED HYDROXYAPATITE (HA) REINFORCED POLYLACTIC ACID COMPOSITE: A 56 DAY STUDY

7.1 Chapter 7 Abstract

The effects of degradation on the mechanical properties of polylactic acid (PLA)/hydroxyapatite (HA) nanofibers and short single-crystal HA whiskers were evaluated using an elevated temperature at 50 °C to accelerate PLA degradation. The surface of HA was first modified with a silane coupling agent and mixed with PLA at weight fractions of 0, 5, and 25 wt%. Mechanical testing specimens were fabricated via an injection molding procedure, then fully immersed in phosphate-buffered saline (PBS) at time intervals of 0, 3, 7, 14, 21, 28, and 56 days. At the end of each time interval, specimens were mechanically evaluated using three-point bending and were measured for changes in mass and dimension. The pH of fluid in the vicinity of degrading PLA and HA/PLA was also measured. Over the first 28 days of immersion (simulated 28 week), the surface modified with 5 wt% HA and 25 wt% HA samples retained 97.2% (115.2 ± 4.5 MPa) and 95.1% (105.4 ± 8.0 MPa) flexural strength, respectively, while the control pure PLA sample's flexural strength decreased by 71.0% (26.2 ± 20.2). The change in mass, cross section, and water absorption was not significantly affected by immersion. The result of the accelerated degradation of HA/PLA composites showed the enhancement in strength retention using a silane surface-modified HA while maintaining pH buffer and dimensional stability.

7.2 Introduction

The attractiveness of polymer absorbable materials, especially polylactic acid (PLA), for orthopedic fixation applications is primarily due to their ability to eliminate the need for secondary surgery which removes the implant after it has served its function. Unfortunately, clinically used PLA implants remain present long after healing has occurred. Complete *in vitro* degradation time at physiological temperatures of 37 °C was reported up to 5.7 years by Bergsma et al. and observed over 4 years clinically by Barber [1-3].

The complete degradation of Poly (L-Lactic acid) PLLA and PLLA/HA composites (HA particles) was well studied by Shikinami et. al. showing absorption periods up to 6 years [4]. Since these *in vivo* and *in vitro* degradation experiments can be extremely time consuming, the attractiveness of accelerated degradation testing has drawn attention in the absorbable polymer biomaterials field.

Bergsma et al. were one of the first groups to study accelerated degradation of PLLA and 96:04 PLLA:PLDA [2]. Under a temperature of 90 °C in a phosphate buffered saline solution, Bergsma found a observable correlation between accelerated degradation and physiologically degraded specimen [2]. Additionally, Weir et al. proposed the degradation mechanisms of PLLA at 50 and 70 °C similar to PLLA at 37 °C [5, 6]. However, Lyu et al. and Agrawal et al. observed distinct variations above the glass transition temperature (T_g) such as hydrolysis activation energies and difficulty fitting molecular weight data above the T_g of the PLA [7, 8].

The aim of the current study was to evaluate polylactic acid and hydroxyapatite (HA/PLA) composites for orthopedic fixation devices in accelerated simulated physiological environments to compare to physiological conditions. Based on literature review, an elevated temperature, although lower than the glass transition temperature, was chosen at 50 °C where the T_g of PLLA was 69 °C. Trials were conducted over 56 days of immersion in phosphate buffered saline (PBS). In vitro changes were evaluated by the mechanical three-point bending test (for flexural strength), scanning electron microscopy (SEM) (for fracture surface morphology), and pH testing in the vicinity of degrading composite.

7.3 Materials & Methods

7.3.1 Materials

Polylactic acid (PLA) was received from the Purac Company (Purac Biomaterials, Netherlands) in pellet form. Hydroxyapatite nanofibers (HANF) and short single-crystal whiskers (HA-w) were synthesized in house. HA nanofibers were synthesized using a wet precipitation method and fibers collected were 100 nm in width and 100 μ m in length. HA whiskers were synthesized from HA nanoparticles using the molten salt synthesis approach sized between 2–5 μ m in width and 10 μ m in length. Silane γ -MPS (3-(Trimethoxysilyl)propyl methacrylate) was received from Sigma-Aldrich (St. Louis, MO, USA).

7.3.2 Methods

PLA pellets as received were first milled in a cryogenic milling procedure and sieved to a powder size under 500 μ m. A silane coating was formed on HA nanofibers and HA whiskers in a similar process as compared to that of Rakmae et al. [9]. PLA

powder and modified HA nanofibers and whiskers were then combined at 0, 5, and 25 wt% in a mortar and pestle. Following mixing, flexural plate specimens were produced via injection molding.

HA/PLA composites as molded were fully immersed in phosphate buffered saline (PBS) as received from Sigma-Aldrich (Sigma-Aldrich, St. Louis, MO, USA) in fully sealed glass vials and stored at 50 °C in a Labnet mini incubator (Labnet International INC., Edison, NJ, USA). At intervals of 0, 3, 7, 14, 21, 28, and 56 days, HA/PLA composites were removed from the incubator for testing.

HA/PLA composites were mechanically tested on a three-point bending fixture with span length of 20 mm. Load and displacement were recorded to calculate flexural strength on an Instron 3367 universal testing machine (Instron, Grove City, PA, USA). Water absorption was calculated using Eq. 7.1, where dried mass is denoted as m_d , and wet mass as m_w . Weight loss was calculated from initial weight and weight after drying for two weeks or until stable at 50 °C in oven.

$$\text{Percentage mass change} = \frac{m_w - m_d}{m_d} \times 100\% \quad (7.1)$$

7.4 Results

7.4.1 Mechanical evaluation

Mechanical properties of the HA/PLA composite were evaluated by three-point bending. In Figure 7.1, the relationship between the flexural strength of HA/PLA composite and immersion time is demonstrated. Each datum point is the mean of 5 measurements with standard deviation.

As shown in Figure 7.1, initial dry state flexural strength of 5 wt% and 25 wt% HA composite demonstrate a vast increase compared to the pure PLA samples. The

flexural strength of the pure PLA was 90.5 ± 14.8 MPa. The HA/PLA composite with 5 wt% and 25 wt% HA had the flexural strength at 118.5 ± 2.6 MPa and 110.9 ± 3.09 MPa, respectively. The flexural strength was improved by 22.6% with 25 wt% HA and 31.0% with 5 wt%. After 14 days immersion, the mechanical strength of pure PLA flexural samples had decreased to 41.2 ± 14.7 MPa, a 54.5% reduction from the dry state. Conversely, samples containing HA maintained initial dry state strength. Moreover, 5 wt% and 25 wt% HA/PLA at 28 days immersion had flexural strengths of 115.2 ± 4.6 MPa and 105.4 ± 8.0 MPa, respectively. The pure PLA from the same immersion period had flexural strength of 26.2 ± 20.2 MPa, a 71.0% decrease. Following 56 days of immersion in PBS, all samples had a drastic decrease in flexural strength. Pure PLA samples could easily be broken when removing from vials or during mechanical testing setup.

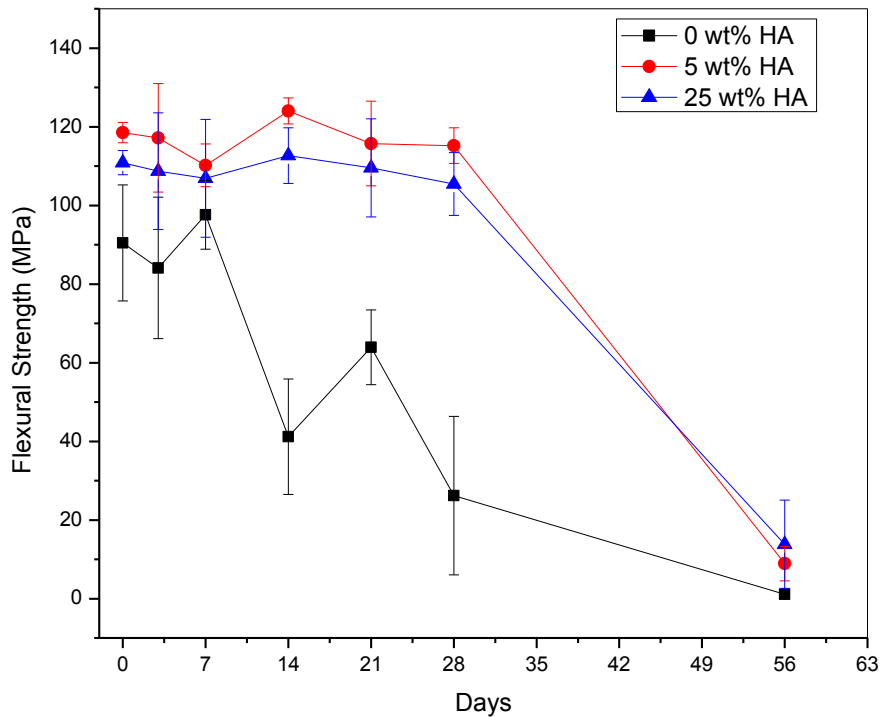


Figure 7.1. Variation of flexural strength with immersion time in PBS at 50 °C

7.4.2 Mass retention

Figure 7.2 shows the percentage of mass retention over the degradation intervals. Up to 28 days of immersion in PBS, there was no change in mass. Between days 28 and 56, the mass loss began. The mass loss of 5 wt% HA/PLA was 2.5% between days 28 and 56. Similarly, the 25 wt% HA/PLA experienced a mass loss of 4.0%, while the pure PLA had the greatest mass loss of 7.1% between days 28 and 56.

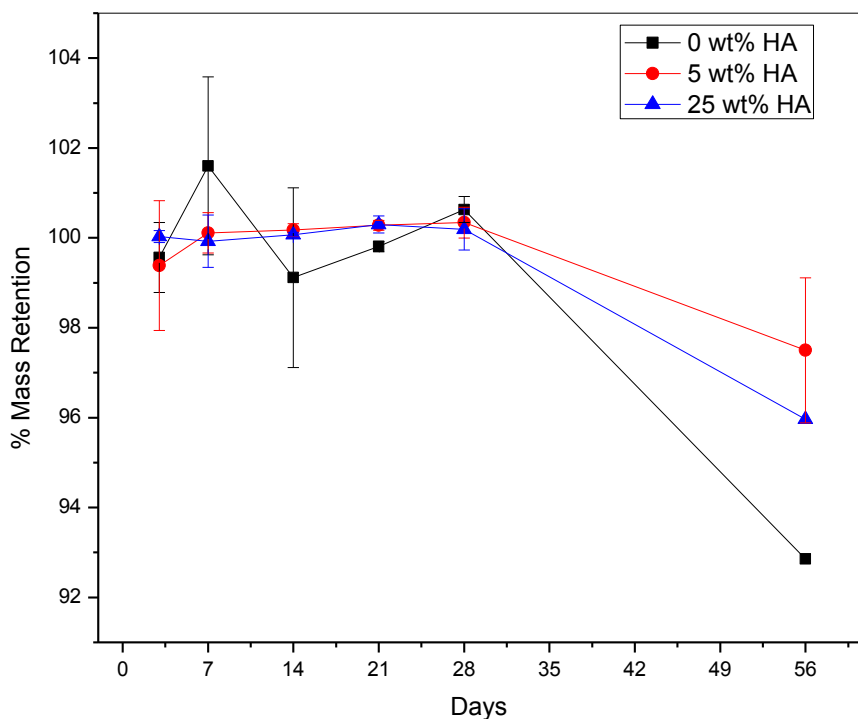


Figure 7.2. Variation of mass with immersion time in PBS at 50 °C

7.4.3 Visual examination

Initially before immersion, pure PLA samples were clear and transparent. After 7 days of immersion in PBS at 50 °C, pure PLA samples became opaque in color and were no longer transparent. This color change continued up to the day 14, after which there was no discernible difference based on immersion time. Samples which contain HA were initially white in color, and remained the same throughout the duration of the study.

7.4.4 Geometric examination and water absorption

Cross sectional area and water absorption of flexural mechanical testing specimen following various immersion times and mass fraction HA are summarized in Table 7.1. The cross sections of the flexural samples measured before and after immersion demonstrated large variations. From this test, no significant difference was observed at 0 wt%, 5 wt%, and 25 wt% which had a cross sectional increases of 0.9%, 1.3%, and 2.7%, respectively. Similarly, no significant variations in water absorption of immersed samples were observed. Water absorption following 56 days immersion period was 2.7%, 1.6%, and 2.2% for 0 wt%, 5 wt%, and 25 wt%, respectively.

Table 7.1. The cross section and water absorption variation of HA/PLA composite immersed in PBS at 50 °C

	Cross Sectional Area (%)			Water Absorption (%)		
	0 wt% HA	5 wt% HA	25 wt% HA	0 wt% HA	5 wt% HA	25 wt% HA
3 days	2.2 ± 1.5	3.7 ± 1.6	0.6 ± 1.3	3.3 ± 0.5	1.7 ± 1.8	1.6 ± 0.5
7 days	0.6 ± 1.8	3.0 ± 1.5	2.9 ± 1.3	0.7 ± 2.2	2.9 ± 1.1	2.7 ± 0.8
14 days	-0.1 ± 2.6	2.5 ± 2.5	0.2 ± 1.9	1.4 ± 2.4	0.8 ± 0.9	1.8 ± 0.1
21 days	2.4 ± 1.7	0.5 ± 1.3	-0.2 ± 2.0	1.0 ± 0.1	1.0 ± 0.2	1.8 ± 0.4
28 days	2.0 ± 1.4	0.3 ± 1.0	-1.6 ± 2.3	1.0 ± 0.8	1.3 ± 0.4	1.4 ± 0.4
56 days	0.9 ± 0.6	1.3 ± 6.6	2.7 ± 1.4	2.7 ± 0.3	1.6 ± 0.2	2.2 ± 1.3

7.4.5 pH evaluation

The changes in pH over the immersion period were recorded without replacing the PBS and are shown in Figure 7.3. The PBS was first buffered to 7.4 pH and sterilized in an autoclave. As shown in Figure 7.3, the pH of all samples remained relatively stable until 21 days, following which the pH of pure PLA samples rapidly decreased from 7.4 ± 0.1 pH to 2.5 ± 0.2 pH. Unlike the pure PLA samples, specimens with 5 wt% and 25 wt% HA remained 6.6 ± 0.2 pH and 6.7 ± 0.3 pH, respectively. Even after 56 days immersion, the pH of samples with HA remained higher than the pure PLA samples.

Additionally, in this trial unlike work previously presented by this research high mass fraction HA demonstrated a stable pH. This may be due to the lowered water absorption compared to unmodified HA nanofibers previously studied.

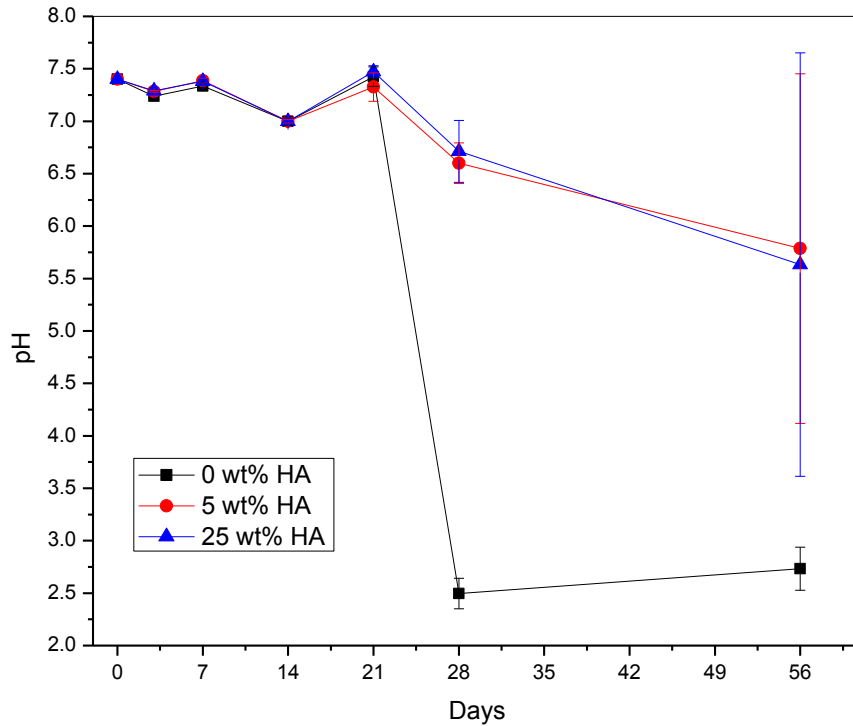


Figure 7.3. The pH variation over immersion intervals with various weight fraction HA.

7.5 Discussion

7.5.1 Accelerated degradation procedure

In the present study, an increased temperature was used to accelerate the degradation of the HA/PLA composite. Accelerated degradation of what has been well studied by Weir, Bergsma, Lyu, and others [2, 6, 7]. However, the examination of HA/PLA composites undergoing accelerated degradation has not been well studied. In the present study, previous data from an *in vitro* degradation at physiological temperatures were used for comparison. Based on published studies, an *in vitro* temperature was chosen under the T_g at 50 °C in order to avoid problems with hydrolysis

activation energy as warned by Agrawal and Lyu et al. [7, 8]. The mechanical strength of HA/PLA composites was recorded at 0, 3, 7, 14, 21, 28, and 56 days. Based on the work by Weir, these intervals approximately correlate to 0, 42, 89, 121, 147, 196, and 298 days from observed changes in molecular weight at 37 °C and 50 °C [6]. However, accelerated degradation tests may closely match early degradation. Caution was advised in late degradation similarities.

7.5.2 Mechanical evaluation

Flexural plate samples were tested under three-point bending. All samples were tested directly after removal from the incubator to conform to ASTM standard. Wong et al. presented a method for mechanical testing fully immersed specimens in PBS, and observed similar strength as those recorded other studies [10]. This method may more closely represent *in vivo* conditions but would not be comparable to previous results and other research studies.

HA is primarily used in orthopedic implants to increase mechanical strength and improve biological properties. The flexural strength increase of 31.0% with the addition of 5 wt% HA nanofibers demonstrated the significant value of using HA nanofiber instead of micro sized fillers to increase the mechanical strength. However, in order to achieve the biological benefit from HA, a higher mass fraction was desired. In orthopedic absorbable devices, 25 wt% calcium phosphate ceramic filler has been a common composite loading rate. In order to achieve this loading rate without degradation of strength, a micro sized HA whisker was used. Since increasing the loading HA nanofiber has been shown to decrease the strength from previous studies due to problems with mixing, the present study combined 5 wt% HA nanofiber with a 20 wt% HA whisker to

create a flexural strength of 110.9 ± 3.1 MPa which maintained a 93.5% strength improvement over the use of 5 wt% HA nanofiber alone.

The mechanical strength of the 5 wt% and 25 wt% HA both demonstrated a maintained strength up to 28 days (which in this research is equivalent to 28 simulated weeks at physiological temperature), while the pure PLA sample lost 71.0% of its strength in the same time period. Note that 28 weeks serves as the standard for completion of the healing process. Similar results were demonstrated by Hile using 25 wt% HA particles [11]. However, after 24 weeks, the strength rapidly decreased and after 50 weeks, the retained strength was less than 20%. Additionally, Russias et al. observed a sharp decrease in strength at 2 days in *Hank's balanced salt solution (HBSS)* by GIBCO[®] and lost 81.8% after 20 days of immersion [12]. However, Russias' HA/PLA composite contained much higher loading, up to 85 wt% HA whiskers [12].

The maintained strength of HA/PLA composites up to 28 days is of vital importance as this correlates to 28 weeks immersion at physiological temperature as shown by Weir. In soft tissue fixation application, such as used in anterior cruciate ligament surgery, typical healing is nearly complete beginning at 24 weeks when patients are told they can return to normal activities [13].

7.6 Conclusions

The accelerated degradation of HA/PLA composite was similar to previous testing of 5 wt% HA nanofiber at 37 °C. The similarities in the two tests validate the use of acceleration in vitro test. The tests conducted in this research to evaluate various different HA/PLA composites in a short time period are essential to the improvement of composites for final use in composite construction of orthopedic fixation devices. The

accelerated degradation of HA/PLA composites in PBS at 50 °C were evaluated based on flexural strength, mass retention, visual change, cross sectional area change, and water absorption. The strength retention as noted up to 28 days in both 5 wt% and 25 wt% HA gives an excellent demonstration of the capability of HA/PLA composites for use in orthopedic fixation devices. Furthermore, 28 days correlates to 28 weeks at physiological temperature, a time at which complete healing should have occurred. Additionally, HA/PLA composites were not drastically effected by immersion. The results from the present study lends positively to the future use of HA/PLA composites.

References

- [1] Bergsma JE, de Bruijn WC, Rozema FR, Bos RRM, Boering G: Late degradation tissue response to poly(l-lactide) bone plates and screws. *Biomaterials* 1995, 16(1):25-31.
- [2] Bergsma JE, Rozema FR, Bos RRM, Boering G, Joziase CAP, Pennings AJ: In vitro predegradation at elevated temperatures of poly(lactide). *Journal of Materials Science: Materials in Medicine* 1995, 6(11):642-646.
- [3] Barber FA, Dockery WD: Long-Term Absorption of Poly-L-Lactic Acid Interference Screws. *Arthroscopy: The Journal of Arthroscopic & Related Surgery* 2006, 22(8):820-826.
- [4] Shikinami Y, Matsusue Y, Nakamura T: The complete process of bioresorption and bone replacement using devices made of forged composites of raw hydroxyapatite particles/poly -lactide (F-u-HA/PLLA). *Biomaterials* 2005, 26(27):5542-5551.
- [5] Weir NA, Buchanan FJ, Orr JF, Farrar DF, Boyd A: Processing, annealing and sterilisation of poly-l-lactide. *Biomaterials* 2004, 25(18):3939-3949.
- [6] Weir NA, Buchanan FJ, Orr JF, Farrar DF, Dickson GR: Degradation of poly-L-lactide. Part 2: Increased temperature accelerated degradation. *Proceedings of the Institution of Mechanical Engineers, Part H: Journal of Engineering in Medicine* 2004, 218(5):321-330.
- [7] Lyu, Schley J, Loy B, Lind D, Hobot C, Sparer R, Untereker D: Kinetics and Time-Temperature Equivalence of Polymer Degradation. *Biomacromolecules* 2007, 8(7):2301-2310.
- [8] Agrawal C, Huang D, Schmitz J, Athanasiou K: Elevated temperature degradation of a 50: 50 copolymer of PLA-PGA. *Tissue Engineering* 1997, 3(4):345-352.
- [9] Rakmae S, Ruksakulpiwat Y, Sutapun W, Suppakarn N: Physical properties and cytotoxicity of surface-modified bovine bone-based hydroxyapatite/poly(lactic acid) composites. *Journal of Composite Materials* 2010, 45(12):1259-1269.
- [10] Wong S, Wu JS, Leng Y: Mechanical Behavior of HA/PLA Composite in Simulated Physiological Environment. *Key Engineering Materials* 2005, 288-289:231-236.
- [11] Hile DD, Doherty SA, Trantolo DJ: Prediction of resorption rates for composite polylactide/hydroxylapatite internal fixation devices based on initial degradation profiles. *Journal of Biomedical Materials Research* 2004, 71B(1):201-205.

- [12] Russias J, Saiz E, Nalla RK, Gryn K, Ritchie RO, Tomsia AP: Fabrication and mechanical properties of HA/PLA composites: A study of in vitro degradation. *Materials Science and Engineering: C* 2006, 26(8):1289-1295.
- [13] Vavken P, Sadoghi P, Murray MM: The Effect of Platelet Concentrates on Graft Maturation and Graft-Bone Interface Healing in Anterior Cruciate Ligament Reconstruction in Human Patients: A Systematic Review of Controlled Trials. *Arthroscopy: The Journal of Arthroscopic & Related Surgery* 2011, 27(11):1573-1583.

CHAPTER 8: PARAMETRIC ANALYSIS AND OPTIMIZATION OF ORTHOPEDIC INTERFERENCE SCREWS IN RELATION TO PULLOUT RESISTANCE

8.1 Chapter 8 abstract

Orthopedic soft tissue fixation using bioabsorbable interference screws has been widely used in anterior cruciate ligament reconstruction. For this application, pullout is accepted as the benchmark for comparison between interference screw devices. A multi-objective parametric study and optimization methodology was applied, consisting of the finite element analysis method, Taguchi method[®], and artificial neural network. Two dimensional axisymmetric finite element models for the pullout of the interference screw were developed and arranged on an L8 orthogonal array. These simulations were used to calculate two objective values for analysis (maximum screw and bone von Mises stresses) while altering thread width, thread radius, proximal and distal half angle, root radius, minor diameter, and thread pitch. From the parametric study, the greatest contributing factors to minimizing the maximum stress in screw and bone were the minor diameter (39.1% screw, and 52.7% bone) and screw thread half angles (32.3% screw, and 16.5% bone). Artificial neural networks were used to estimate an optimal design which had the lowest stresses in both the screw and bone. The near optimal solutions of the interference screw were obtained by a random search method. The results showed that the near optimal designs had lowered stress in both the screw (1.8%) and the bone (11.8%). The neurogenic approach effectively decreased the time and effort required in determining the near optimal design.

8.2 Introduction

In previous research a novel polymer nanocomposites with improved elastic modulus and mechanical strength was developed in order to better provide orthopedic fixation in soft tissue surgeries such as anterior cruciate ligament reconstruction (ACLR). Due to improvements in material properties it is of critical importance to develop and optimize devices which can best utilize the enhanced material properties.

Although pullout force of interference screws is not the most common mode of failure, pullout testing is often utilized in the development of orthopedic fixation screw devices [1-5]. This method is commonly used as it can give a general idea of screw strength to compare to existing interference screw devices.

The evaluation of the bone stresses generated during pullout is complex and not easily solved by analytical methods. Therefore, the necessity of finite element analysis (FEA) is often required. There are three types of FEA considered for solving this problem as shown in literature: axisymmetric, two-dimensional and three-dimensional [6-9]. Two-dimensional models are flawed in that stresses outside the plane of analysis are disregarded, while 3D models require large number of elements and, consequently, long calculation times. The axisymmetric model can be regarded as a good compromise between 2D and 3D, where the only simplification is that the screw thread is modeled as a disk.

Bone material is mostly modeled in literature as isotropic, elastic, and homogeneous material, while in reality bone is anisotropic because of its trabecular structure [10]. In this study bone was considered to be isotropic to obtain general results

and was defined by elastic modulus, Poisson's ratio, and density. The polymer nanocomposite was modeled in a similar fashion.

In the literature, geometric parameters of the screw geometry are generally considered as pitch, proximal and distal half angles [3, 4, 8]. Several authors have considered fillet and root radius, while many models have sharp edges [11]. These sharp edges in interference screws have led to graft lacerations in ACLR, which is undesirable in soft tissue fixation applications. The present study determines the critical geometric parameters which most influence the pullout strength of orthopedic interferences screws. Various models were developed using the mechanical properties of newly developed polymer nanocomposites containing polylactic acid (PLA) and Hydroxyapatite (HA). A parametric analysis was undertaken to assess how pullout strength of the interference screw system varies for different values of thread width, thread radius, proximal and distal half angle, root radius, minor diameter, and thread pitch.

8.3 Materials and Methods

8.3.1 Finite Element Model

The model shown in Figure 8.1 was developed using Abaqus 6.9 FEA software (Dessault Systems). The bone consists of cancellous bone modeled as an isotropic homogenous material with a density of 0.47 g/cm^3 , Poisson's ratio of 0.33, and elastic modulus of 0.66 GPa. The polymer nanocomposite (HA/PLA) was modeled as an isotropic, homogenous material with Poisson's ratio of 0.45 and elastic modulus of 4.5 GPa. The constraints and boundary conditions corresponding to a pullout test are shown in Figure 8.1. In this model, the created screw was cut from the bone model to form a perfect fitting screw in bone. The meshes of the bone and screws were defined using a

global seeding of 0.05. A 4-node bilinear axisymmetric quadrilateral meshing was used. The mean number of elements generated per model was 73,502.

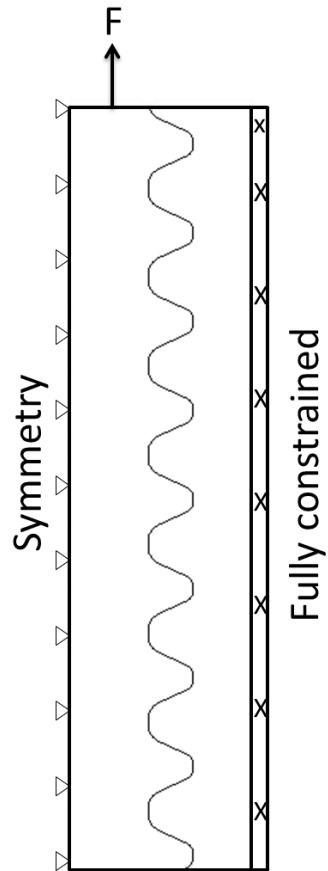


Figure 8.1 Set-up for FEA pullout test

8.3.2 Taguchi Method[®] for parametric study

With the Taguchi method[®], six different design variables of an interference screw thread were considered: thread width, thread radius, proximal and distal half angle, root radius, minor diameter, and thread pitch. With these variables, an L8 orthogonal array was selected which included six parameters and two levels. The remaining screw variables were kept constant. This method leads to the creation of eight different models to be analyzed in the FEA simulation. All screws were modeled with symmetric distal

and proximal half angles, and the pitch remained constant along the screw axis. The general geometries of the simulated screws and the mesh details are summarized in Figure 8.2 and Table 8.1.

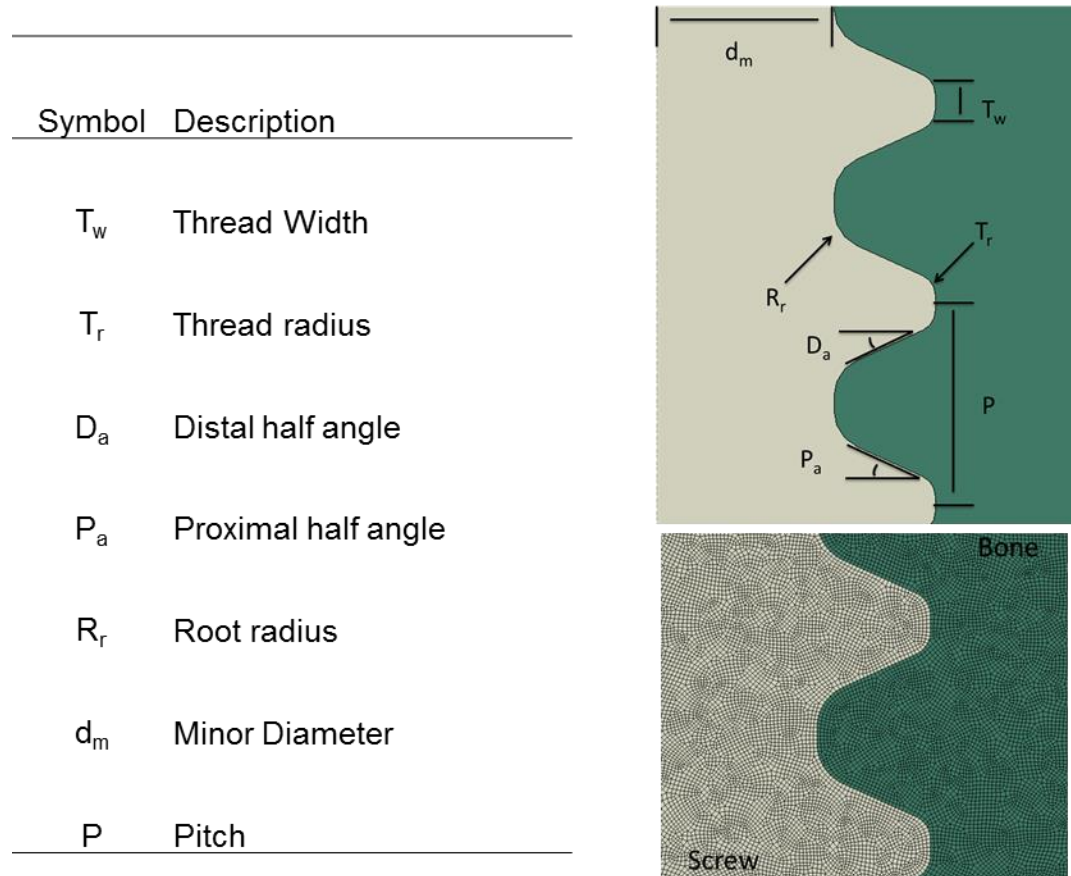


Figure 8.2 Screw geometric parameters and detail of mesh.

Table 8.1 Geometric parameters of screws

Screw Model	Thread Width (mm)	Thread radius (mm)	P/D angle	Root radius (mm)	minor Diameter(mm)	Pitch (mm)
1	0.62	0.31	103.55	0.57	2.55	2.74
2	0.62	0.31	103.55	0.63	2.81	2.88
3	0.62	0.34	114.45	0.57	2.55	2.88
4	0.62	0.34	114.45	0.63	2.81	2.74
5	0.68	0.31	114.45	0.57	2.81	2.74
6	0.68	0.31	114.45	0.63	2.55	2.88
7	0.68	0.34	103.55	0.57	2.81	2.88
8	0.68	0.34	103.55	0.63	2.55	2.74
Opt.	0.62	0.33	114.33	0.53	2.29	1.93

8.3.3 Artificial Neural Network

Interference screw thread geometry was optimized using an artificial neural network (ANN). A three-layer architecture consisting of six input neurons, three hidden neurons, and one output neuron, was used in the present study. The hidden layer had three neurons where a hyperbolic tangent function was used as an activation function. The number of learning iterations used was 12,000. The learning rate was 0.5, and the momentum for learning was 0.25.

Optimal values for iterations, learning rate, and momentum were obtained using an iterative process to increase convergence while minimizing the time. The ANN validation was performed by removing two of our eight function sets. The ANN was then taught using the remaining six function sets and were tested against the two removed function sets. Based on this method it was determined 12,000 iterations were sufficient to predict the objective values of removed function sets. This process was done several times to ensure the accuracy of the prediction. Next, ten additional designs were created,

which were used to further validate our ANN; these designs were also used in additional training. From the 18 sets, an optimal design was generated by the ANN through a random search which minimized the maximum von Mises stress on the screw and bone. The ANN was coded using python 2.7 and modified from an existing module program [12].

8.4 Results

Figure 8.3 shows the von Mises contour plot of screw from Experiment 3. From these plots the maximum von Mises stresses were recorded in the screw and in the bone of each evaluated screw. These maximum stresses were used to minimize the stress in the screw and bone during pullout. As shown in Figure 8.3, the highest stress in the screw is localized on the inner portion of the first few threads of the screw while the highest stress in the bone is located at the tip of the screw thread. Furthermore, limited stress is shared by the last few threads of the interference screw.

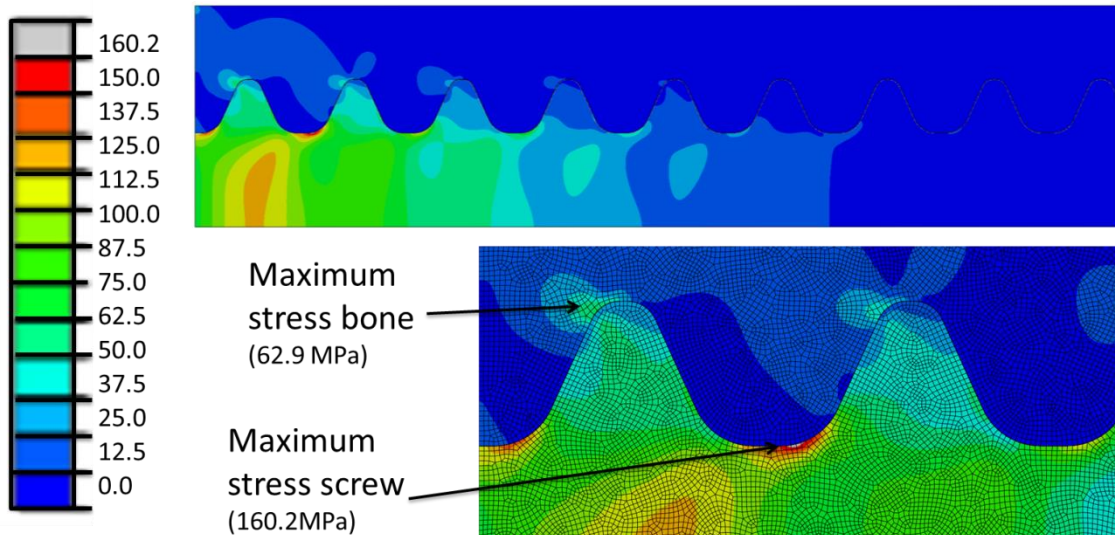


Figure 8.3 Maximum von Mises stress resulting from pullout of Screw6

The Taguchi method[®] used in the parametric study of the maximum von Mises stress of the interference screw geometry reveals the effects of thread width, thread radius, proximal and distal half angles, root radius, minor diameter and pitch on pullout resistance. Based on the signal-to-noise plot shown in Figure 8.4, the major contributing factors to the maximum stress in the screw and bone were proximal and distal half angles and minor diameter. The contribution of each of these factors as percentages is shown in Table 8.2.

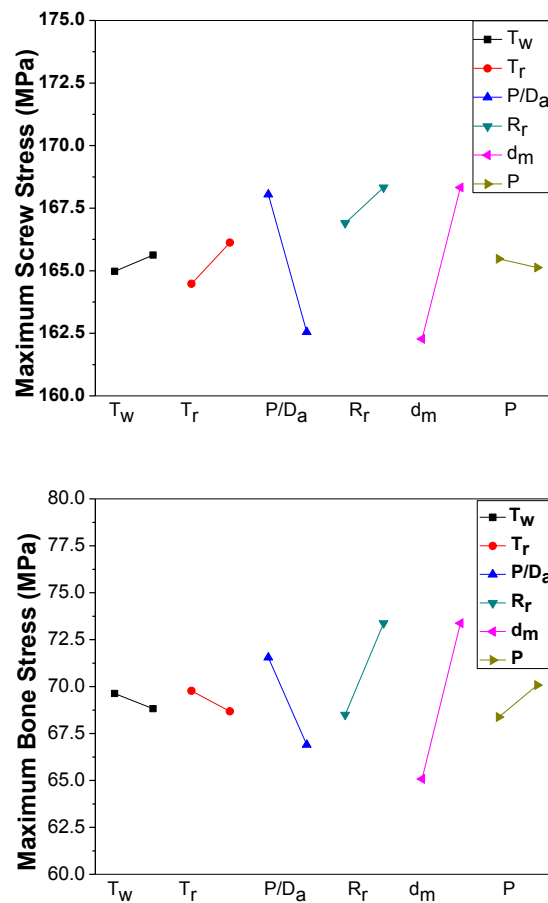


Figure 8.4 Signal to noise plots of the total von Mises stress at each level of each design parameter.

Table 8.2 Percentage contribution of thread geometric parameter to screw and bone maximum stress

	Screw (%)	Bone (%)
Thread Width (T_w)	0.5	0.5
Thread radius (T_r)	2.9	0.9
Proximal/Distal half angle (P/D_a)	32.3	16.5
Root radius (R_r)	25.0	27.1
Minor Diameter (d_m)	39.1	52.7
Pitch (P)	0.1	2.2

Table 8.3 shows the effectiveness of the artificial neural network in optimizing the thread geometry of an interference screw. With the use of the ANN, both the screw stress and bone stress were minimized, with the maximum screw stress decreased by 1.8% and the maximum bone stress decreased by 11.8%.

Table 8.3 Maximum von Mises stress in screw and bone from finite element analysis

Screw Model	Screw Stress (MPa)	Bone Stress (MPa)
1	166.9	66.6
2	166.9	78.4
3	160.2	62.9
4	165.9	70.6
5	165.6	69.8
6	158.5	64.3
7	174.9	74.7
8	163.5	66.5
Optimal	155.7	55.5

The stress distribution between threads in the screw and bone are shown in Figure 8.5. In the screw, the maximum stress was found in the second thread of every examined screw. The bone however, had the highest stress at the first thread, and stress decreased at every thread thereafter.

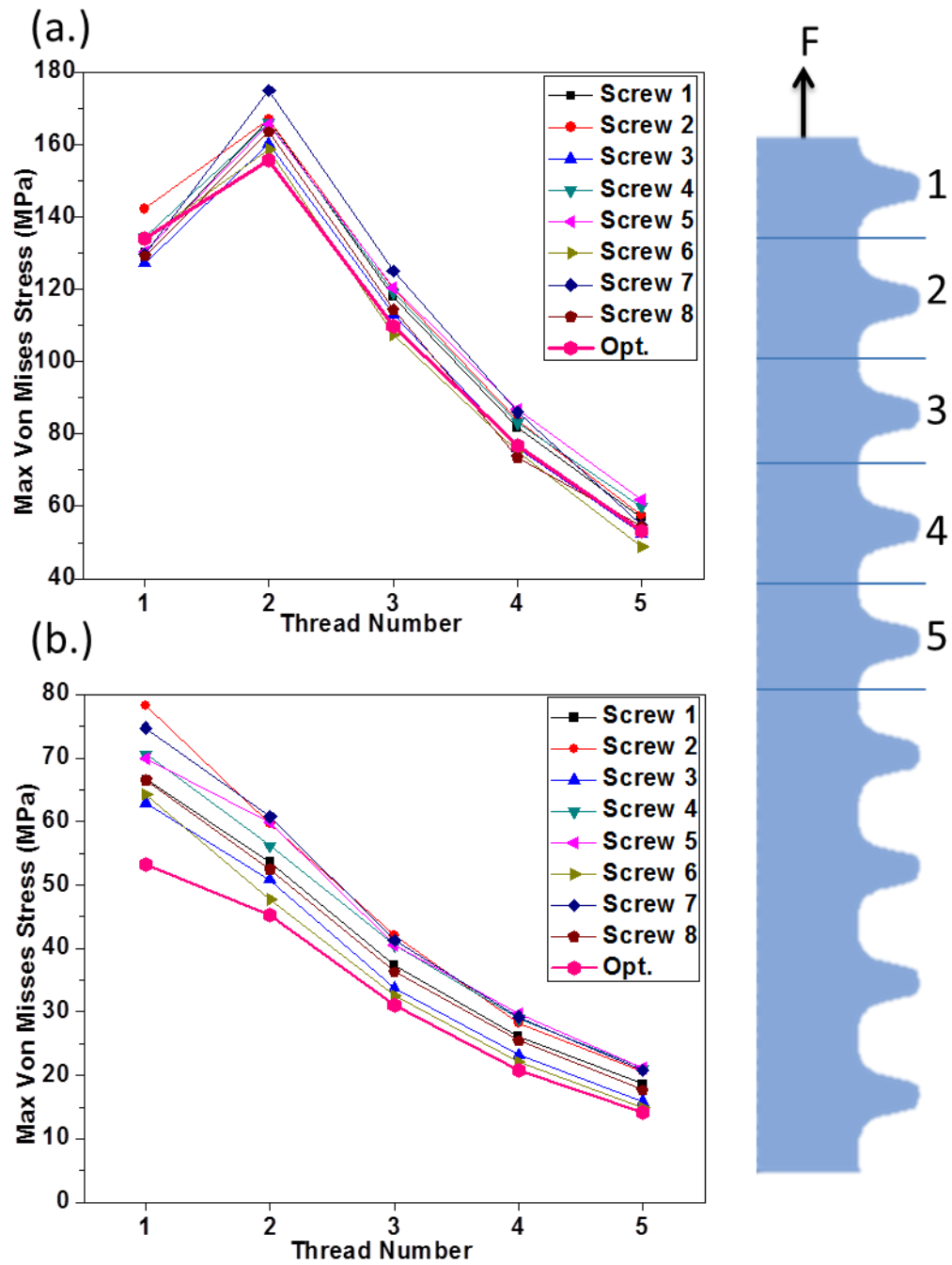


Figure 8.5 Stress distributions between screw and bone thread geometry in screw (a) and bone (b)

8.5 Discussion

8.5.1 FEA

In the present study, an FEA-based Taguchi Method was employed to evaluate the pullout strength of interference screws and to assess the effects of thread geometry. Pullout strength has been widely accepted as a means to evaluate orthopedic screws, specifically for comparison of interference screws. The pullout strength of interference screws is closely related to their structures [3, 11]. In particular, the thread geometry may markedly affect the pullout resistance more so than would the material properties of the screw [11]. Therefore the preliminary evaluations using FEA limits the number of devices necessary for prototyping and evaluation.

The FEA analysis in the present study gave the location of the maximum stress in the first few threads of the screw and bone. This is common for this loading method [13, 14], though better sharing of the load may be beneficial for orthopedic devices. It may also be beneficial to consider a push-out test of interference screws, as interference screws may experience this loading type in anterior cruciate ligament reconstruction.

The influence of mesh density was studied in this FEA model by altering the mesh size and measuring the effect on maximum stress. It was found that stress concentrations rose at the inner root of the thread in the screw and at the tip of the screw in the bone when mesh size became too large. For numerical stability the mesh density was refined in order to avoid stress concentrations. At a seed size of 0.1 these artifacts were removed and 0.05 was chosen to ensure stability over all modeled screw geometries. The FEA model for pullout testing was designed to mimic testing setup for future validation studies.

8.5.2 Taguchi Method

The Taguchi robust design method is a scientifically disciplined tool for evaluating improvements and conducting analyses in materials, products, equipment, and processes. The improvements in the present study enhanced the desired overall performance of interference screw thread geometry. The Taguchi Method[®] largely reduced the number of experimental trials necessary for FEA.

The Taguchi[®] robust design method lends itself well to FEA [15] and is a powerful tool for improving the quality of engineering designs. This method reduces the number of experimental trials while still accurately measuring the sensitivity to variation. With fractional factorial design and using an L8 orthogonal array, only eight models were required. An L8 orthogonal array evenly distributes the effect of the interaction between any pair of factors over the columns and gives the most realistic simulation of the actual effects of the parameters [16]. Among the geometric parameters of the screw thread, the proximal and distal half angle and minor diameter were the most important in determining maximum stress in the bone and screw. This result is understandable as a larger half angle should avoid large stress risers in the screw thread between screw and bone. Additionally, the smaller minor diameter allows for more stress to be distributed in the bone. Since the screw was modeled in two dimensions with a symmetric plane, the effect of inner drivers, common on interference screws, was not considered, nor was the rotation of the thread geometry. In the present study, the interference screw was considered as a disk geometry. In future studies a three dimensional model should be considered.

8.5.3 Artificial Neural Network (ANN)

Hsu et al. [17] and Chao et al. [18] have used a neural genetic approach to effectively analyze and optimize orthopedic bone screws. Much like a biological network, an artificial neural network utilizes a network of neurons to perform a specific function or task. In an artificial neural network, artificial neurons are created to perform this function or task and estimate a cost [19]. The learning algorithm will search through the solution space to find a function that has the smallest possible cost. In this research, an ANN was used to gain understanding of an interference screw thread geometric design and to avoid creating a large number of models. This dramatically reduced time on developing models and computation. In order to utilize the benefits of an ANN, the program must be taught. In learning, the program can find connections that minimize the cost of each variable change. For this study, a supervised back propagation artificial neural network was utilized. Supervised learning was utilized because we had a relatively large data set sample from the Taguchi orthogonal array. Back propagation method is a form of supervised learning where the cost of a function is known or can be calculated. In this method, the ANN was taught using a normalized set of from the taguchi orthogonal array. The cost or outputs which were used for learning are the outputs from each of the models for maximum von Mises stress in the bone and screw calculated by finite element analysis. In this method, the weights of each connection were updated at each iteration of the training set so as to more accurately predict the cost of each function set.

The approach in the present study was able to minimize the stress in both the bone and the screw simultaneously, though the percentage decrease in the screw was only

1.8% compared to the lowest stress in the screw in the first eight experiments. The lowest stress in the bone from Experiment 3 (62.9 MPa) had a maximal stress in the screw of 160.2 MPa (a 2.8% reduction from optimal). Similarly, the minimal stress in the screw Experiment 6 (158.5 MPa) had a maximum bone stress in of 64.3 MPa (a 13.7% reduction). Additionally, the bone is considered to be the weaker material, which makes it more susceptible to failure. Not only was the maximum von Mises stress in the bone and screw reduced, the distribution of stress throughout the screw was also observed, especially in the bone where the optimal screw had the lowest maximum stress at every thread (Figure 8.5).

8.6 Conclusions

An FEA model of an orthopedic interference screw was constructed and evaluated to understand the effects of geometric parameters on pullout stress. It was demonstrated that the minor diameter and half angle had the greatest effect by using the Taguchi Method[®] and an L8 orthogonal array. This information will be very valuable for future orthopedic bone screw devices that are required to resist pullout as a mode of failure. With the use of an artificial neural network the interference screw geometry minimized the maximum stresses by 1.8% and 11.8% in the screw and bone, respectively. The ANN approach effectively reduced the time and effort required for searching the optimal design. However, the FEA model and optimized screw require experimental testing in order to validate and confirm the solution as the optimal interference screw design.

References

- [1] Barber, F.A., O. Hapa, and J.A. Bynum, *Comparative Testing by Cyclic Loading of Rotator Cuff Suture Anchors Containing Multiple High-Strength Sutures*. Arthroscopy: The Journal of Arthroscopic & Related Surgery, 2010. **26**(9, Supplement): p. S134-S141.
- [2] Barber, F.A. and M.A. Herbert, *Cyclic Loading Biomechanical Analysis of the Pullout Strengths of Rotator Cuff and Glenoid Anchors: 2013 Update*. Arthroscopy: The Journal of Arthroscopic & Related Surgery, 2013. **29**(5): p. 832-844.
- [3] Chapman, J., *Factors Affecting the Pullout Strength of Cancellous Bone Screws*. Journal of Biomechanical Engineering, 1996. **118**: p. 391-398.
- [4] Wang, Y., *Proximal half angle of the screw thread is a critical design variable affecting the pull-out strength of cancellous bone screws*. Clinical Biomechanics, 2009. **24**(9): p. 781-785.
- [5] Zantop, T., et al., *Graft Laceration and Pullout Strength of Soft-Tissue Anterior Cruciate Ligament Reconstruction: In Vitro Study Comparing Titanium, Poly-D,L-Lactide, and Poly-D,L-Lactide–Tricalcium Phosphate Screws*. Arthroscopy: The Journal of Arthroscopic & Related Surgery, 2006. **22**(11): p. 1204-1210.
- [6] Abshire, B.B., *Characteristics of pullout failure in conical and cylindrical pedicle screws after full insertion and back-out*. Spine Journal, 2001. **1**(6): p. 408-414.
- [7] Gefen, A., *Optimizing the biomechanical compatibility of orthopedic screws for bone fracture fixation*. Medical Engineering & Physics, 2002. **24**(5): p. 337-347.
- [8] Gefen, A., *Computational simulations of stress shielding and bone resorption around existing and computer-designed orthopaedic screws*. Medical and Biological Engineering and Computing, 2002. **40**(3): p. 311-322.
- [9] Zhang, Q.H., S.H. Tan, and S.M. Chou, *Investigation of fixation screw pull-out strength on human spine*. Journal of Biomechanics, 2004. **37**(4): p. 479-485.
- [10] Currey, J.D., *Bones : structure and mechanics*. [2nd ed. 2006, Princeton, N.J. ; Oxford: Princeton University Press. xii, 436 p.
- [11] Suchenski, M., *Material Properties and Composition of Soft-Tissue Fixation*. Arthroscopy: The Journal of Arthroscopic & Related Surgery, 2010. **26**(6): p. 821-831.

- [12] Schemenauer, N. *Python Stuff*. 2004 [cited 2011 5/24]; Available from: <http://arctrix.com/nas/>.
- [13] Zanetti, E.M., *Parametric analysis of orthopedic screws in relation to bone density*. The open medical informatics journal, 2009. **3**: p. 19.
- [14] Budynas, R.G. and J.K. Nisbett, *Shigley's mechanical engineering design*. 2008: McGraw-Hill New York.
- [15] Dar, F.H., J.R. Meakin, and R.M. Aspden, *Statistical methods in finite element analysis*. Journal of Biomechanics, 2002. **35**(9): p. 1155-1161.
- [16] Fowlkes, W.Y., C.M. Creveling, and J. Derimiggio, *Engineering methods for robust product design: using Taguchi methods in technology and product development*. 1995: Addison-Wesley Reading.
- [17] Hsu, C.C., J. Lin, and C.K. Chao, *Comparison of multiple linear regression and artificial neural network in developing the objective functions of the orthopaedic screws*. Computer methods and programs in biomedicine, 2010.
- [18] Chao, C.-K., *A Neurogenetic Approach to a Multiobjective Design Optimization of Spinal Pedicle Screws*. Journal of Biomechanical Engineering, 2010. **132**(9): p. 091006.
- [19] Michalski. *The Machine Learning Dictionary*. 2011 [cited 2011 5/10]; Available from: <http://www.cse.unsw.edu.au>

APPENDIX I: FABRICATION AND MECHANICAL EVALUATION OF HYDROXYAPATITE AND POLYLACTIC ACID (HA/PLA) NANOCOMPOSITES USING HOT PRESSING

A.1 Appendix I Abstract

In the present study, hydroxyapatite (HA) nanofibers were incorporated into a bioabsorbable polylactic acid (PLA) composite to form HA/PLA nanocomposites using a hot pressing process. The objective of this combination was to improve mechanical strength. In this fabrication method, polymer resin was completely dissolved in methylene chloride and combined with HA using mechanical mixing and sonication. The HA/PLA solution was then dried and hot-pressed uniaxially into specimens for three point bending evaluation. Three point bending results from hot pressed samples indicated flexural strength increased with more hydroxyapatite mass fraction by 25.8% with 5 wt% to 143.6 MPa. Furthermore, the HA nanofibers' mass fraction, up to 25 wt%, was examined, and demonstrated an increase in modulus up to 4 GPa, a 150% increase. Additionally, the hot pressed samples scanning electron microscopy (SEM) of the fracture surface from the three point bend test revealed good dispersion from 5 wt% to 20 wt% for HA nanofiber mass fraction. HA/PLA composites with greater nanofiber loading demonstrated the formation of fiber bundles and areas without nanofibers. From this test, the influence of HA nanofibers, using a hot pressing process, has shown improvement to the HA/PLA nanofibers by improving the HA/PLA nanocomposite's flexural strength, flexural modulus, and the material's viability for orthopedic fixation application.

A1.2 Introduction

In the orthopedic fixation field polylactic acid (PLA) has proven viable as a bioabsorbable polymer in the composition of interference screws, suture anchors and craniomaxifacial plates [1-3]. PLA has demonstrated excellent properties, including biocompatibility, stress sharing, implant absorption not requiring removal, and superior imaging characteristics, as compared to metal counterparts [4-6]. These beneficial properties led to the increased use of PLA interference screws compared to metal. However, pure PLA devices have several disadvantages. Pure PLA devices are substantially weaker than the metal screws, have risk for inflammatory response [5] and have shown little bone bonding potential [7-10].

The concerns of inflammatory response and bone bonding potential associated with pure PLA devices have been well studied. Hunt et al. showed an increase in bone bonding with the addition of hydroxyapatite (HA) [11]. The subsequent improved biological properties of HA/PLA composites and have heightened the critical need to increase the mechanical strength of absorbable polymer devices for use in orthopedic fixation applications [12-14].

The studied mechanical reinforcement of PLA typically utilizes particles or microsized fibers of ceramic material, typically HA or calcium phosphate [15-18]. In the present study, HA nanofibers are used to improve the composite mechanical strength. HA is widely used in orthopedic fixation applications due to its similarity to the mineral component of bone [14]. The addition of HA is shown to have a near linear increase in the flexural modulus but has demonstrated limited reinforcement and typically decreases the overall strength of the PLA [19, 20]. Surface modification to the HA nanofibers have

been considered and are believed to increase the interface between the PLA polymer and HA to improve mechanical properties [21-25]. However, limited increase in strength has been observed.

In order to investigate the influence of the HA nanofibers and PLA matrix, a processing method was chosen to limit the effect of other variables. Polymer nanocomposites, such as HA/PLA, have demonstrated good processability using many fabrication techniques, such as injection molding, casting, and transfer molding [15, 21, 26, 27]. In order to study the influence of only HA nanofibers in PLA for mechanical reinforcement, this investigation used hot pressing. Hot pressing is a form of transfer molding chosen for its ease of operation, ability to simulate the temperature and pressure experienced in the HA/PLA industrial production method, and low cost. PLA has demonstrated sensitivity to high temperature, greatly impacting PLA's mechanical properties [15, 28]. Moreover, in order to limit the temperature experienced by the hot pressing procedure, an experiment was conducted based on the Taguchi Method[®] to develop ideal processing parameters and reduce the time in which the HA/PLA composite was held above melting temperature [29]. The primary goals of the Taguchi Method[®] are to 1) focus on a consistent iterative procedure, regardless of the variation in materials or process effects and 2) to design the product in such a way that the variables cannot alter the results. Taguchi made sure that the causes of variation (noise) were dealt with so that their effect on the robustness of the final procedure is minimal. This processing method was established as the primary protocol to form near ideal processing parameters using hot pressing of PLA. This ensures that only HA nanofibers are considered as the reinforcement and not due to processing changes.

The aim of the present study was to determine the effect of fiber filler on the structure and mechanical properties of HA/PLA composite. This was accomplished by fabricating HA/PLA composite under uniaxial pressure at elevated temperature. An evaluation of the mechanical flexural strength was determined using three point bending to define material flexural modulus and strength. HA fiber dispersion was investigated using scanning electron microscopy (SEM) to evaluate the fiber dispersion from the three point bending fracture surface. Furthermore, the processing procedure was used to evaluate the feasibility of transfer molding for HA/PLA composite biomaterial fabrication.

A1.3 Materials and Methods

A1.3.1 Hydroxyapatite nanofiber

HA nanofiber material was fabricated by a chemical precipitation method. The synthesis procedure was modified from Zhan's method for producing HA nanorods [30]. In this synthetic process, calcium nitrate, sodium dihydrogen phosphate dihydrate, gelatin, and urea were combined in an aqueous solution. The solution was then heated to 95 °C and kept at that temperature for 72 hours. Following this, HA nanofibers were filtered, washed with distilled water, and dried at room temperature. In this synthesis, the final dimensions of the nanofiber bundles are 5-20 μm in width and 100-200 μm in length. The HA nanofibers were used to make an HA/ PLA composite in mass fraction from 0 to 25 wt% as displayed in Figure A1.1.

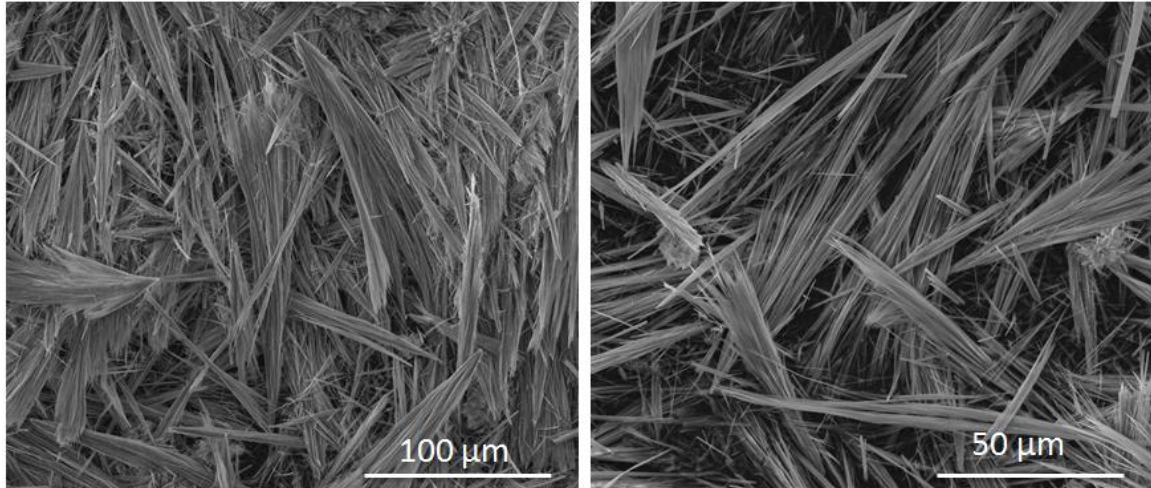


Figure. A1.1. Hydroxyapatite fibers created by chemical precipitation method.

A1.3.2 Polylactic acid

Commercially available, high molecular weight, medical grade PLA, was received from PURAC Company (PURAC Biomaterials, Netherlands). PLA pellets were used with pellet size ranging between 1-4 mm.

A1.3.3 HA nanofiber surface modification

A surface modification of the HA nanofiber procedure, similar to the methods employed by Zhang et al., was explored in the present study [22]. In this procedure, 5 grams of HA nanofibers were added to a 5 wt% Trimethoxy(propyl)silane (γ -MPS) (Sigma-Aldrich, St.louis, MO, USA) solution containing 70% acetone and 30% DI water. The mixture was heated to 50 °C for 3 hours with constant magnetic stirring, followed by additional heating at 60 °C for 5 hours. Once this process had been completed, the mixture was filtered and washed to remove the residual γ -MPS and dried in the oven (Isotemp oven model 655f, Fisher Scientific, Agawam, MA, USA) at 110 °C [22-24].

A1.3.4 Hot pressing fabrication of PLA & HA/PLA

After HA nanofibers were dried, the nanofibers were milled with mortar and pestle. The PLA pellets were processed by the solvent method alone. Entrapment of HA in PLA was achieved by using a similar processing strategy to that employed by Kasuga et al. [31]. In the present study, 30 g of polylactic acid was dissolved in 300 ml methylene chloride (Sigma-Aldrich, St. Louis, MO, USA). Once fully dissolved, HA nanofibers, in appropriate mass fraction, were added by weight percent from 0 to 25 wt%. Nanofiber dispersion was enhanced by mechanical mixing and sonication with an ultrasonic horn (Branson Sonifier 450, Branson Ultrasonics, Danbury, CT, USA). Samples were then dried at room temperature in a beaker in a vacuum oven to remove toxic residue of methylene chloride in composite. After 48 hours, samples were removed and weighed to ensure the majority of the methylene chloride was evaporated and methylene chloride further be removed at high temperature in hot pressing. This experimental setup can be separated into several crucial steps and is depicted in sequential order in Figure A1.2. This processing procedure was studied with the use of the Taguchi Method[®] to obtain a near ideal processing procedure while limiting temperature and time [29, 32]. Once near ideal processing parameters in the hot pressing application were established, experimental procedures were strictly controlled to ensure repeatability.



Figure.A1.2. The complete hot pressing procedure:(A) pure PLA pellets and methylene chloride solution are first added; (B) pellets are completely dissolved in methylene chloride solution (C) HA is mixed with PLA using ultra-sonic horn and mechanical assistance (D) methylene chloride solvent forms an HA/PLA solution (E) Methylene chloride is evaporated using a vacuum oven (F) from vacuum oven HA/PLA emerges as a composite disk (G) Hot pressing procedure yields (H) mold removal and (I) samples are cut and tested under three point bending on an universal texture analyzer.

In a fabrication procedure, similar to that used in literature [15, 31], round disk-like structures, due to the geometry of the beaker, prepared with the solvent method, are placed directly into a stainless steel mold for a flat plate specimen 64.5 mm X 64.5 mm

and 3.2 mm in thickness. Great care was taken in fabrication of the mold to ensure parallelism in thickness. Parallelism of the top and bottom surface of the mold is required to ensure that polymer cannot escape from the mold at high pressure. The sample is placed in the bottom platen and allowed to heat from direct contact. The upper platen is lowered to a height similar to the height of the disk. After 20 minutes, the disk begins to melt and the upper platen is lowered further to better distribute heat to the polymer specimen. Both heating platens temperature was controlled at 217 °C with no pressure applied to the sample. After an additional 20 minutes, the upper platen was once again repositioned to further heat the polymer disk. The platen then stays at this position for 10 minutes to finish the melting process. Next, the sample was pressed at 16,000 pounds of force, which is equivalent to 2,500 psi on the molded specimen. Once pressed, the sample was removed from the press and air quenched until reaching room temperature. Again processing parameters were chosen based on the Taguchi Method[®] in order to minimize exposure time to temperature and optimized strength [29]. After the sample had sufficient time for cooling, it was removed from the mold. The samples were further processed by using a diamond saw to cut samples 6 mm in width to conform to ASTM standard D790 [33].

A1.3.5 Taguchi method

A taguchi method was used to establish near ideal processing parameters for the hot pressing procedure using an L8 orthogonal array. In this procedure, milling time, ultrasonic horn time, ultrasonic horn percent power, vacuum oven time, pressure, press time, and annealing temperature were evaluated with other variables remaining the same, as shown in Table A1.1.

Table A1.1 Parameters evaluated for fabrication of HA/PLA composite using Taguchi method

Levels	1	2
Milling (min.)	1	5
Ultra Sonic Horn (min.)	1	5
Vacuum Oven(hr.)	24	48
Press Time (min.)	5	10
Pressure(lbs.)	16,000	20,000
Annealing (°C)	25	110
Ultrasonic horn (% power)	50	80

A1.3.6 Mechanical testing: three point bending

The flexural properties of the hot pressed specimens were tested from controlled rate testing of a rectangular cross-section, as prescribed by ASTM standard D790 [33]. A three point bending mechanical evaluation technique was used for the evaluation of HA/PLA composite subjected to a hot pressing procedure and is shown in Figure A1.3. This test gathers information of flexural strength, flexural modulus, and failure mode.

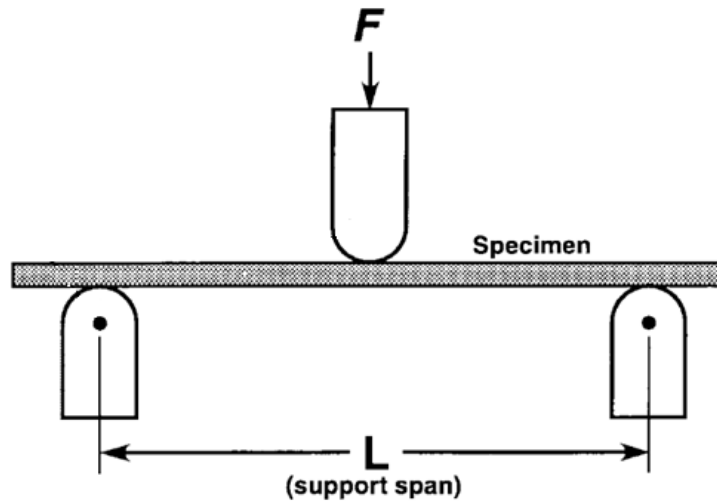


Figure A1.3. Schematic diagram of the three point flexural test designed according to ASTM standard D790 [1].

Using the three point bending test, stress is measured using the Equation A1.1 below:

$$\text{Stress} = \sigma = \frac{3FL}{2bd^2} \quad (\text{A1.1})$$

where F is the force, L is the length of the support span, b is the base dimensions and d is the depth dimension. Similarly, Equation A1.2 is given for strain as

$$\text{Strain} = \epsilon = \frac{6Dd}{L^2} \quad (\text{A1.2})$$

where D is given as the deflection. From this information, flexural modulus and stress at failure can be computed [33]. HA/PLA composite specimens were tested on a universal texture analyzer three point bending apparatus using a 20 mm support span with a controlled rate at 5 mm/min. A minimum of four specimens were tested to calculate flexural strength and flexural modulus, averages, and standard deviations.

A1.3.7 Scanning electron microscope fracture surface

Scanning electron microscopy (SEM) was used to characterize the structure and dispersion of the HA nanofibers from the fracture surface of the three point bending specimens. Samples were platinum coated to reduce charging effect and to better visualize nanofiber dispersion. An accelerating voltage of 5kV was used to examine the fracture surface following three point bending using SEM (FEI Quanta 600F environmental scanning electron microscope, FEI Co, Hillsboro, OR, USA) as shown in figure A1.4.



Figure A1.4. Scanning electron microscope (SEM Quanta) used to image the fracture surface of HA/PLA composite.

A1.4 Results

A1.4.1 Mechanical testing

The Taguchi Method[®] was very useful to allow for near ideal processing parameters to be utilized in the formation of HA/PLA composites. As shown in Figure A1.5, the variation between processing was 104.7 ± 6.9 MPa (Experiment 8) to 130.7 ± 15.1 MPa (Experiment 3). Additionally, gained from the Taguchi Method was the effect of temperature to flexural strength, where strength degradation was present with increased exposure to temperature.

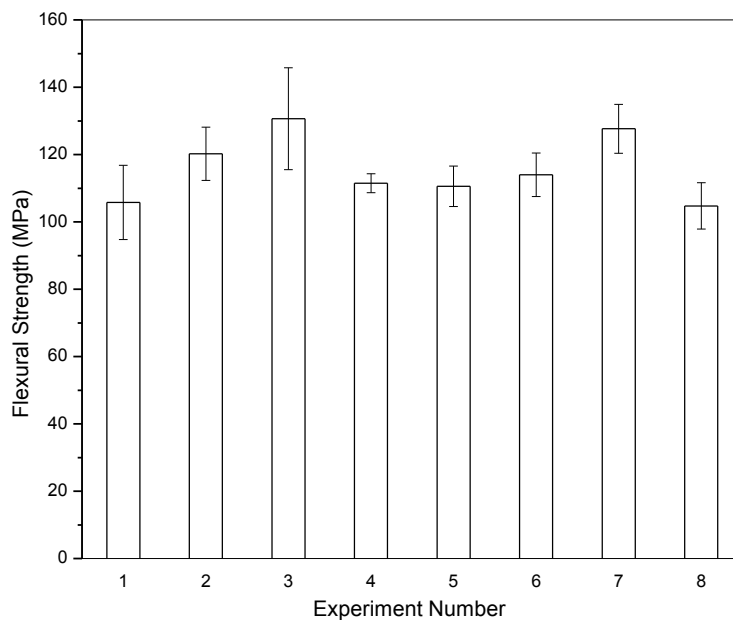


Figure A1.5. Flexural strength from Taguchi method[®] for processing study.

The three point bending test with HA nanofibers revealed a maintained or enhanced mechanical strength of the HA/PLA composite material. This is demonstrated in Figure A1.6, where flexural strength is maintained between 10 and 20 wt% hydroxyapatite (HA) in polylactic acid (PLA), when compared to pure PLA. The HA/PLA composite reached a peak in strength at 5 wt% HA a 25.8 percent increase. Overall, the HA/PLA composite samples maintained or had limited decrease in strength with fiber loading up to 25 wt%. The flexural modulus was increased from 1.6 GPa to almost 4 GPa, as shown in figure A1.7, which is similar to human bone, which has a flexural modulus between 3-20 GPa.

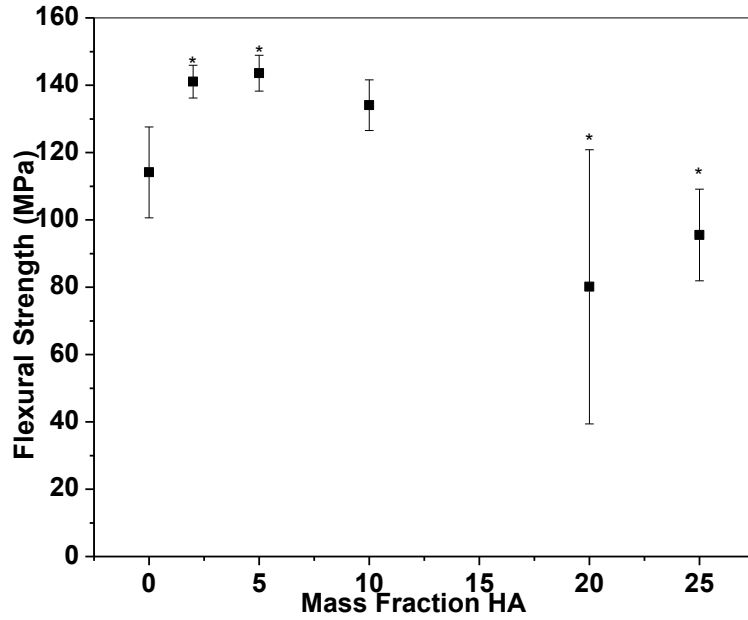


Figure A1.6. Flexural strength average from hot pressed samples of PLA with silane modified HA fibers (* $P < 0.05$)

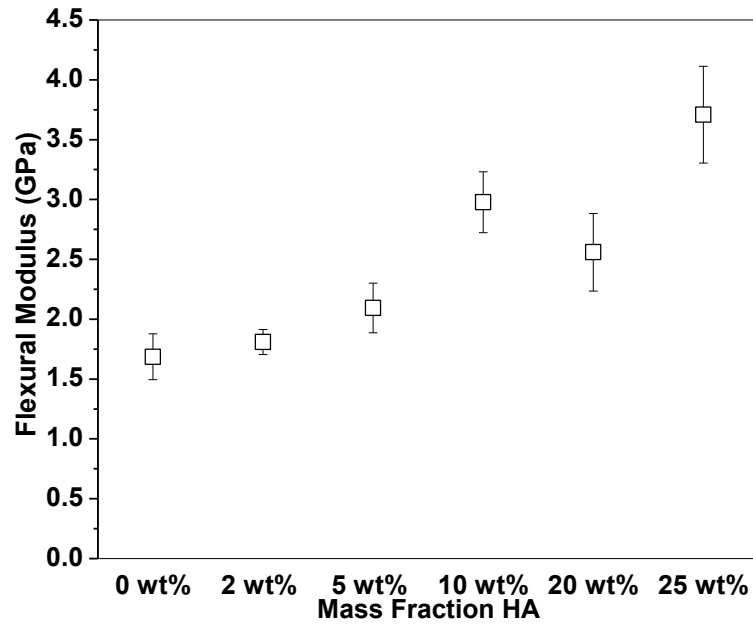


Figure A1.7. Flexural modulus PLA and HA/PLA for hot pressed samples

In addition to the flexural strength and modulus, a stress strain relationship from the three point bending test was created and is shown in Figure A1.8. With this information, the failure mode can be better explained. In the PLA control specimen, a distinct peak is observed prior to its final rupture. This feature is broadened with the

addition of the hydroxyapatite nanofibers. This can be observed as a more ductile failure, and the HA/PLA composite material bends substantially before its final failure. With the addition of 25 wt%, a return of the neat PLA fracture mode occurs, and a more brittle failure is observed.

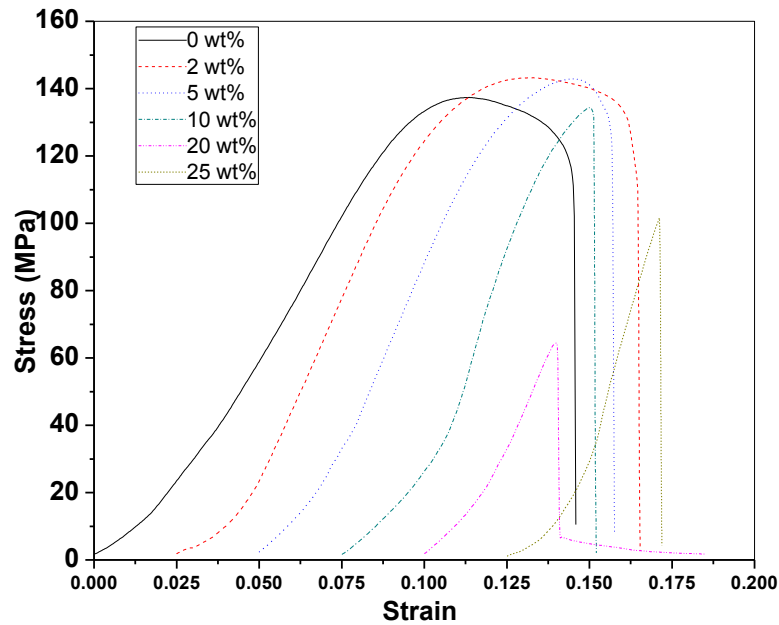


Figure A1.8. Stress versus strain graph of high molecular weight PLA and HA/PLA for hot pressed samples where an offset of .025 was used for visualization purpose.

A1.8.2 Scanning electron microscope

Following three point bending test, fractured surfaces from hot pressed specimens were evaluated using scanning electron microscopy, as shown in Figure A1.9. Good fiber dispersion was exhibited in nanofiber mass fraction to approximately 20 wt%, whereby the formation of HA nanofiber bundles were observed, which could not be removed using the solvent processing and sonication method. Little fiber pull-out was observed in any fracture surface micrograph, which can indicate a limited fiber matrix interface. Additionally, as the HA nanofiber mass fraction in composite is increased, the area of

fiber bundles also increased. This can be seen in Figure A1.7 at 25 wt% HA; obvious areas of pure PLA were observed.

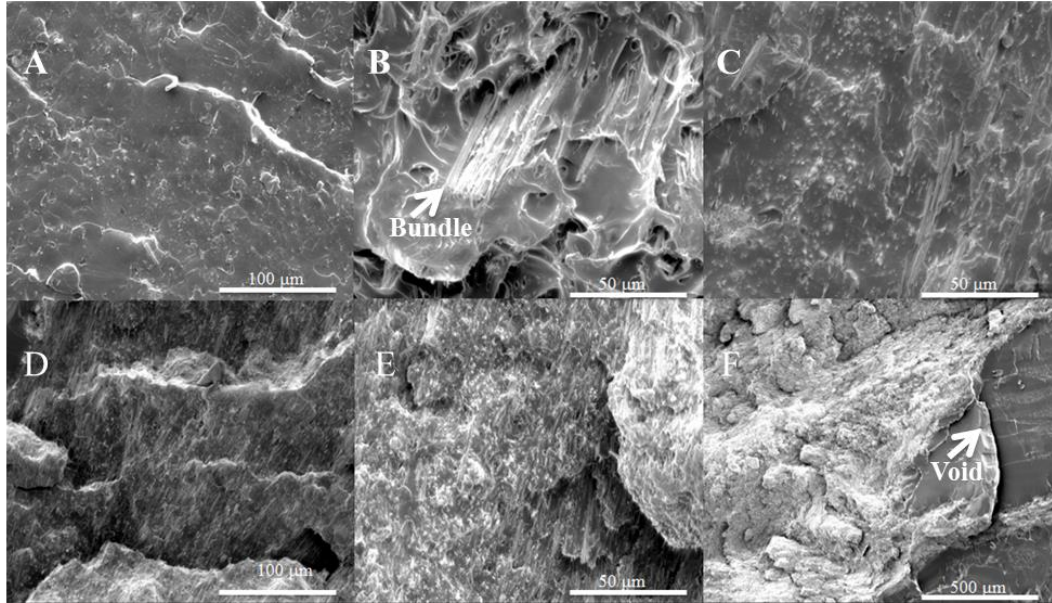


Figure A1.9. Scanning electron micrograph of fracture surface of hot pressed specimen under three point bending: (A) pure PLA (B) 5% HA (C) 10% HA (D) 15% HA (E) 20% HA (F) 25% HA

A1.9 Discussion

The design and fabrication of HA/PLA composites with increased mechanical properties were achieved with heat and high pressure in a hot pressing application. The hot pressing parameters were studied with the use of the Taguchi Method[®]. This was to ensure near ideal processing parameters were used for the HA/PLA composite synthesis, similar to result demonstrated by Olsson et al. [34]. The Taguchi Method revealed the sensitivity of PLA and HA/PLA composites to temperature greater than melting temperatures (190 °C) and time of exposure to temperature. This sensitivity is similar to that described by Altpeter and Ignjatovic in their study of HA/PLA composites using hot pressing [15, 28]. Unfortunately, there was great variability in control samples from

sample to sample and batch to batch. This was observed as the difference in each of the experimental controls where the pure PLA control samples ranged from 70 MPa to 115 MPa in some trials even though the processing parameters remained unchanged. This variability in the processing limits the feasibility of this processing technique for medical devices in the future.

The solvent processing method was a concern for further use in medical applications due to the solvent being unsuitable for use in the human body. Complete solvent removal is critical and was ensured by weight measurement. The solvent residue in the processing evaluated by Kasuga et al. [31] was completely removed and verified with laser Raman spectra after 8 hours evaporation at 25 °C. Specimens in the present study were subjected to 48 hours in a vacuum oven at the same temperature which represents an effort to ensure that all solvent would be removed. However, further work should be done to verify complete removal of solvent in the composite.

The HA/PLA improvements in the modulus were similar to that found in literature [19, 20, 36]. However, in the present study, the flexural strength is greatly increased with the incorporation of HA nanofiber. The greatest enhancement in flexural strength of HA/PLA composite is shown with the addition of 5 wt% nanofiber with silane surface modification. An improvement from 115 MPa (PLA control) to 140 MPa is shown with 5 wt% silanized HA nanofibers in PLA. With this composite, a 66% increase in the flexural modulus was also observed. This result is very promising, as typically the reinforcement effect with the addition of the HA only represents a mass fraction of 5-10%. With this processing technique, only flexural three point bending tests were made, so there is no data regarding the tensile strength. The improvement in the modulus and

maintenance of the flexural strength make HA a strong candidate for PLA reinforcing materials. Further mechanical evaluations should be considered before applying as a permanent reinforcing material, such as tensile testing, where the dispersion of filler will better be examined and have a high sensitivity to agglomerations of filler, as shown by Shikinami, where a decreased reinforcing effect was observed [36].

The SEM images demonstrated good dispersion of the nanofibers in the PLA similar to the dispersion observed in literature [16, 31, 35]. However, the solvent mixing method did not always achieve the same uniformity. This was shown as a large nanofiber bundle in the 5 wt% HA/PLA composite fracture surface. The silane coupling agent used in this study proved to be an excellent choice based on dispersion and mechanical evaluation. Furthermore, this is similar to Rakmae's evaluation of silane as a coupling agent recommended in the production of HA/PLA composites with HA particles [24]. In the present study, limited pull-out of fiber was observed from SEM micrograph from the PLA matrix. The limited pull-out can be an indication of a weak interface between the PLA and HA material. Further study of silane coupling agents is needed to better understand the interaction between PLA and HA nanofiber.

A1.10 Conclusion

Hot pressing a form of transfer molding, utilizes temperature and pressure to form well dispersed HA/PLA composite specimens. The dispersion of the HA nanofibers in the PLA matrix to 20 wt% indicates that silane is a good coupling agent for use with PLA composites. Though good dispersion was observed up to 20 wt%, the increase in strength was not increased past 10 wt% HA nanofiber concentration. However, it was demonstrated that the increase in mass fraction of HA nanofibers did positively impact

the flexural modulus to obtain a similar value as human bone (4.1GPa, 25 wt%). Increasing to 25 wt% HA/PLA composite did not demonstrate an increase in strength, but it may still be beneficial for non-load-bearing medical devices. In this procedure, it was observed that the reinforcing enhancement of mechanical properties can be observed with HA nanofiber mass fraction of 5 wt%. An improvement from 114.1 MPa pure PLA to 143.6 MPa is shown with 5 wt% HA nanofiber in PLA (25.8%) and a 66 % improvement in modulus. This increase in the modulus and flexural strength demonstrates the composite's potential for use in the biomedical field. However, further investigation in fiber dispersion, reinforcement, and mass fractions should be more thoroughly examined in future research.

References:

- [1] Garlotta, D., *A Literature Review of Poly(Lactic Acid)*. Journal of Polymers and the Environment, 2001. **9**(2): p. 63-84.
- [2] Douglas, T., *Porous polymer/hydroxyapatite scaffolds: characterization and biocompatibility investigations*. Journal of Materials Science: Materials in Medicine, 2009. **20**(9): p. 1909-1915.
- [3] Daniels, A.U., *Mechanical properties of biodegradable polymers and composites proposed for internal fixation of bone*. Journal of Applied Biomaterials, 1990. **1**(1): p. 57-78.
- [4] Hall, M.P., D.M. Hergan, and O.H. Sherman, *Early fracture of a bioabsorbable tibial interference screw after ACL reconstruction with subsequent chondral injury*. Orthopedics, 2009. **32**(3): p. 208.
- [5] Gefen, A., *Optimizing the biomechanical compatibility of orthopedic screws for bone fracture fixation*. Medical Engineering & Physics, 2002. **24**(5): p. 337-347.
- [6] Hou, S.-M., *Mechanical tests and finite element models for bone holding power of tibial locking screws*. Clinical Biomechanics, 2004. **19**(7): p. 738-745.
- [7] Andreas Weiler, *Biodegradable Implants in Sports Medicine: The Biological Base*. The Journal of Arthroscopic and Related Surgery, 2000. **16**(03).
- [8] Barber, F.A. and W.D. Dockery, *Long-Term Absorption of Poly-L-Lactic Acid Interference Screws*. Arthroscopy: The Journal of Arthroscopic & Related Surgery, 2006. **22**(8): p. 820-826.
- [9] Park, M.C. and J.E. Tibone, *False Magnetic Resonance Imaging Persistence of a Biodegradable Anterior Cruciate Ligament Interference Screw With Chronic Inflammation After 4 Years In Vivo*. Arthroscopy: The Journal of Arthroscopic & Related Surgery, 2006. **22**(8): p. 911.e1-911.e4.
- [10] Marumo, K., *MRI study of bioabsorbable poly-L-lactic acid devices used for fixation of fracture and osteotomies*. Journal of Orthopaedic Science, 2006. **11**(2): p. 154-158.

- [11] Hunt, J. and J. Callaghan, *Polymer-hydroxyapatite composite versus polymer interference screws in anterior cruciate ligament reconstruction in a large animal model*. Knee Surgery, Sports Traumatology, Arthroscopy, 2008. **16**(7): p. 655-660.
- [12] Grayson, M., *Encyclopedia of composite materials and components*. Encyclopedia reprint series. 1983, New York: J. Wiley. xxviii, 1161 p.
- [13] Bayraktar, H.H., *Comparison of the elastic and yield properties of human femoral trabecular and cortical bone tissue*. Journal of Biomechanics, 2004. **37**(1): p. 27-35.
- [14] Orlovskii, V.P., V.S. Komlev, and S.M. Barinov, *Hydroxyapatite and Hydroxyapatite-Based Ceramics*. Inorganic Materials, 2002. **38**(10): p. 973-984.
- [15] Ignjatovic, N., *Evaluation of hot-pressed hydroxyapatite/poly-L-lactide composite biomaterial characteristics*. Journal of Biomedical Materials Research, 2004. **71B**(2): p. 284-294.
- [16] Murariu, M., *Polylactide compositions. Part 1: Effect of filler content and size on mechanical properties of PLA/calcium sulfate composites*. Polymer, 2007. **48**(9): p. 2613-2618.
- [17] Ambrose, C.G. and T.O. Clanton, *Bioabsorbable Implants: Review of Clinical Experience in Orthopedic Surgery*. Annals of Biomedical Engineering, 2004. **32**(1): p. 171-177.
- [18] Wong, S., J.S. Wu, and Y. Leng, *Mechanical Behavior of PLA/HA Composite in Simulated Physiological Environment*. Key Engineering Materials, 2005. **288-289**: p. 231-236.
- [19] Hile, D.D., S.A. Doherty, and D.J. Trantolo, *Prediction of resorption rates for composite polylactide/hydroxylapatite internal fixation devices based on initial degradation profiles*. Journal of Biomedical Materials Research, 2004. **71B**(1): p. 201-205.
- [20] Wright-Charlesworth, D.D., *In vitro flexural properties of hydroxyapatite and self-reinforced poly(L-lactic acid)*. Journal of Biomedical Materials Research Part A, 2006. **78A**(3): p. 541-549.
- [21] Fried, J.R., *Polymer science and technology*. 2nd ed. 2003, Upper Saddle River, NJ: Prentice Hall Professional Technical Reference. xvii, 582 p.

- [22] Zhang, S.M., *Molecular Modification of Hydroxyapatite to Introduce Interfacial Bonding with Poly (Lactic Acid) in Biodegradable Composites*. Key Engineering Materials, 2005. **288-289**: p. 227-230.
- [23] Zhang, H.-p., *Molecular dynamics simulations on the interaction between polymers and hydroxyapatite with and without coupling agents*. Acta Biomaterialia, 2009. **5**(4): p. 1169-1181.
- [24] Rakmae, S., *Physical properties and cytotoxicity of surface-modified bovine bone-based hydroxyapatite/poly(lactic acid) composites*. Journal of Composite Materials, 2010. **45**(12): p. 1259-1269.
- [25] Wang T., *Improve the Strength of PLAHA Composite Through the Use of Surface Initiated Polymerization and Phosphonic Acid Coupling Agent*. Journal of research of the National Institute of standards and Technology, 2011. **116**: p. 785-796.
- [26] Menges, G., W. Michaeli, and P. Mohren, *How to make injection molds*. 3rd ed. 2001, Munich, Cincinnati: Hanser ; Distributed in USA by Hanser Gardner Publications. xvii, 612 p.
- [27] Malloy, R.A., *Plastic part design for injection molding : an introduction*. 1994, Munich ; New York Cincinnati: Hanser Publishers ; Hanser/Gardner Publications. xii, 460 p.
- [28] Altpeter, H., *Non-conventional injection molding of poly(lactide) and poly(ϵ -caprolactone) intended for orthopedic applications*. Journal of Materials Science: Materials in Medicine, 2004. **15**(2): p. 175-184.
- [29] Taguchi, G.B., S. Chowdhury, and Y. Wu, *Taguchi's quality engineering handbook*. 2005, Hoboken, N.J. Livonia, Mich.: John Wiley; ASI Consulting Group. xxxii, 1662 p.
- [30] Zhan, J., *Biomimetic Formation of Hydroxyapatite Nanorods by a Single-Crystal-to-Single-Crystal Transformation*. Advanced Functional Materials, 2005. **15**(12): p. 2005-2010.
- [31] Kasuga, T., *Preparation and mechanical properties of polylactic acid composites containing hydroxyapatite fibers*. Biomaterials, 2000. **22**(1): p. 19-23.

- [32] Fowlkes, W.Y. and C.M. Creveling, *Engineering methods for robust product design: using Taguchi methods in technology and product development*. Engineering process improvement series. 1995, Reading, Mass.: Addison-Wesley Pub. Co. xxiv, 403 p.
- [33] *Standard Test Method for Determination of Modulus of Elasticity for Rigid and Semi-Rigid Plastic Specimens by Controlled Rate of Loading Using Three-Point Bending*. Annual Book of ASTM Standards, 2002. **08**(01): p. 4.
- [34] Olsson, N.E.J., T.S. Lundström, and K. Olofsson, *Design of experiment study of compression moulding of SMC*. *Plastics, Rubber & Composites*, 2009. **38**(9/10): p. 426-431.
- [35] Russias, J., *Fabrication and mechanical properties of PLA/HA composites: A study of in vitro degradation*. *Materials Science and Engineering: C*, 2006. **26**(8): p. 1289-1295.
- [36] Shikinami, Y. and M. Okuno, *Bioresorbable devices made of forged composites of hydroxyapatite (HA) particles and poly-L-lactide (PLLA): Part I. Basic characteristics*. *Biomaterials*, 1999. **20**(9): p. 859-877.

VITA

Richard Joseph Lebens III

Permanent Address: 253 Penwood Court, Chesterfield, MO, 63017

The author Richard Joseph Lebens III was born in Wichita, Kansas, USA in 1985. His family moved to the St. Louis area in 1989. He attended the University Missouri in Columbia Missouri from 2004 to 2008 and received a Bachelor of Science in Mechanical Engineering in 2008. He began work toward a Doctorate of philosophy in Mechanical Engineering at the University of Missouri College in 2009.

Richard began his pursuit of a doctoral degree funded by the GAANN fellowship. After that Richard worked as a TA in introduction to materials and was a graduate research assistant in the mechanical engineering department. His work experience included manufacturing and processing of polymer nanocomposites. While his emphasis was injection molding of absorbable polymer composites, he was exposed to various materials and methods, including dental composite, bone cement, and HA fabrication. Richard's interest in medical devices is clear and he is always ambitious to learn more cutting edge medical technologies. Additionally, Richard was responsible for the fabrication of molds and experimental design and setup.